UiT The Arctic University of Norway

Faculty of Science and Technology
Department of Physics and Technology

Pumped Hydropower Conversion and Renewable Hybrid Power Plants at Senja

Ina Løvvold

EOM-3901 Master's thesis in Energy, Climate and Environment – September 2020

Abstract

With an increasing demand for power on a global scale, and an increasing interest in renewable energy sources, both solar and wind power is growing fast. Their efficiency is increasing while the prices are decreasing, and the forecasts for these technologies shows a promising future. Along with these intermittent energy sources, storage solutions are also continuously developing, whereas pumped hydropower is the most prevalent. Even if Norway is mainly self-supplied by renewable hydropower production, the population and energy demand is increasing, and so is installation of wind and solar power. Norway, with its mountains and fjords, have some challenges regarding power supply, since there often is long distances between production and demand. One of these locations is found at the northern part of Senja, where voltage drops are causing severe challenges for the seafood industry and contributing to the rise of this thesis. A total upgrade of the power network at northern Senja is estimated to cost in the order of 45M€, and an alternative solution is being sought to solve this challenge.

In this thesis, an evaluation is performed regarding locally produced solar and wind power, so that production is closer to the demand. In addition, power production is normally more profitable than network construction. One of the main challenges for solar and wind power is their intermittent nature, demanding a source for storage. Therefore, the main focus in this thesis is on the possibility of converting already existing hydropower plants into pumped hydroelectricity storage, and by this constructing a renewable hydro power plant. Several suitable solutions are found, and even the most expensive is estimated to cost 4/5 of a total upgrade of the power network. It is also found that solar and wind resources act as complementary sources. While wind power could help off with power production during the heavy load period at wintertime, solar power could work as a good source for seasonal energy storage of pumped hydro. Based on the findings in this thesis, suggestions to topics of further work is given.

Acknowledgements

v

Contents

List of Tables

List of Figures

Abbreviations

AC   Alternating Current

AM   Air Mass

ARC   The Arctic Centre of Sustainable Energy

BEP   Best Efficiency Point

CSP   Concentrated Solar Power

DC   Direct Current

ECMWF   The European Centre for MediumRange Weather Forecasts

ERA5   ECMWF reanalysis 5

GHI   Global Horizontal Irradiation

HAWT   Horizontal-Axis Wind Turbines

HOMER   Hybrid Optimization Model for Multiple Energy Resources

HPP   Hybrid Power Plant

HRW   Highest Regulated Level of Water Height

IRENA   International Renewable Energy Agency

LCOE   Levelized Cost of Energy

LRW   Lowest Regulated Level of Water Height

masl   metres above sealevel

MET   The Norwegian Meteorological Institute

NREL   National Renewable Energy Laboratory

NVE   The Norwegian Water Resources and Energy Directorate

OED   The Ministry of Petroleum and Energy

PaT   Pump as Turbine

PHES   Pumped Hydroelectric Storage

PPA   Power Purchase Agreement

PR   Performance Ratio

PV   Photovoltaic

RENEW   Transformation to a Renewable & Smart Rural Power System Community

RTE   Roundtrip Efficiency

SSB   Statistics Norway

STC   Standard Testing Condition

TKN   Troms Kraft Nett

TKP   Troms Kraft Produksjon

UiT   Norways Arctic University

WWEA   World Wind Energy Association

Nomenclature

Symbol:	Description:	Unit:
A	Area	m^2
c	The Weibull scale parameter	m/s
C_k	Temperature parameter	unitless
e	Energy equivalent	kWh/m^3
E_{pot}	Potential Energy	J
FF	Fill factor	unitless
h	Head	m
I	Current	A
I_{mpp}	Current at mawimum power point	A
I_{SC}	Short circuit current	A
J	Current density	A/cm^2
J_0	Saturation current density	A/cm^2
J_L	Ideal current source	A/cm^2
k	The Weibull shape factor	unitless
l	Roughness length	m
L_{min}	Minimum PV row distance	M
m	Mass	kg
$\dot{m}$	Mass flow	kg/s
n	Diode ideality factor	unitless
η	Efficiency	unitless
p	Pressure	Pa
P_0	Ideal power	W
P_{gen}	Generated Power	W
P_{in}	Radiation intensity	W/m^2
P_{kin}	Kinetic power	W
P_{mpp}	Power at maximum power point	W

P_{pump}	Pumping power	W
P_{rad}	Incident solar radiation power density	W/cm^2
Q	Fluid flow	m^3/s
R_S	Series resistance	Ω
R_{SH}	Shunt resistance	Ω
T	Temperature	K
T_{amb}	Ambient temperature	K
T_{mod}	Module temperature	K
u	Fluid speed	m/s
v	Speed	m/s
v_0	Measured wind speed	m/s
V_{mpp}	Voltage at maximum power point	V
V_{OC}	Open circuit voltage	V
Y	System yield	kWh/kWp
Y_f	Final yield	kWh/kW
Y_r	Reference yield	kWh/kW
z	Tower height	m
z_0	Wind speed measurement height	m
α	Solar angle above the horizon	Degrees
β	Module inclination angle	Degrees
γ	Efficiency degradation factor	%/K
δ	Declination angle	Degrees
Θ	Zenith angle	Degrees
ρ	Density	kg/m^3
ω	Hour angle	Degrees

Introduction

1.1 Background

The modern society relies on stable power supply. While rapidly growing renewable energy sources are positive aspects regarding environmental issues, they have some challenges regarding such required stability. Many renewable sources are intermittent, causing unstable production, but solutions are evolving to reduce this problem. This also gives rise to a growing share of renewable hybrid power plants, where power producing technologies are combined with storage. Another challenge for stable power supply rises when the distance between production and demand is great, such as for certain locations that are situated at the far end of the power distribution network. One of these locations is the northern part of Senja, a large island in the far north of Norway. At the moment, the island is supplied by only one main feeder, a 66 kV cable that is nearing its capacity due to rapid growth in the seafood industry at Senja. The northern part of Senja is subject to unstable voltage quality due to long radial feeders in the 22 kV distribution network, and the hydro power plants that are located along those radials are a crucial player to maintain a satisfactory voltage level.

1.2 Scope of the Study

Troms Kraft Nett, the local power distributor, in cooperation with the Arctic Centre for Sustainable Energy, which is an interdisciplinary center affiliated with UiT, Norway's arctic university, wishes to seek solutions to improve the power challenges at northern Senja. There are several options to consider, without investing in a new, costly distribution network. Along with a quest to reduce costs, are also a desire to move in a more sustainable direction, and this paper seeks to evaluate the possibility of a hybrid sustainable energy system. The way it is considered in this paper is by evaluating the potential at Northern Senja for the two fastest growing renewable energy technologies, solar and wind power. Different layouts of a solar power plant at Northern Senja are evaluated, as well as how they could be complemented by wind power. One challenge for renewable energies is their intermittent production, often

demanding a storage alternative. In this paper, pumped hydro power is chosen for storage evaluation, since it is the leading technology when it comes to storing large amounts of energy for a longer time period, at the same time as hydropower plants already exits at the location. The capacity and suitability of converting already existing hydro power plants at Senja into pumped hydro energy storage is evaluated. This option would be able to store surplus energy from the considered renewable energy installations, and it could also help to relieve the network in times of high demand.

1.3 Outline of the Thesis

Excluding the introduction, this thesis will have the following division:

- **Chapter 2** – In this chapter necessary theoretical background knowledge is presented. This includes basic knowledge of the Norwegian power system and the renewable energy technologies considered. Hydropower, pumped hydroelectric storage, solar power and wind power is presented, as well as a combination of those, forming renewable hybrid power plants.

- **Chapter 3** – This chapter provides information about the sites of interest regarding the power network, already existing power plants, and sites evaluated for new power plants.

- **Chapter 4** – Provided data used in this study is presented in this chapter, followed by a firm explanation of how this data was evaluated, processed and further used for the study. Software's used are also introduced here.

- **Chapter 5** – This chapter presents all the results from the study performed. An evaluation is done of 2018 as a normal year regarding precipitation, as well as an evaluation of solar resource measurements. The given results are firmly evaluated and discussed, and rough cost analysis are given.

- **Chapter 6** – Conclusions regarding the results are given in this chapter, and also suggestions to topics of further work based on the findings in the study.

2 Theoretical Background

This chapter will provide basic theoretical background knowledge about definitions, regulations and technologies considered in the evaluation of a potential renewable hybrid system at Senja in Norway. Knowledge required is about the Norwegian power grid and marked, power production from hydro, solar and wind, as well as pumped hydroelectric storage and hybrid systems.

2.1 Power Distribution in Norway

A reliable power supply and distribution network is crucial in modern societies. The geology of Norway has provided the country with stable hydropower, and it makes up 94.3% of the Norwegian power production. During the last years, more wind power has been integrated, and it now holds a share of 3.4% of the total Norwegian power production (OED, 2020b). Norway have been trading power abroad for a long time, and for the period between 1993 and 2017, as much as 17 years had a net export (SSB, 2018).

The Norwegian geology, with great amounts of mountains and fjords, and great distances between production and demand may cause various challenges. Power must be used immediately when it is produced, so a balance between production and consumption is crucial, and planning ahead is important. The length of the Norwegian power network is about 130 000 km (OED, 2020), consisting of three different grid levels. The central grid has the highest voltage, between 300 kV and 420 kV, and in some regions 132 kV. It consists of the nationwide network, as well as networks abroad, which makes it possible to trade power in times of surplus or deficit. The regional grid is also a high voltage grid, between 33 kV and 132 kV, which distribute power from the central grid to the distribution grid. It may also be connected to producers and consumers at higher voltage levels. The distribution grid is at a lower voltage, between 230 V and 22 kV, and it is the part of the network that supplies consumers. Between the grid levels are substations that step up and down the voltage to the desired level (OED, 2020).

In Norway, as in many other countries, the power distribution is strictly regulated. The administrator of the Norwegian power supply is the state-owned company Statnett, while NVE regulates and oversees network operations. NVE is The Norwegian Water Resources and Energy Directorate, which is a directorate under the Ministry of Petroleum and Energy. The power grid is a natural monopoly because it is expensive to build, and it is relatively inexpensive to operate. The mean price of it decreases the more it is used, so it makes little sense to build parallel competing networks. Norway is therefore divided into sections where local network companies have monopoly. Since consumers cannot choose network operators, the operators are strictly regulated to ensure consumers a decent price, as well as satisfactory quality of the network (OED, 2014).

Since the power distribution requires momentaneous balance, the power marked depends on production availability, planning and regulations. The sellers and buyers in the power marked, whom are the power producers and distributors, agree on the next day's trade, both the amount of power for each hour as well as the price. The latter is set in Nord Pool, which is owned by the Nordic and Baltic transmission system operators. Based on these daily agreements Statnett forms the basis to maintain the coming days momentaneous balance (Statnett, 2018).

2.2 Hydropower

Still water at an elevation, and flowing water, contains considerable amounts of energy, potential and kinetic energy, respectively. This energy has for decades been extracted by mankind, by converting mechanical energy into electricity, either by run-of-the-river systems or by building reservoirs. In reservoirs the potential energy is stored and converted to kinetic energy when allowing water to flow through a turbine. Run-of-the-river hydroelectricity is a type of hydroelectric generation plant whereby little or no water storage is provided. It often has less capacity than dammed reservoirs and is highly dependent on the river flow (BOR, 2005). Run-of-the-river systems cannot be used as storage facility in hybrid systems, since they have little, or no, storage capacity, so such systems will not be considered in this paper.

In this chapter the basic theory behind conventional hydro power is presented.

2.2.1 Conventional Hydropower Plants

The potential energy in the water conserved in a reservoir is converted into kinetic energy by letting this water flow through tunnels or pipes, called a penstock. By the usage of turbines this kinetic energy can be extracted and further converted into electricity. The amount of energy one can extract from the water in a reservoir depends on the size of the reservoir, the flow of water, turbine efficiency, resistances in pipes and the head level. The head is the vertical distance between the inlet of water and the turbine (Andrews & Jelley, 2007).

Figure 2-1 shows a general layout of a conventional hydro-power plant and its basic components, which are numerated in parenthesis in the following explanation.
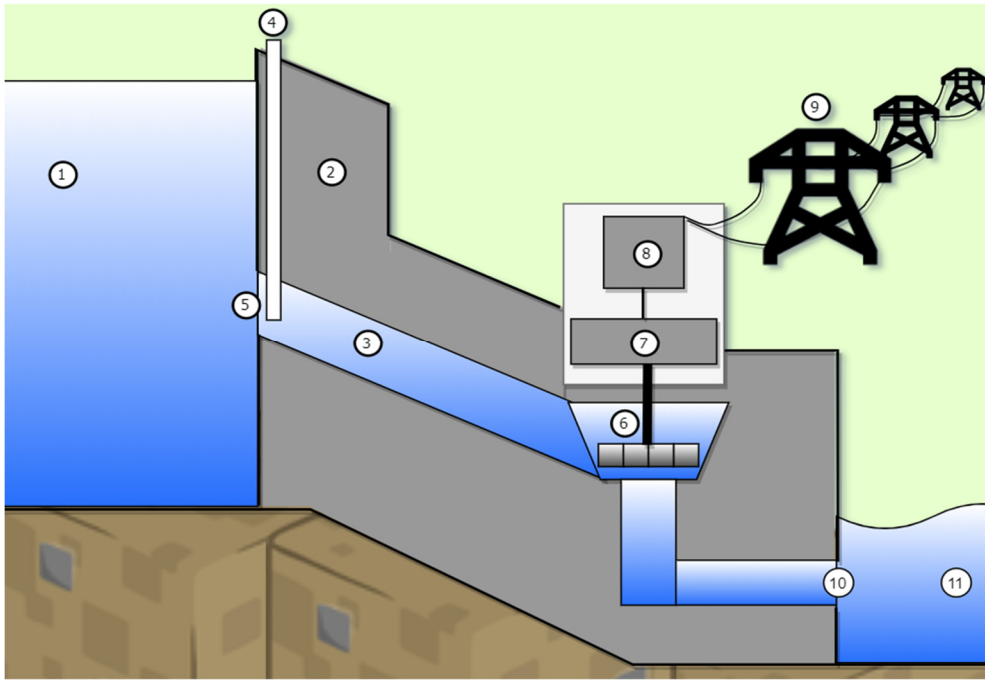
Figure 2-1 General layout of conventional hydro power plant [Self-produced figure, 2020]

The reservoir, or magazine, and the overlying water flow are normally referred to as upstream (1), while the river/stream below the outlet (10) of the power plant is referred to as downstream (11). At the inflow (5) of the penstock (3) is a control gate (4) where water flow is regulated according to preferred production. The turbine (6) and generator (7) are located in the powerhouse, and this is the site where energy is converted to electricity and further transformed by a transformer (8) to higher voltage and transported to the power network (9) (Bonsor, 2019).

The potential energy in a dam, given in J, is calculated from equation 2-1.

$$E_{pot} = mgh \hspace{3cm} (2-1)$$

, and the generated power, given in W, from equation 2-2.

$$P_{gen} = \eta \rho g h Q \hspace{3cm} (2-2)$$

Here, m is mass [kg], ρ is density of water [kg/m³], g is the gravitational acceleration, h is the head level [m], Q is the flow of water [m³/s], and η the efficiency (unitless) (Andrews & Jelley, 2007).

The efficiency is further a product of the different efficiencies from the turbine, the generator and the transformer, found by equation 2-3 (Bonsor, 2019).

$$\eta Power\ plant\ =\ \eta Turbine\ *\ \eta Generator\ *\ \eta Transformer \qquad (2-3)$$

Another useful definition for hydro power plants is the energy equivalent, e, which is the amount of energy produced for each cubic meter of water through the turbine (NVE, 2010), and it is found by equation 2-4.

$$e = \frac{\eta \rho g h}{3600} \qquad (2-4)$$

The energy equivalent has the unit kWh/m3, and it provides easier comparison between output generation from different hydro power plants independent of their size, installed capacity etc.

2.2.2 Water Turbines

There are two main types of hydroelectric turbines (Andrews & Jelley, 2007); impulse turbines and reaction turbines. Impulse turbines, where Pelton turbines are the most known, are open systems where water is steered on to the blades, transferring kinetic energy from the water to the turbine blades, hence causing rotation. Reaction turbines are closed systems where difference in pressure causes water to push the blades into rotation. Francis turbines and Kaplan turbines are the most commonly used reaction turbines. Which turbine to install is site dependent. While Kaplan turbines are most suitable for low head and high flow rate, Pelton turbines are so for high head and low flow rate. Francis turbines have a wider range of usage but are often installed for medium head and medium flow (Andrews & Jelley, 2007).

Since this paper focuses on hydroelectric power plants with medium head and flow, and as explained later in section 2.3.2, Francis turbines are the most commonly used turbine in pumped hydro power, the next paragraph gives a firmer description of only this type of turbine.

In a Francis turbine the water is spiraled into the runner to distribute water equally from all directions, hence increasing the efficiency, which often reaches between 90-95% (Breeze,

2014). Francis turbines are sometimes called mixed-flow turbines, because the water flow enters the turbine in a radial direction and leaves at the axial direction. The blades of the turbine are shaped such that to extract a maximum amount of energy. Guide vanes and stay vanes, which water passes through before entering the runner, are positioned in given angles for the same reason. Also, these vanes regulate the amount of flow for optimization. At the most optimal operation point, called the best efficiency point, <u>BEP</u>, the head, flow, speed of rotation and gate positions are optimal, and all the vanes are angled perfectly (Nielsen, 2015).

2.2.3 Regulations and Definitions

Hydropower plants in Norway are strictly regulated by laws and concessions, by the parliament, the Ministry of Petroleum and Energy (<u>OED</u>), the Norwegian Water Resources and Energy Directorate (<u>NVE</u>), and some external directives (OED, 2015). Hydropower plants are required to comply with legislation on such as minimum water flow in rivers, dam construction security and passage for fish. Also, all dams are regulated by a highest and lowest regulated level of water height, <u>HRW</u> and <u>LRW</u>, respectively. The defined magazine volume is the volume between these two levels. If levels are found outside of the limits, the power plant is fined. Exceptions are if the violation is caused by natural consequences, as flooding etc. (NVE, 2007).

The magazine capacity is defined as the amount of power that can be produced during an average year, if the magazine is full in the beginning of the year and empty at the end. Put in other words; The full magazine, plus the precipitation throughout a normal year (TKP, 2020b). Installed power is the power for which a turbine and generator is designed for, and a power plant of less than 10 MW is classified as small-scale hydro. Hydropower plants are also classified with an average annual production. This production estimate is based on historical data about water inflow in a reference period of about 30 years (Rosvold & Hofstad, 2019). Based on the power plants production capacity an estimation is done of the theoretical mean annual production during the reference period. This is used as an estimate of predicted production over the years to come and is normally given in GWh.

The production capacity of a hydropower plant is dependent on its storage capacity and the inflow of water from the watercourse's precipitation field. Water inflow varies greatly annually, seasonally, and geographically (OED, 2015). Wintertime in Norway generally has low inflow, mostly due to that precipitation comes in the form of snow. There are great differences though, especially for coastal and inland area. Coastal areas in Norway often have greater inflow than inland areas during wintertime due to higher temperatures, more often above freezing level, so hydropower plants near the coast have less annually variations (NVE, 2010).

The water level in Norwegian hydropower plants normally follow a seasonal pattern, where inflow is high during summer. By the end of autumn reservoirs are full, prepared for low inflow during winter. Then, the water level is gradually decreasing during wintertime, and reservoirs are almost emptied at spring, preparing for spring flooding caused by snow melt (Patocka, 2014). Figure 2-2 illustrates a mean year concerning inflow and power consumption in Norway.
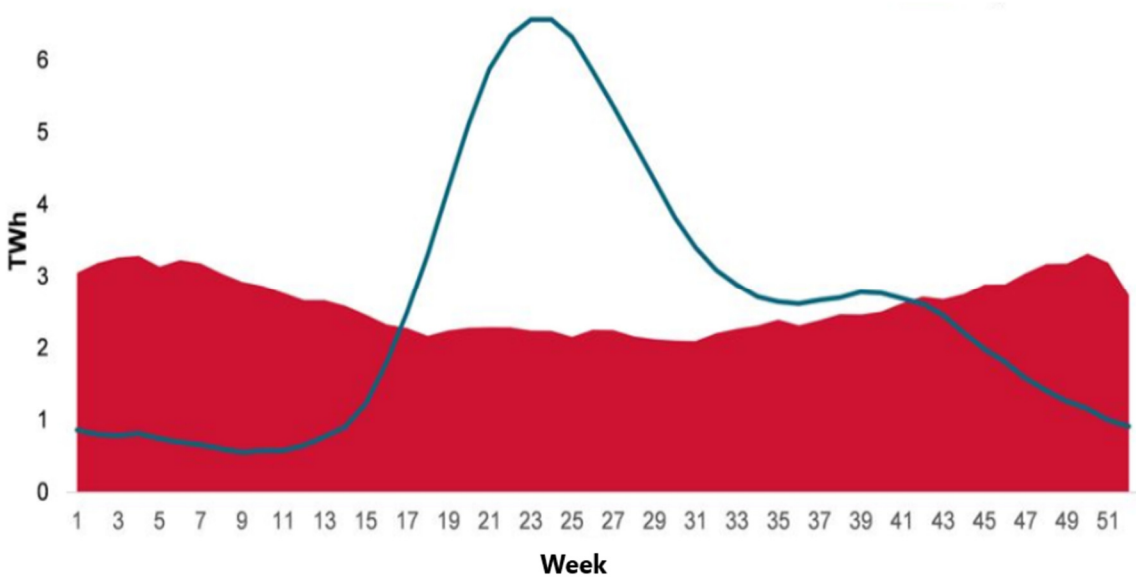
Figure 2-2 Typical inflow (blue) and consumption (red) during a mean year in Norway (NVE, 2019b)

The storing capacity in hydropower magazines enables production to be distributed throughout the year, and this results in the fact that hydropower makes up for well above 90% of Norwegian power production (NVE, 2019c). The annual inflow varies greatly over the years, so for Norway

to be dependent on hydropower, the storage capacity is crucial. Annual inflow for a 15-year period is illustrated in figure 2-3, and the lowest and highest inflow differ with about 50TWh.
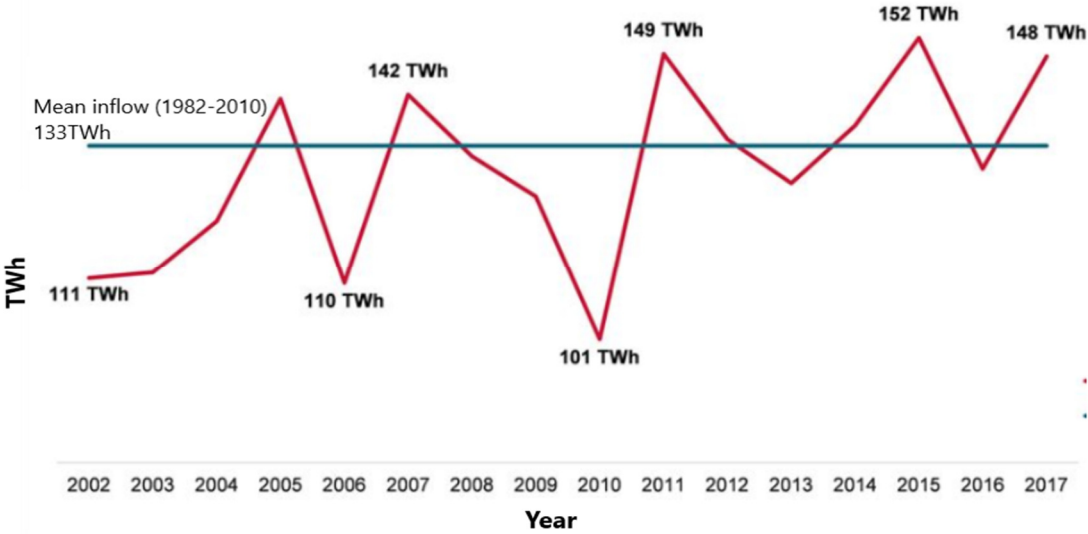
Figure 2-3 Annual inflow, actual (red) and median (blue), in Norway for a 15-year period (NVE, 2019b).

2.2.4 Development and Economy

Renewable energy accounted for a third of global power capacity in 2019 (IRENA, 2019c), and during 2019 renewable energy capacity grew more than three times faster than non-renewable capacity. Hydropower accounts for about 1/6 of all power generation globally (Statkraft, 2019). At the end of 2019, it made up the largest share, 47%, of all installed renewable energy, with a capacity of 1190 GW (IRENA, 2020). Hydropower has had an annual growth of up to 3% between 2013 and 2018, but with a decreasing trend (IEA, 2019). The addition of installed capacity was unusually low in 2019 with only 1%, but this is estimated to be caused by the postponement of the completion dates of some large projects (IRENA, 2020).

Most power plant technologies, renewable ones as well, have both positive and negative consequences concerning the environment. There are lots of positive aspects to hydropower, such as low operating costs, the impact on the atmosphere is low, quick response time if needed and the lifetime of a plant is long – often between 40 and 100 years. There are also considerable negative aspects to account for, the greatest one being massive intervention in nature and

10

environment (Andrews & Jelley, 2007). For hydropower though, it seems that in many cases the benefits outweigh the disadvantages considered against other power production alternatives.

Investments in dams are very costly and they have a long payback time (Andrews & Jelley, 2007). The investment cost is very much site dependent, but typically ranges from 850 €/kW to 3000 €/kW. The levelized cost of energy (LCOE) on the other hand, is low. This cost calculation takes the life span into account and distributes the investment and operational costs over the total production during the plant's entire life. Typical LCOE for hydropower ranges from 17 €/MWh to 230 €/MWh for small scale hydro, and from 17 €/MWh to 160 €/MWh for large scale hydro (IRENA, 2012). The LCOE for hydropower in Norway have been stable for many years, about 31 €/MWh for large scale hydro and 37 €/MWh for small scale. This price is expected to remain about the same until at least 2040 (NVE, 2019d).

The main obstacle for hydropower in Norway is the tax system, requiring a minimum of 59% from hydropower producers. In comparison, other energy production forms are only taxed with ordinary corporation taxes of 22%, so it is in many cases more profitable to invest in other energy sources than hydropower (Skårerud, 2020). Nevertheless, the Norwegian tax regime for power producers is currently being addressed at governmental hold. In the Finance Committee's recommendation for a revised national budged, that was recently published, the political majority tends towards tax cuts for hydropower producers (Stortinget, 2020).

2.3 PHES - Pumped Hydroelectric Storage

Pumped hydroelectric storage (PHES) works in the same way as conventional hydropower with reservoirs, except they can be refilled using a water pump, and hence work as energy storage as well. The main difference is that PHES requires at least one extra, lower reservoir, or large and stable enough river, from which they can extract water for pumping. A general layout of a PHES is shown in figure 2-4, but what is not shown in the figure is that the pump/turbine should be submerged relative to the outlet, as explained further in chapter 2.3.3.
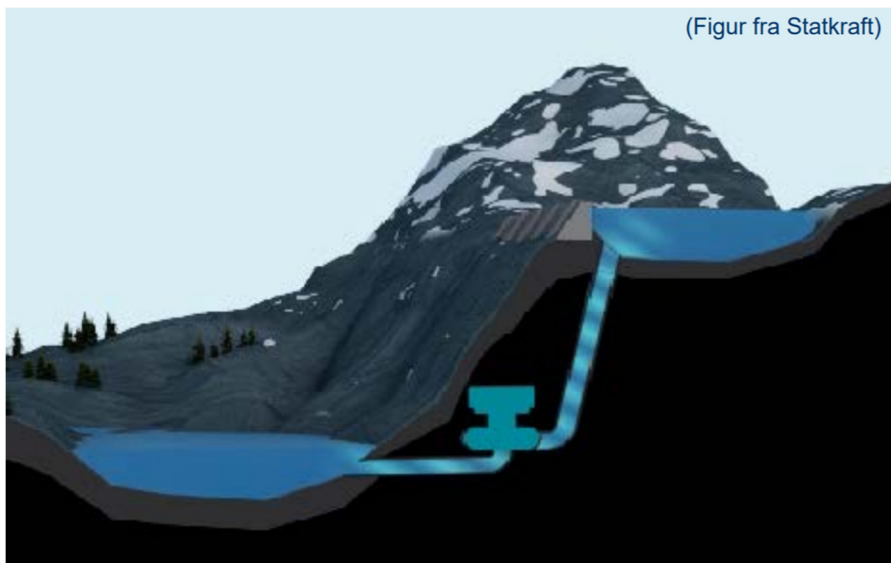
Figure 2-4 Pumped Hydroelectric storage, with two reservoirs and a reversible turbine or pump/turbine between (Statkraft, 2019).

Due to, amongst other factors, a long life cycle, low maintenance cost, efficiency, availability, flexibility and the size of storage capacity, PHES is a well-established energy storage alternative. It is the largest-capacity form of grid energy storage available, and in 2017 it accounted for over 95% of all active energy storage installations worldwide (DOE, 2017). PHES is advantageous due to short response time. Depending on the plant construction, full generating mode is often achieved within less than two minutes from standstill, while for full pumping mode it often takes less than five minutes from standstill. A PHES plant generating at 50% capacity are often able to achieve full generating mode in about 15 seconds (EERA, 2016).

PHES is also effective when it comes to power network regulations and is widely used to balance baseload power plants. Modern PHES are excellent suppliers of system services, as

frequency control and voltage control, and they may operate almost continuously. They are able to provide spinning reserves for the power grid, and their ability to convert large amounts of power within limited time is highly valuable in the power system (Lia, Vereide, & Kvaal, 2016).

2.3.1 PHES Efficiency

The efficiency of PHES is a product of the pumping efficiency and the power generation efficiency, called the roundtrip efficiency, <u>RTE</u>, found from equation 2-5.

$$RTE = \frac{P_{gen}}{P_{pump}} \qquad (2-5)$$

The generated power, P_{gen}, is the same as for conventional hydro power (<u>eq. 2-2</u>) (Antal, 2004), while the pumping power, P_{pump}, is the power input required to drive the pump, calculated by equation 2-6 (Milnes, 2017), and both is given in W.

$$P_{pump} = \frac{\rho g Q h}{\eta} \qquad (2-6)$$

Here, ρ is the density of water, g the gravitational acceleration, Q is flow rate, h is the head level and η is the efficiency of the pump.

Due to the long life span of hydro power plants, the roundtrip efficiency for <u>PHES</u> varies significantly between old and new installations, from lower than 60% for the oldest technology, to above 80% for new, more efficient installations (Yang, 2016). Some important factors for effective <u>PHES</u>, in addition to a pump/turbine with high efficiency, is a geographical topography allowing high head and shortest possible intake tunnel, penstock and outlet. This is to reduce friction losses and initial investments, and a high head allows for smaller pump/turbine units (Antal, 2004). In other words, the best possible designs are magazines situated in a close horizontal distance and a relatively high vertical distance.

2.3.2 PHES Designs

There are several different designs of PHES, the two main types being combined/hybrid/pump-back PHES and pure off-stream/closed loop system PHES (Yang, 2016). Pump-back PHES often make use of an already existing hydropower plant, so it is fed both by natural water inflow as well as pumped back water. Pure off-stream PHES is often man-made reservoirs where the only water supply is the introduced pumped water, hereunder also saltwater reservoirs. Other types of PHES includes decentralized systems, underwater and underground reservoirs.

The pumping system design may also vary. For instance, a separate pump can be installed in addition to the turbine, which may already exist at the location, or a pump as turbine (PaT), can be used. A PaT is a hydraulic pump that can be reversed, and it is relatively cheap. It is often the best economic solution for micro hydropower schemes of less than 100 kW, even if the efficiency is lower than for regular turbines (Kougias et al., 2019).

The most common turbines used for larger pumped hydropower schemes is reversible turbines with a reaction turbine design. There are both single speed units and adjustable speed units. Adjustable speed units are by far the most efficient, and their operational range allows for adjustment of input power and helps to avoid reverse flow when operating at high heads. It also allows for control of electrical power frequency on the power grid during pumping mode and helps to avoid cavitation under low head operation. However, adjustable speed units are also more expensive and require a greater powerhouse size (Antal, 2004). For adjustable speed units, a Francis type turbine is often used. A variable-frequency drive then needs to be coupled to the motor/generator to be able to change between pumping and generating mode, as well as to drive pumping and generation as efficient as possible (Marabito & Hendrick, 2019).

2.3.3 Conversion of Conventional Hydropower Plants into PHES

One promising option for PHES, considering economics and permits, is conversion of already existing conventional hydro-power plants into PHES (Perán & Suárez, 2019). There are numerous ways to do this, and the design and cost is very much site dependent. The designs,

already mentioned in chapter 2.3.2, vary from installation of just a pure water pump, reversing turbines that can do so, or substituting the original turbine with a reversible turbine or PaT.

There are several challenges though. A reversible turbine, unlike a regular turbine, should be submerged relative to the outlet at the lower reservoir, defined as the plant's submergence. This to avoid cavitation in pumping mode, and already installed turbines put in reverse are normally not adequately submerged. In addition, it is hard to obtain optimal pumping efficiency compared to a variable speed reversed turbine. The latter is more expensive and requires more space. (Perán & Suárez, 2019). It is not straightforward to replace a turbine with a reversed turbine either. In practice, a new plant is often required to be constructed to replace the original one (Storli, 2020). In common for all solutions is that the project timeline is often substantially shorter compared to constructing PHES "from scratch", since a concession to operate a hydropower plant is already given, and it is also normally much cheaper (Perán & Suárez, 2019).

When considering conversion of conventional hydropower plants into PHES there are several issues that must be addressed. An evaluation must be performed regarding the original plant's limiting factors and input data, preliminary assessment of the electrical equipment, budget etc. (Perán & Suárez, 2019). The geology of the site must be thoroughly examined for each site considered, since PHES operation of lakes often results in more rapid water level fluctuation. This can affect the reservoir banks differently than conventional power plant operation, and in some situations, this causes the banks to get more prone to avalanches. In Norway it can also impact the ice-cover, which often will be thinner and last for a shorter period for PHES operated lakes (Patocka, 2014). The biology is also affected and must be evaluated for each case.

2.3.4 Development and Economy

Globally, more than 1.6 TWh installed capacity of pumped hydroelectric storage have been realized (DOE, 2020), and the capacity is estimated to grow for a long time to come (EERA, 2016). The main competitor of PHES is batteries, especially considering their rapidly increasing efficiency and decreasing prices (Perán & Suárez, 2019). Even though, PHES has a competitive

investment price and ability to store massive amounts of energy for a long time, so it is predicted to remain the most important and economical player for energy storage for the years to come. Improvement in construction techniques, electromechanical equipment design and manufacturing has also reinforced its flexibility and competitiveness (Perán & Suárez, 2019).

The technical life time of a PHES installation is between 40 and 80 years (EERA, 2016), and it has over the years reduced the required installation costs (Perán & Suárez, 2019). The installation cost and the development time highly rely on the site and scope of the projects, from 1500-2000 €/kW, and more than 10 years' time, for designs "from scratch". For the simplest conversions of already existing hydropower plants into PHES, the investment cost may be as low as 100-300 €/kW, and it has a substantially shorter project time, (Perán & Suárez, 2019).

LCOE for PHES is normally low, and for Norway it is around 0.070 €/MWh (Charmasson, 2016). Due to the fluctuating electricity prices in Norway, given an optimistic efficiency ratio of $\eta_{Turbine-mode} = 0,9$ to $\eta_{Pumping-mode} = 0,85$, it could yield a price difference of >30%, based only on efficiency losses (Lia et al., 2016). Expected investment costs in Norway for upgrading conventional hydropower plants into PHES was in 2007 estimated to be between 1680 €/kW and 2525 €/kW (Sira-Kvina, 2007). It is estimated that such investments could yield some small profits, and with more fluctuating electricity prices the more profitable (Lia et al., 2016). It is important to keep in mind though, that energy storage often gives more stable energy production, and hence less variation in electricity prices. In that case the investment profit gets annihilated by the PHES construction itself, but the effect of this is very unpredictable and is probably less valid for small scale projects. The most common way to solve such unpredictive investment obstacles is by long-term power purchase agreements, PPAs (Lia et al., 2016).

Hydropower as an energy source is a mature technology, and hence the efficiency development has stagnated, though at a relatively good level. Further development primarily focuses on increasing efficiencies at power plant operations deviating from the BEP. For PHES there is also potential for improvement regarding digitalisation of control management (Kougias et al., 2019). The forecast for PHES in Norway is probably dependent on the outcome of the tax regime revision that is currently being addressed, explained in section 2.2.4. Because of the high taxes at the moment, the profit is normally not adequate for investment, even if there is a great amount of capacity for PHES (Skårerud, 2020).

2.4 Solar Power

The energy from the sun is abundant and is actually the origin of many other energy sources. It provides energy to Earth as photons are absorbed and converted to heat, and the uneven distribution gives rise to pressure differences, both horizontally and vertically. This in turn, along with Earth's rotation and tilt, results in weather, fluid dynamics in the atmosphere and ocean. These fluid dynamics give rise to energy sources such as wind, wave, hydro, tidal, biomass etc. Without the sun, fossil fuel would have never existed either. In addition to being abundant, solar energy is a clean, renewable energy source, it is environmentally friendly, pollution free, and is more or less available all around the world, even though some locations have a varying income throughout the year. Earth receives 1.8×10^{11} MW power from the sun, which is several thousand times greater than our total current power consumption (Solanki, 2016).

In this chapter the basic theory behind solar energy is presented and based on the scope of this thesis only photovoltaic electricity generation technologies will be included.

2.4.1 Energy From the Sun

The amount of solar radiation that reaches the top of Earth's atmosphere, the extra-terrestrial solar irradiation, is also known as air mass zero, AM0. It is given by the solar constant, S = 1367 W/m², which is in fact an average value. It varies with difference in sun emission intensity, as well as throughout the year due to the annual variation in sun-earth distance (Solanki, 2016). Due to absorption and scattering in the atmosphere, not all this irradiation reaches the surface of Earth. When the extra-terrestrial radiation from the sun reaches Earth's atmosphere, four outcomes are possible. It can either be reflected back to space (~6%), it can penetrate the atmosphere and be absorbed (~16%), it can be directly radiated to Earth, or it can be scattered, leading to a redistribution of radiation randomly in all directions. The part of the scattered radiation that reaches Earth's surface is called diffuse radiation, and the ratio between direct, also called beam, radiation and diffuse radiation depends on the sun's position on the sky and

the amount of clouds, aerosols and other particles in the atmosphere. Albedo, or reflected, radiation is the radiation that is reflected by Earth's surface and depends on the surfaces' texture. Global radiation is then the total sum of direct, diffuse and albedo radiation that reaches a given point on the surface (Solanki, 2016). A radiation overview is illustrated in figure 2-5.
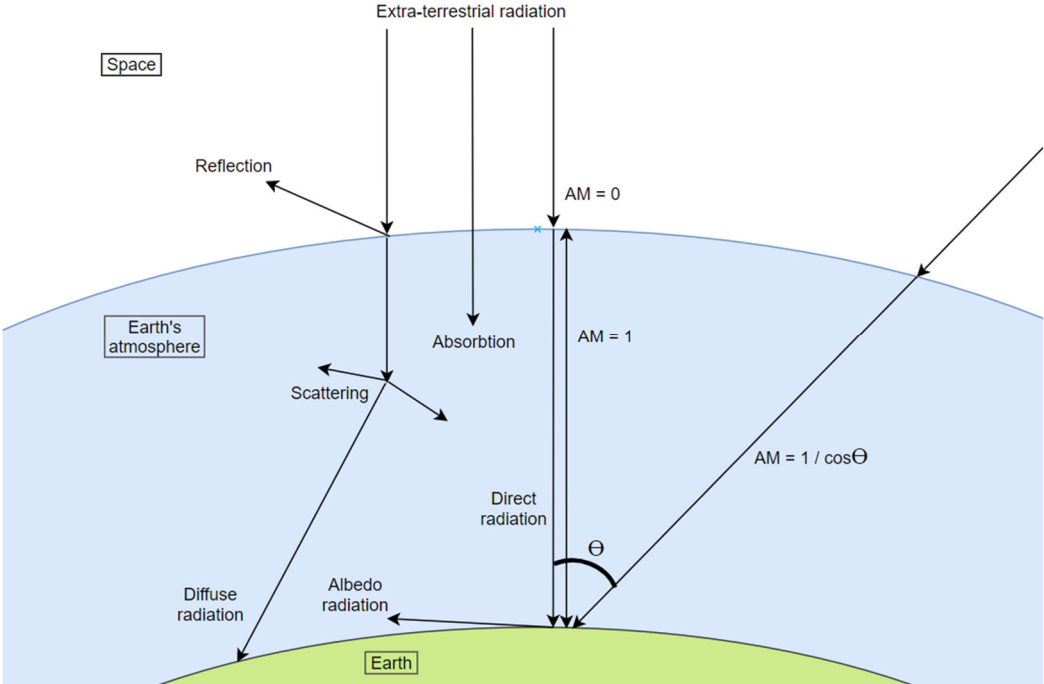
Figure 2-5 Extra-terrestrial radiation's interaction with the atmosphere [Self-produced figure, 2020]

Global radiation is in general higher for the sun in an overhead position, <u>AM</u>=1, than for sunrays with a high incoming angle relative to the vertical, the zenith angle, Ө, (see figure 2-5), where <u>AM</u> is found by equation 2-7.

$$AM = \frac{1}{\cos(\theta)} \qquad (2-7)$$

This is due to that the radiation must travel a longer distance through the atmosphere, meaning through a greater air mass, causing more absorption and scattering. High latitudes experiences greater <u>AM</u> than low latitudes since the sun does not reach an overhead position here. Also, <u>AM</u> values varies throughout the year and the day, because of Earth's motion with respect to the sun. The rotation of Earth, the tilt of its rotational axis and its revolution around the sun causes a variation in the angle of incoming solar radiation. During a year, the angle between

18

the lines joining the centre of the earth and the sun, with the projection on the equatorial plane of Earth, called the declination angle, δ, varies between ± 23.45°. It is zero at the two equinoxes of the year, and at maximum at the two solstices. During a day, the hour angle, ω, varies between ±180°, where 0° is at noon, positive values are before and negative values are after noon (Solanki, 2016).

It is also worth mentioning that because of the tilt of Earth and its elliptic path around the sun, the northern hemisphere receives more sun hours annually than the southern hemisphere. In fact, the North Pole experiences more sun hours than the equator, but sun hours are not equivalent to the amount of time that the sun rays reaches the ground (Sanden, 2011). For this, the topography and weather have a greater impact, whether there are a lot of shadowed area, clouds etc. All of this has an impact on the solar energy that reaches a specific point on Earth's surface, and the possibility to harvest the sun's energy there.

2.4.2 PV - Solar Photovoltaics

There are numerous technologies exploiting the energy from the sun, the two main types being solar thermal energy, in the form of heat collection, and electricity generation. The latter can be done either by concentrated solar power (CSP) or photovoltaics, PV. CSP requires high amounts of direct irradiance and is hence most promising for tropical areas (Bristol, 2016). Therefore, only PV will be considered here, and amongst different technologies, the crystalline silicon solar cells are the most common one.

Solar cells are constructed from semiconductors, allowing the photovoltaic effect to be exploited by exciting electrons across a P-N junction. This causes a state of voltage difference across the junction, and the natural state seeks an electron relaxation, meaning a recombination of electron-hole pairs, which is most easily obtained by the electron moving through an external circuit. This creates a current in the circuit, that can be harvested as electric power (Solanki, 2016). The amount of voltage and current that can be obtained depends on the construction of the photovoltaic device and the losses occurring. Figure 2-6 illustrates a simple model of an ideal solar cell device, with voltage V and resulting current I.
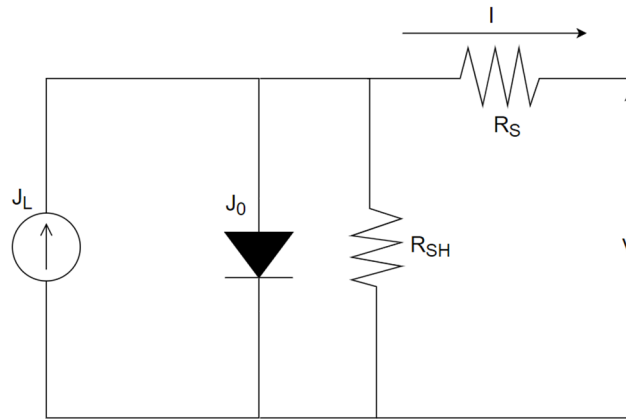
Figure 2-6 Equivalent circuit of a P-N junction solar cell
[Self-produced figure, 2020]

The equivalent circuit has a current source with light generated current density, J_L, representing an ideal solar cell, and the optical losses are included here, so the generated current, I, is proportional to the light input. The losses within the solar cell are represented by a diode for the recombination of electron-hole-pairs, called the reverse saturation current density, J_0, and resistances for ohmic losses. The ohmic losses present in a solar cell is series resistance, R_S, occurring in the path of the current flow, and the shunt resistance, R_{SH}, also referred to as the leakage path of the current. The shunt resistance is the resistance the current experiences when going in the opposite direction than desired. Therefore, the most optimal situation is a high shunt resistance and a low series resistance. From this equivalent circuit of a simple solar cell model, the I-V equation is given by equation 2-8 (Solanki, 2016).

$$J = J_L - J_0 * \exp\left(\frac{q(V + IR_S)}{nkT}\right) - \frac{V + IR_S}{R_{SH}} \qquad (2-8)$$

Here, J is current density, q is the charge of an electron, V is the given voltage, and n is the diode ideality factor which can take on values between 1 and 2, where 1 implies ideal diode. k is the Boltzman constant and T the temperature in Kelvin.

2.4.3 PV Characteristics

Figure 2-7 shows a plot of the I-V equation (2-8), called an I-V curve. The figure also shows the short circuit current, I_{SC}, and the open circuit voltage, V_{OC}, which are important characteristics of solar cells and used for comparison between different cells. These are the solar cell's highest obtainable currents and voltages, and I_{SC} will occur if the cell is short circuited, while V_{OC} will occur when the cell is open circuited. Their values can be found by solving equation 2-8 for V=0 and for I=0, respectively (Solanki, 2016).
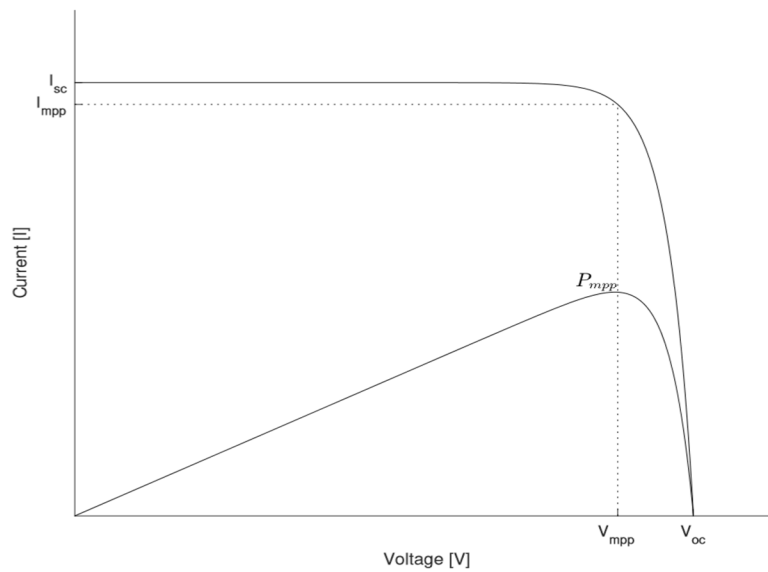
Figure 2-7 Typical I-V curve of a solar cell (Jacobsen, 2019).

Figure 2-7 is also illustrating the power produced by the solar cell, and P_{mpp} is the point of maximum power production, while I_{mpp} and V_{mpp} is the current and voltage, respectively, at this point.

Other important comparison characteristics of solar cells include the fill factor, FF, and efficiency, η. The fill factor is the ratio between the physically possible maximum power, P_{mpp} = V_{mpp} x I_{mpp}, and the ideal power, P_0 = V_{OC} x I_{SC}, of that specific solar cell. The equation for fill factor then becomes equation 2-9.

$$FF = \frac{V_{mpp}I_{mpp}}{V_{oc}I_{sc}} \qquad (2-9)$$

FF represents the squareness of the I-V curve and is given in percentage. Good cells typically have values of 0.80 or more, but it is not possible to obtain 100% because of losses that will occur, mainly resistive losses. In the best case, the fill factor could be 0.89 (Solanki, 2016).

Efficiency is defined as the ratio between power output and power input, where for PV power input is the power of solar radiation, P_{rad}. The international standard for characterization of solar cells uses P_{rad} = 1000 W/m^2 as test conditions. For power output the maximum power point is used, hence the equation for efficiency becomes equation 2-10.

$$\eta = \frac{P_{mpp}}{P_{rad}} = \frac{V_{mpp}I_{mpp}}{P_{rad}} = \frac{V_{OC}I_{SC}FF}{P_{rad}} \qquad (2-10)$$

For silicon, which is the most common material, a theoretical maximum efficiency is found to be about 29% with an indirect bandgap of 1.14 eV (Andreani, Bozzola, Kowalczewski, Liscidini, & Redorici, 2019).

The reason for the limitation in efficiency is due to fundamental losses, and the greatest loss is by thermalization and transmission losses (~56%). Thermalization losses are caused by photons having energy larger than the band gap, so only part of the photons' energy is utilized, while the rest is lost to heat. Transmission losses are due to photons having less energy than the band gap, so their energy is not sufficient to excite electrons to the next, required energy level, and hence these photons are transmitted right through the solar cell. (Solanki, 2016).

Other losses in a solar cell are voltage losses caused by the electron-hole recombination and fill factor losses as mentioned earlier. In addition to the fundamental losses, which cannot be avoided, there are other losses that are dependent on the quality and fabrication technique of the solar cell. Examples of such losses are optical losses due to reflection, shadowing and non-absorbed radiation, and electrical losses due to ohmic losses in material and recombination of electron-hole pairs.

2.4.4 The Effect of Temperature on PV Performance

Temperature has a large impact on PV performance, and in general the efficiency degradation factor, γ, for a typical silicon PV module is about -0.45%/K (Solanki, 2016). The standard testing condition, STC, for solar cells is an irradiance level at 1000 W/m^2, AM1.5 spectrum, and a temperature of 25°C. The temperature varies greatly around the globe, and in addition the working temperature for a PV module is often higher than the ambient temperature. This is a result from trapping of infrared light by the glass cover used as protection on the modules, as well as by the transmission and thermalization losses from radiation that cannot be utilized. The value of the module temperature is estimated by equation 2-11 (Solanki, 2016).

$$T_{mod} = T_{amb} + KP_{in} \qquad (2-11)$$

Here, T_{mod} and T_{amb} are the module and ambient temperature, respectively, and P_{in} is the radiation intensity given in W/m^2. K is a site and situation dependant constant, determined by wind speed, humidity and other factors that can affect cooling or heating of modules, and it can take on values between 0,02 and 0,03. The lowest value is obtained under the most effective cooling situation (Solanki, 2016).

I_{SC} actually increases with temperature since the band gap value is reduced, but simultaneously V_{OC} decreases by the same reason, and the latter is more prominent, hence the total results in lower efficiencies with higher temperatures.

2.4.5 PR - Performance Ratio

When evaluating PV systems, there are several different comparison methods, where performance ratio, PR, is one that have gained wide acceptance globally (Khalid, Mitra, Warmuth, & Schacht, 2016). It is the ratio of final power output to the grid to actual available power input, meaning available irradiance, after all losses to the environment and minus the energy consumed by the operation process. Therefore, it is an indicator of losses from shading, temperature, cell mismatch, inverter problems, wiring, reflection, outages etc. The advantage

of comparing PR is that external factors as solar irradiation, temperature etc. are taken into account. As mentioned earlier PV systems are classified by STC, but the actual working conditions varies greatly, so PR might be considered a better comparison method to evaluate a PV system's performance at a specific site. Continually PR measurements could also be helpful in failure detection and system analyzation (Khalid et al., 2016).

PR is unitless, and normally takes on values between 0 and 1, and values of 0,8 and above is considered a good performance, while values of 0,75 and less indicates problems (Khalid et al., 2016). Defining final system yield and reference yield as Y_f and Y_r, respectively, the equation for calculation of PR is given by 2-12.

$$PR = \frac{Y_f}{Y_r} \qquad (2-12)$$

Y_f and Y_r can be calculated by equation 2-13 and 2-14 (Khalid et al., 2016).

$$Y_f = \frac{Final\ energy\ output\ (kWh)}{Nominal\ DC\ power\ (kW)} \qquad (2-13)$$

$$Y_r = \frac{Total\ in-plane\ irradiance\ \left(\frac{kWh}{m^2}\right)}{PV\ reference\ irradiance\ \left(\frac{kW}{m^2}\right)} \qquad (2-14)$$

The final energy output is the energy delivered to the grid, in AC, while nominal DC power is the power output determined under STC, and the final system yield normalizes the energy produced with respect to the system size. The total in-plane irradiance is site dependent, while the PV reference irradiance is the STC irradiance of $1000kW/m^2$. Equation 2-14 can further be corrected for seasonal variations by a temperature parameter, C_k, given as 2-15 (Hukseflux, 2007).

$$C_k = 1 + \gamma\left(T_{mod} - T_{ref}\right) \qquad (2-15)$$

, where T_{mod} is the module temperature and γ the efficiency degradation factor, both presented in section 2.3.5. T_{ref} is the <u>STC</u> temperature of 25°C, and by using this seasonal temperature correction, equation 2-14 becomes 2-16.

$$Y_r = \frac{Total\ in - plane\ irradiance\ \left(\frac{kWh}{m^2}\right)}{C_k * PV\ reference\ irradiance\ \left(\frac{kW}{m^2}\right)} \qquad (2-16)$$

2.4.6 PV Orientation

One crucial factor for PV performance is the angle of the cells. The most optimal situation is when the cells are placed orthonormal to the sunrays, and the angle relative to this is called the incidence angle, γ. It is 0° at the most optimal, meaning when it coincides with the normal of the module's surface. Any other angle would result in more reflection, hence more energy losses to the environment (Solanki, 2016). Since the sun's angle, relative to the ground, varies throughout the day, the most optimal construction, concerning angles, is tracking systems for PV panels. There exists both one-axis and two-axis tracking systems, whereas the latter is the most optimal. However, such systems are substantially more costly, and with more mechanics and electronics involved, they also require more maintenance and are more prone to failure.

For stationary systems the optimal angle depends on the desired output for a preferred part of the year or time of the day. If the desired output is a total maximum current and there are no shadings involved, the general optimum is an azimuth angle of 0°. The azimuth angle is the angle relative to south, so 0° represents directly south at the northern hemisphere and directly north at the southern hemisphere.

The most optimal angle of the tilt of a module, called the inclination angle, β, depends on the latitude of the system and the time of the year. For instance, at the equator at equinox it should be 0° degrees, meaning parallel to the horizon. For higher latitudes the inclination angle should be steeper, corresponding to the sun's position at the sky (Solanki, 2016). In addition, in the case of snow-covered surfaces, an even steeper inclination angle might be more optimal since it allows for collection of albedo radiation as well. This will also help prevent snow build up at

the panels. On the other hand, in the case of restricted area where modules must be installed in rows, a smaller angle is preferable. This is because the front panels will cast a shorter shadow, allowing less spacing between rows. To calculate minimum row spacing, L_{min}, for a certain solar angle above the horizon, one can use the sine theorem to calculate the cast of the shadow, as in equation 2-17.

$$L_{min} = \frac{x}{\sin(\alpha)} * \sin(\beta) \qquad (2-17)$$

Here, x is the length of the panel, α is the solar angle above the horizon, and β is the inclination angle of the panel.

2.4.7 Solar Power Plants

One single solar cell is relatively small and has quite small output values. A standard Si solar cell is 6" x 6", and the normal <u>STC</u> output values from such cells are $V_{OC} = 0{,}55V$ and $I_{SC} = 30mA/cm^2$ (Solanki, 2016). To increase these values, several solar cells are series and parallel connected to form a module, and typical modules consist of either 32, 36, 48, 60, 72 or 96 cells. When connecting approximately identical cells in series the current will take on the value of the least current producing cell, while the voltage will be the sum of all solar cell voltages in that series. The opposite is true for parallel connection, where the voltage is identical to the cell with the lowest voltage, while the current output is the sum from all parallel series.

Modules are further manufactured with frames and glass protection to form a PV panel, and from there one can construct PV systems of preferred size. By connecting modules in series and in parallel, forming arrays, one obtains the same result as with cells, by increasing voltage and current.

All PV systems that want to output <u>AC</u> power needs an inverter, and there are several different types of inverters with varying efficiencies. Sizing of inverters relative to the PV system is crucial for the system performance. As a general rule of thumb, the inverter size should be similar to the <u>DC</u> rating of the PV system. Too small inverters will result in clipping, where it is not able to convert energy produced by the PV system above a certain amount. The efficiency

of an inverter is greatest when it is running closest to its overall capacity, so an oversized inverter will mainly work at a lower efficiency than desired. Also, larger inverters are often more costly, so financially it beneficial to choose the smallest inverter without compromising the power output (energysage, 2020).

To avoid failure or damage of a PV system, which may be caused by shadings or short currented cells, different types of bypass diodes are also often implemented, in order to prevent reversed biasing. Blocking diodes are also used, to prevent current from flowing in the wrong direction in dark conditions, as at night-time (Solanki, 2016).

PV systems can be off-grid, grid connected, or part of a hybrid system, and they exist in various sizes around the world. Utility scale systems are called solar power plants, PV power stations, solar parks or solar farms. The characterization is somewhat different from country to country, but normally the capacity is given in one of the three following:

- The nameplate capacity, meaning the rated kW_p under <u>STC</u>, where kW_p is the maximum power output under these conditions.
- Area and efficiency.
- Rating by the converted lower nominal power output in MW_{AC}. By doing so one accounts for losses from inverters, cable resistances etc, which allows for easier comparison between solar power plants. It also allows for comparison between the output power from solar power plants to other types of power plants. This is the reason for why this characterization method has gaining broader acceptance (NREL, 2013).

Other characterization parameters used to compare different PV systems is generated energy and specific yield. Generated energy is simply the amount of energy generated, often given for a period of one year. Specific yield is the amount of energy, in kWh, generated for every kWp of capacity, also normally given for a duration of one year.

The average lifetime of PV power plant's is estimated to be about 30 years, and their end-of-life management seems promising for recycling of materials (IRENA, 2016). Most PV manufacturers have warranties guaranteeing 90% efficiency after 10 years and 80% efficiency after 25 years, and the efficiency of commercial Silicon modules ranges between 18% and 22%

under STC (EERE, 2020). The degradation of PV panels is only time dependent, and not affected by the amount of production (Solanki, 2016).

To maximize production from a PV module, the placement and orientation is crucial. Available irradiation is a key factor, but there are also other aspects that needs to be addressed when considering PV installations. Shadings should obviously be avoided, and the climate of the area has huge impact, considering clouds, temperature and wind. The most optimal area would be a sunny, windy and cold climate. Areas with snowy surfaces would add more reflected radiation, but this will only be an advantage as long as the snow does not cover the PV panels. Other impacts that can affect the performance of PV is partly shading effects from sand cover or saltwater spray etc. from nearby environment.

2.4.8 Development and economy

Amongst renewable energy technologies, the fastest growing is, by far, solar energy. With an increased capacity of 20% in 2019, it then amounted for 586 GW globally (IRENA, 2020). About 95% of this was PV installations (Sönnichsen, 2019). This makes it the third largest renewable energy installed capacity, and with a steep increasing technology learning curve and decreasing economic learning curve, the trend is estimated to continue. Cumulative solar PV capacity is expected to be six times higher by 2030 compared to 2018 levels (IRENA, 2019a).

The total installation cost of PV was 1023 €/kW in 2018, compared to 3909 €/kW in 2010. Estimations done by the International Renewable Energy Agency (IRENA) in 2019, forecasts a decrease to between 288 €/kW and 705 €/kW by 2030 (IRENA, 2019a).

The LCOE for PV is highly site dependent. Since degradation of PV panels is independent on the production rate, the LCOE is highly affected by the power output during the lifetime of the system. Because of this, the LCOE ranges from 27 €/MWh for utility scale PV, up to above 200 €/MWh for some residential systems (LAZARD, 2019). For Norway, industrial PV had a LCOE of about 78 €/MWh in 2018. It had then decreased 47 € since 2016, and is estimated to continue the decrease towards 2040, when it is estimated to be about half the price than today, equalling 39 €/MWh (NVE, 2019e). Norway is estimated to be one of the last countries where

PV can compete with other technologies regarding price, due to the low electricity prices caused by the highly available hydropower production (Vartiainen, Masson, & Breyer, 2017).

The main advantages of Silicon PV power technology are the abundant and environmentally friendly materials it is made up of (Solanki, 2016). It can also be utilized anywhere the sun shines, and PV panels can be placed on fields, mountains, floating on water, mounted on top of or integrated in buildings etc, so area is basically available anywhere where there is sparse amount of shadowing. The main disadvantage is the large amount of highly purified silicon feedstock needed – about 15 tons for every MW_p module (Solanki, 2016).

The average module efficiency for mono crystalline has increased from 14.7% in 2006 to 18% in 2019, and this positive trend is estimated to continue through 2030 (IRENA, 2019d).

2.5 Wind Power

Kinetic energy of wind arises due to an uneven distribution of solar energy throughout the globe, which in turn creates pressure differences in the atmosphere. Air expands when heated, which increases the pressure, causing air to move from high to low pressure, resulting in winds (Wizelius, 2010). The rotation of Earth, the content of the air, and several physical forces creates a complex weather system, resulting in both geographical, annual and daily variations of wind. Even though, wind energy can be exploited in one form or another at basically any corner of the world. Some areas, however, are sheltered from wind at ground level, but when moving to higher altitudes the rotation of Earth leads to an origin of wind practically anywhere. Some technologies are evolving towards exploiting this but will not be considered in this thesis.

In this chapter the basic theory behind wind power is presented, as well as the technology constructed at the site of interest.

2.5.1 Energy in The Wind

What gives rise to the kinetic energy in the wind is the momentum and density of the particles in the air. The power of the wind, given by equation 2-18, is proportional to its speed per cubic metre. A doubling in speed increases its power eight times (Wizelius, 2010).

$$P_{kin} = \frac{1}{2}\dot{m}v^2 \qquad\qquad (2-18)$$

, where P_{kin} is kinetic power given in W, v is speed [m/s], and $\dot{m}$ is mass flow, given by equation 2-19, where ρ is the density of the air [kg/m^3] and A is area [m^2].

$$\dot{m} = \rho A v \qquad\qquad (2-19)$$

From these equations one can see that since air is denser when colder, the mass flow will be greater, and hence the power of cold wind is greater than of warm wind of the same speed. Therefore, winds in colder climate holds greater power capacity than in warm climate.

It is worth reminding the reader about the important difference between energy and power. Energy is defined as the quantitative physical property needed to induce work or heat, and is given in Joules, J, while power is the amount of energy per time, given in Joules per second, J/s, or Watt, W.

2.5.2 Wind Potential Calculations

Due to the eight times proportionality between wind speed and power, calculating the wind power potential for a given location is rather complicated, but it is crucial when considering installation of wind power harvesting constructions. The mean wind speed cannot be used, but instead one needs to know the occurrence of different wind speeds, the frequency, during a normal year, and the speed may differ from one instance to another (Wizelius, 2010). Also, the temperature and air pressure have impact on the air density, which in turn impacts the mass flow in equation 2-19. Some simplifications are used in rough calculations, such as a standard pressure at sea level of 1 bar and a temperature of 9°C, which gives an air density of 1,25 kg/m^3.

Even though exact prediction calculations are complicated, there are a method of simplification that has proven to be reasonably accurate. When knowing the mean wind speed, most sites seem to follow a probability distribution known as the two-parameter Weibull-distribution, equation 2-20 (HOMER, 2020).

$$f(v) = \frac{k}{c}(\frac{v}{c})^{k-1} \bullet \exp\left[-\left(\frac{v}{c}\right)^k\right] \qquad (2-20)$$

Where v is wind speed (m/s), k is the Weibull shape factor (unitless) and c is the Weibull scale parameter (m/s). c is proportional to the wind velocity (Bowden, Barker, Shestopal, & Twidell, 1983), and the relationship, within 1%, is given by equation 2-21, given $1,6 \leq k \leq 3,0$.

$$v = \frac{1}{2} \bullet \left(\pi exp(^1/_2)\right) \bullet c \qquad (2-21)$$

k decides the shape of the Weibull curve, and for wind speed it is normally bell shaped. It is site dependent, and takes on values between 1 and 3, where high values indicate stable winds, and low values indicates great variability in wind speed. For k < 1,6 equation 2-20 cannot be used, but there are other estimations for those scenarios. k is normally greater than 1,6 for most of the globe, except within ~5° of the equator and areas characterized by extremely long lull periods, like the Sahara (Bowden et al., 1983). Since this paper focuses on an area far north of the equator, other estimations of k are not included.

Wind speed is also dependent on the shape of the terrain and height above ground. This is due to that rough terrain results in greater friction between the air and the terrain, slowing down the wind, while at smooth surfaces the wind can travel more freely (Wizelius, 2010). As known from fluid dynamics, air has a low viscosity, but it is enough to cause inner friction, resulting in high external friction at the ground causing a decreased speed high above the ground. There are several different techniques to estimate wind speed at great heights. One way is by the usage of roughness length, l, which describes the terrains effect on external friction (Djohra, Mustapha, & Hadji, 2014), and table 2-1 summarizes some typical values.

Table 2-1 Typical roughness lengths for different terrain types (Djohra et al., 2014).

Terrain:	l [m]
Very smooth ice	0.00001
Calm, open sea	0.0002
Blown sea	0.0005
Snow surface	0.003
Fallow field	0.03
Crops	0.05
Few trees	0.1
Forests and woodlands	0.5
Suburbs	1.5

The values given in table 2-1 can further be used to estimate wind speed at different height by formula 2-22, called the logarithmic wind profile (Masters, 2013). Here, a simplification is

made, assuming a constant pressure gradient. In other words, constant air density is assumed at the lower atmosphere, where wind power is normally harvested.

$$\frac{v}{v_0} = \frac{\ln\left(\frac{z}{l}\right)}{\ln\left(\frac{z_0}{l}\right)} \tag{2-22}$$

In this formula, z is the tower height in metres and v the wind speed at this height. z_0 is the height at which the measured wind speed, v_0, is done. The roughness lengths of the terrain have substantial impact on the wind speed at these heights, shown in the plot in figure 2-8, where the wind speed profile is calculated for selected roughness lengths. The profiles are calculated from a measured wind speed, v_0, of 8 m/s at an altitude of 10m.
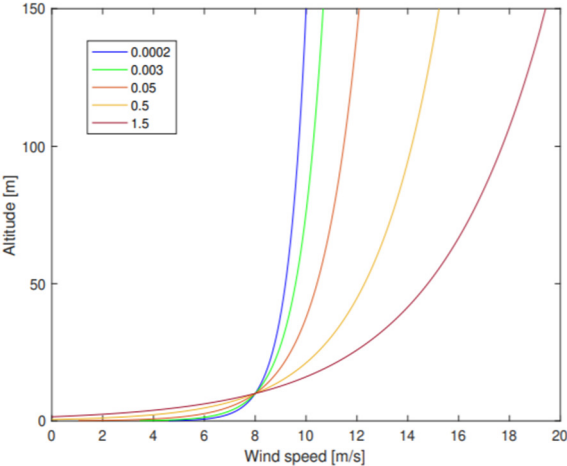
Figure 2-8 Wind speed profile for selected roughness lengths, l, for altitudes up to 150m. Measured wind speed, v0, at 10m is 8 m/s (Jacobsen, 2019).

Geological factors as mountains, fjords etc. may also cause severe local wind trends. Due to this, as well as climate, terrain and wind speed profiles, it is crucial that a thoroughly evaluation of sites are performed when considering installation of wind power harvesting technologies.

2.5.3 Wind Power Technologies

Wind power is a rapidly growing technology with several different designs, where the most common one, both on and offshore, are horizontal-Axis wind turbines (HAWT) with three rotor

blades attached to a horizontal shaft (NVE, 2019). Since the site considered in this paper consists only of such turbines, this will be the only technology presented here. The general design is illustrated in figure 2-9, followed by a description with numerations in parenthesis.
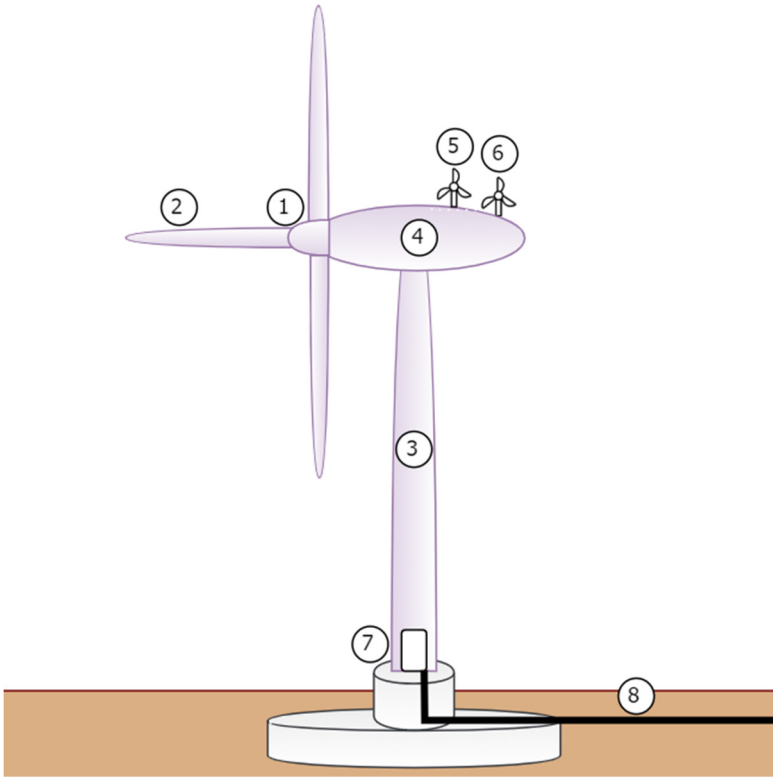
Figure 2-9 general layout of a horizontal-Axis wind turbines with three rotor blades attached to a horizontal shaft [Self-produced figure, 2020]

The rotor blades (2), attached to the hub (1), are shaped to extract as much lift- and drag force as possible. Different shapes and different materials are used, and the technology is still evolving rapidly, causing a learning curve towards higher efficiency. At high latitudes, where average temperature, and hence air density and the power of the wind, differs greatly throughout the year, pitch regulated turbines have proven to be suitable. Such turbines can rotate the angle of the rotor blades, optimizing the spinning speed and hence the energy extraction (Wizelius, 2010). An optimal production at low density air for a given turbine, will result in overload for that generator at the same wind speed at high density air. Therefore, the ability to rotate the blades to slow down the speed of the hub is crucial to protect the generator at high wind speed when the temperature is low, and still maintain optimal annual production. To measure the wind speed, an anemometer (5) is utilized.

The hub is attached to the nacelle (4), which contains all the generating components. Inside the nacelle, a bearing attached to the hub rotates, driving a generator where electricity is produced. A gear box optimizes the rotational speed in the generator, and a brake system is used to slow down and stop the turbine if the speed becomes too high. Several other components are housed in the nacelle, such as cooling systems, yaw drives, hydraulic system, control panel and so on. The nacelle is attached on top of the tower (3), which for most HAWT's has an entrance at the bottom (7), a latter at the inside, and in most cases an elevator. Inside the tower one also finds the power cable (8) that exports power from the generator to the grid (Wizelius, 2010).

Most often, a transformer is connected between the turbine and the grid to optimize the power quality delivered. The placement of the transformer varies, from inside the nacelle, inside the tower, under the tower in the fundament, or somewhere outside the tower. On top of the tower the nacelle can rotate to adjust for optimal wind angle, which is found by the wind vane (6).

A useful term for power production, often used to characterize wind turbines is the capacity factor. This is the unitless ratio of actual power output to the maximum possible power output for that turbine, over a given period of time. Average capacity factor of wind turbines has been steadily increasing over the years, and as of 2019, it is about 34% (IRENA, 2019b). It has been estimated by Betz limit that the maximum capacity factor for wind turbines is 59% (Andrews & Jelley, 2007). The reason for this limit, is that some of the wind passing through the cross-sectional area swept by the turbine's blades, is required to keep some of its kinetic energy to maintain an air flow downstream. Needless to say, an air stream is required for the turbine to function.

Since some of the kinetic energy of the wind that flows through a turbine is extracted, the downstream air flow will slow down, experience a pressure drop and hence expand. This can be seen from the simplified form of Bernoulli's equation for a horizontal fluid flow, given in equation 2-23 (Andrews & Jelley, 2007).

$$\frac{P_1}{\rho} + \frac{1}{2}u_1^2 = \frac{P_2}{\rho} + \frac{1}{2}u_2^2 \qquad (2-23)$$

p is here pressure, ρ is density, and u is fluid speed. The sub number 1 and 2 represent before and after a given area.

Another reason for why wind turbines cannot extract all the energy in the wind is because of their operation range. If the wind speed is too low, there are not enough power in the wind to cause rotation. If the wind speed is too high, turbines are at risk of being damaged and therefore stopped. This is called the cut-in and cut-out wind speed, respectively. Typical values for cut-in wind speeds are 4-5 m/s, and about 25 m/s for cut-out wind speed. The wind speed that the turbine is designed for is called the rated wind speed, and the generation at this point is called the rated power. All wind speeds greater than the rated wind speed will be limited by the rated power. For turbines of rated power at 2-5MW, the rated wind speed is typically around 12-15 m/s (Tande, 2006). The power curve of such turbines is illustrated in figure 2-10.
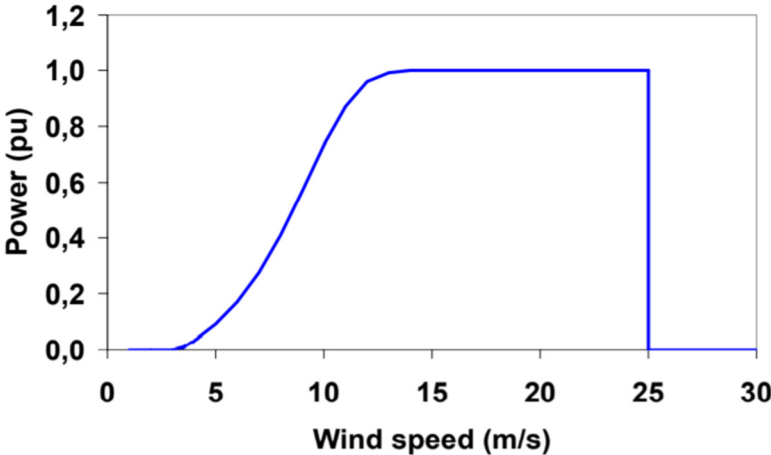
Figure 2-10 Power per-unit curve of a wind turbine (Tande, 2006).

2.5.4 Wind Power Plants

Wind power plants, also called wind farms or wind parks, are a delimited land or sea area, with a range of wind turbines from a few, to a couple of hundred. As previously mentioned, the wind potential at those land areas are most often thoroughly evaluated before considering installation. Placement of turbines within the plants is also well calculated since, as explained in the previous chapter, air flow expands when passing a turbine. The larger area of downstream wind with low pressure and speed may therefore cause losses for other turbines (Andrews & Jelley, 2007). This is one of the reasons for why turbine sizes tend to be increasing over the years. More air flow can be utilized, operation at higher heights results in increased mean wind speed, and

fewer turbines are hence needed for the same production. This also decreases the land area and infrastructure needed, which also decreases the investment and operation costs (Andrews & Jelley, 2007).

The lifetime of a wind power plant is estimated to be around 20-25 years (Wizelius, 2010). Characterization parameters often used for wind power plants are the installed nameplate capacity and the plant production. The installed nameplate capacity is the capacity each turbine is designed for at rated power, times the number of turbines at that plant. Actual production is estimated by multiplying the nameplate capacity with the capacity factor.

2.5.5 Development and Economy

Wind power is the second fastest growing renewable energy source, with a 10% increase during 2019 (IRENA, 2020). According to statistics presented by the World Wind Energy Association (WWEA) the installed capacity reached 650,8 GW at the end of 2019 (WWEA, 2020). Wind power technology is relatively cheap, and in large parts of the world it is already cheaper to install wind power plants than coal or gas plants (Statkraft, 2020). Still, the economic learning curve is decreasing, and the efficiency learning curve is increasing. New wind turbines are getting more robust and efficient, and they produce more energy, have a longer life cycle and requires less maintenance (Statkraft, 2020). The biggest obstacle for wind power installation is the land area required, environmental impact and resistance from the public and environmental organizations. Another issue recently addressed is the deposition of turbines. While the steel tower may be recycled, the turbine blades often ends up as land fill (Jacobson, 2016).

Total installation cost for onshore wind power was about 1615 €/kW in 2010, about 1264 €/kW in 2018, and is estimated to decrease to between 675 and 1140 €/kW by 2030 (IRENA, 2019b). The LCOE in Norway is for now 32 €/MWh and is estimated to decrease to 20 €/MWh by 2040 (NVE, 2019e).

The capacity factor is estimated to increase, but the uncertainty is great, so estimations for 2030 ranges from 30% to 55% (IRENA, 2019b).

2.6 HPP - Hybrid Power Plants

The rapid growing marked for renewable, intermittent, energy production, also causes a need for energy storage for when the production is higher than the demand. A hybrid power plant, HPP, combines energy production sources with energy storage technology.

There are several different storage opportunities, such as compressed air, a vast variety of batteries, flywheels, hydrogen fuel cells etc, but as mentioned previously PHES accounted for over 95% in 2017. Based on this, and the scope of this thesis, only hybrid power plants consisting of PV, wind power, hydro power and PHES will be considered further. A general layout of such system is presented in figure 2-11.
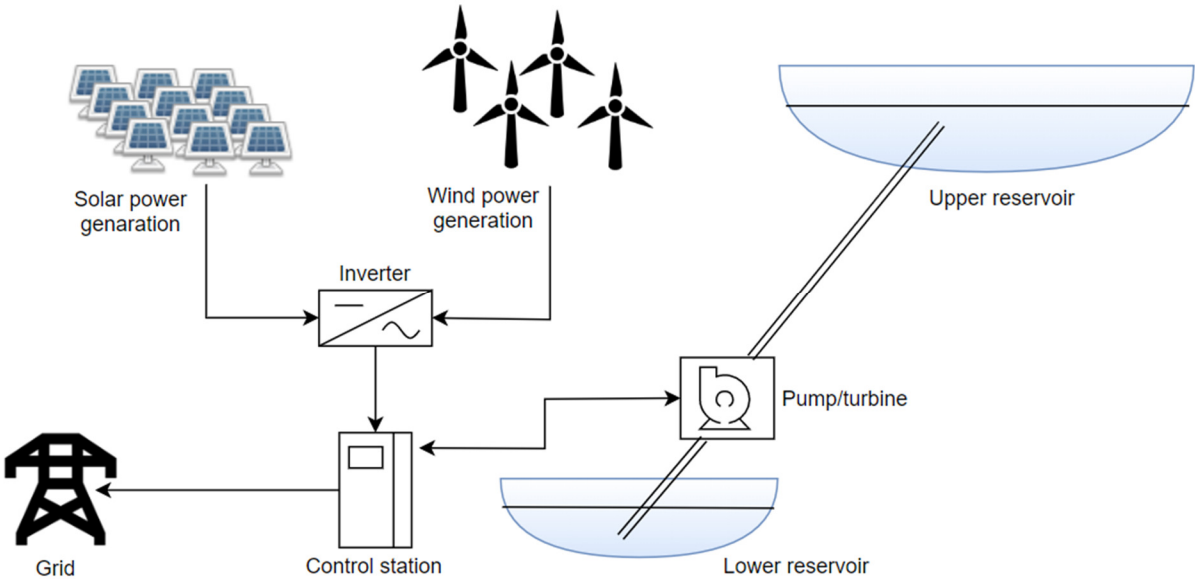
Figure 2-11 General layout of a PV/wind/PHES hybrid power plant (Self-produced figure, 2020)

The different power production technologies have their own pros and cons. For the same installed amount of MW, wind power often requires twice as much land area than PV, while LCOE is more than twice the price for PV than for wind power in Norway at the moment. For hydro and PHES the area required depends on the size and depth of the regulated lakes, and the

costs varies greatly depending on site and size. There are different ways to compare economics of the different technologies, and a rough estimate of installation costs and <u>LCOE</u> in Norway is given in table 2-2, based on the previously mentioned costs in chapter <u>2.2.4</u>, <u>2.3.4</u>, <u>2.4.8</u> and <u>2.5.5</u>.

Table 2-2 Rough cost comparison between technologies considered

Technology:	Installation cost:	LCOE in Norway:
PV:	1023 €/kW	78 €/MWh
Wind:	1264 €/kW	32 €/MWh
Hydro:	850 €/kW - 3000 €/kW	31 €/MWh – 37 €/MWh
PHES:	100 €/kW - 2000 €/kW	0.070 €/MWh

One of the greatest advantages of a renewable hybrid power plant is that the sources for production for each component often occurs at different times. In situations of overproduction from solar and wind power, where sometimes production must be stopped, energy can instead be used to pump water from a low to a higher reservoir to store this energy as potential energy. In periods of low solar and wind production, a considerable large part of this energy can be retrieved. In this way, water can be reused, and it is also a beneficial way to allow for more integration of renewable energy sources to the grid. Historically, in part from when there is overproduction from solar and wind, the pumping process seems to be ran at night-time, when electricity prices are normally at its lowest, while electricity production from PHES often is run at peak demand periods at daytime (Antal, 2004).

<u>HPP</u>s' can also be utilized as seasonal storage. For Norway, wintertime is normally dry season, at the same time as consumption of power spikes due to electric heating of domestic houses occurs. Water storage for the winter have therefore always been a high priority (Lia et al., 2016).

It is also found that some of the energy sources complement each other, such as when the sun is shining, precipitation is absent. It is also shown that for some locations sun and wind are complementary sources (Diaf, Notton, Belhamel, Haddadi, & Louche, 2008). For Norway, it is found that the expected annual variation in wind power production and hydro inflow are complementary, as shown in figure 2-12, which also illustrates expected annual consumption in Norway (Tande, 2006). The solar resource varies between different regions, especially

between north and south, coastal and inland. The coastal climate in the north of Norway results in highly fluctuating occurrence of precipitation, wind and sun (Dybdahl, 2016).
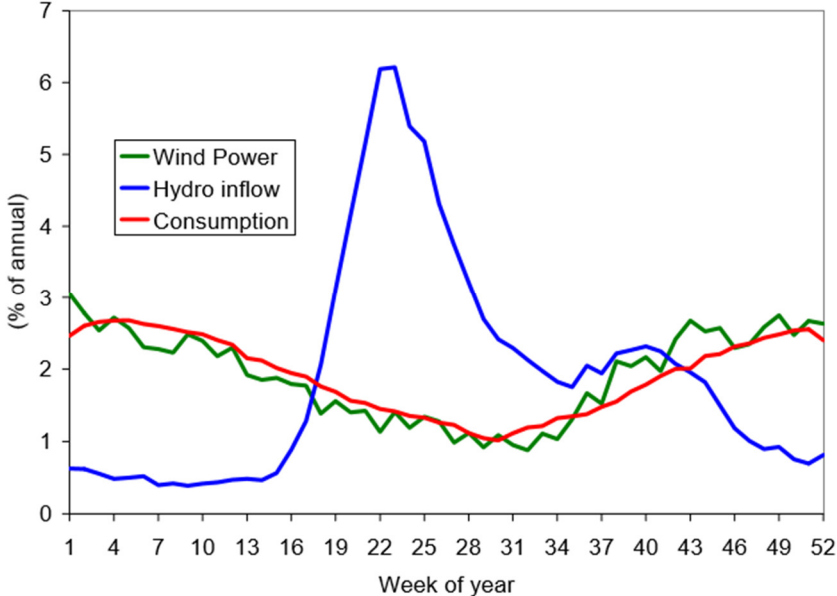
Figure 2-12 Estimated annual variation over the weeks of a year for wind power production, hydro inflow and consumption (Tande, 2006).

3 Sites of Interest

This chapter will provide information about the sites of interest, background for why this study was initialized, and evaluation of suitable locations for the renewable hybrid system components.

3.1 Senja

Senja is Norway's second largest island with its 1 589,35 km², located at the coastline about 69° north, well above the polar circle. There are about 8000 inhabitants, many of whom are relying on fishery and the seafood industry, and some on the growing tourism. The geological design of the island is mountainous with a vast number of fjords and valleys. This is probably the main reason for why there are so many distinct, small communities spread across the island. This thesis will have a main focus on two of these communities located at the north of Senja, namely Senjahopen and Husøy, which are located at the far end of the power distribution network. Such locations are often associated with challenges regarding voltage drops due to long power line distribution distances.

The scope of this thesis is in line with ARC's and Troms Kraft's cooperation project, called the Transformation to a Renewable & Smart Rural Power System Community RENEW, where solutions to Senja's network issues are sought. ARC is The Arctic Centre of Sustainable Energy, an interdisciplinary centre affiliated with UiT, Norway's Arctic University, and Troms Kraft is a local power company. Troms Kraft also has a similar project internally, called "Smart Senja", and both projects are evaluating innovative solutions to meet the increasing demand of power in a community where the power network is nearing its capacity. Methods as power flow control, cooperation agreements with customers about regulated purchase of power, usage of batteries and cooperation agreements with local power producers are considered (ARC, 2020). Also, alternatives for local power production and storage are considered, and that makes up the origin of this thesis. In the following chapters evaluation of a solar park, wind power and pumped hydroelectricity storage is done.

41

The map of Senja in figure 3-1 is used as a reference throughout this chapter, and all sites of interest are marked in the map and listed with description below.
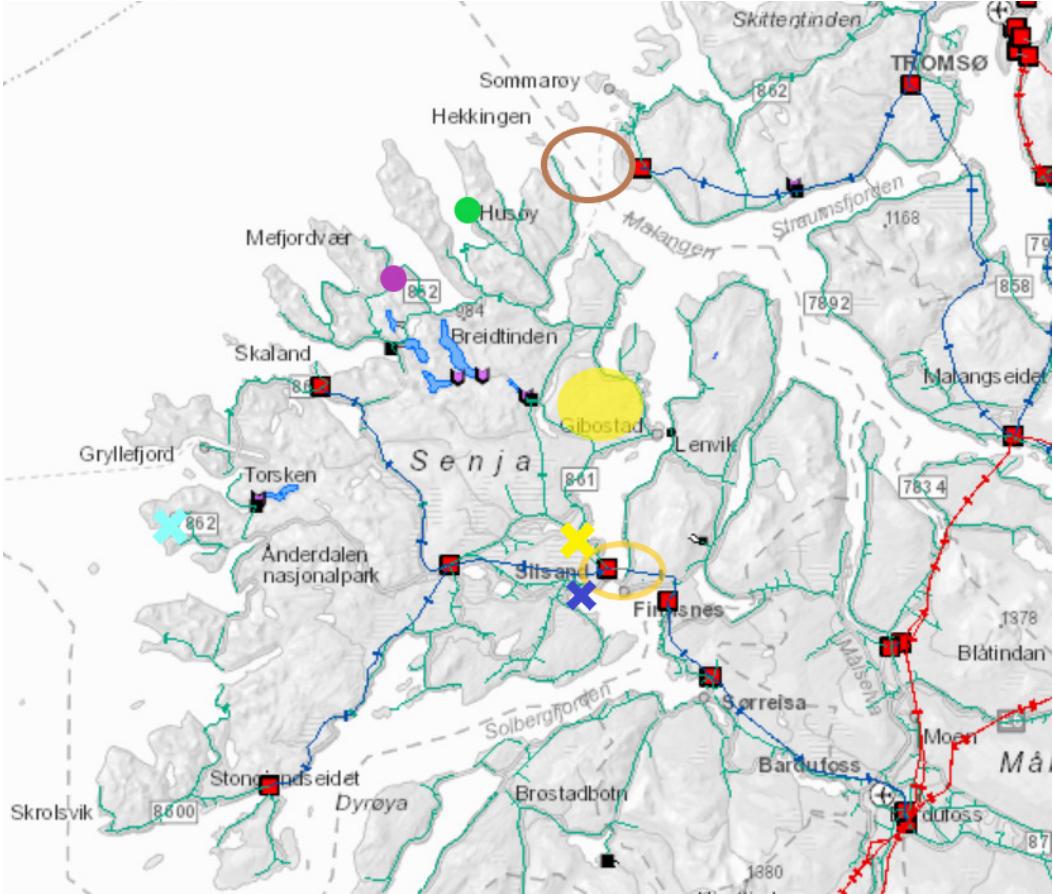
Figure 3-1 Map of Senja, showing all sites of interest (NVE Atlas, 2020).

- Lakes in blue: Existing hydro power plants
- Network in red: Central grid
- Network in blue: Regional grid
- Network in green: Distribution grid
- Red squares: Substations
- Circled orange: Network connection between Finnfjordbotn and Silsand
- Circled brown: Pre-registered supply line connection between Senja and Kvaløya
- Purple and green dot: Senjahopen and Husøy, respectively
- Yellow, filled circle: Snauheia
- Yellow cross: Pyranometer at Silsand
- Light and dark blue cross: Grunnfarnes and Laukhella measurement stations, respectively

3.1.1 Power Network and Consumption

The power supply network at Senja, shown in figure 3-1, is built by Troms Kraft Nett (TKN), the local network company. Most of the network was built during the 1950th and 60th, with some new networks, and some of the original have been significantly upgraded during its time (SKS, 2019). The age profile of the network is shown in figure 3-2.
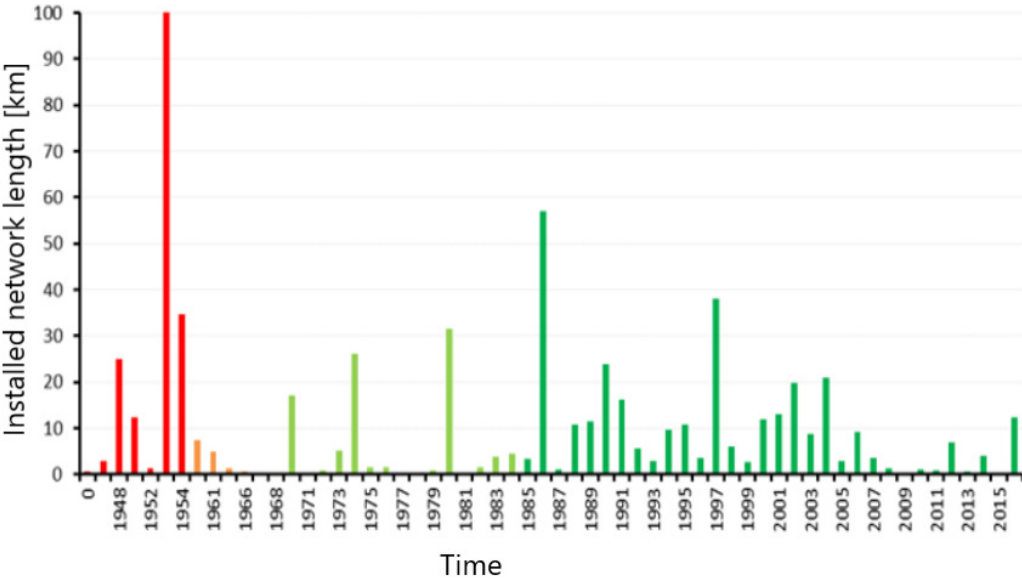
Figure 3-2 Age profile of the 22kV power supply network at Senja (SKS, 2019).

The power supply network is vulnerable due to long distances between supply and demand, and the 66kV regional network line from Finnfjordbotn, circled in orange in figure 3-1, is the only supply line from the mainland at the moment. This transmission line is nearing its capacity, and with growth in general at Senja, and especially rapid growth in the seafood industry, a solution to this power supply challenge must be found soon (SKS, 2019).

The seafood industry is a great power consumer, and the largest businesses at Senjahopen is Nergård, Aksel Hansen AS and Coldwater Prawns Production. At Husøy there is only one big player, Brødrene Karlsen AS (SKS, 2019). Examples of their part of total peak load demand is illustrated in figure 3-3, where it is also shown that residential power demand takes little share.
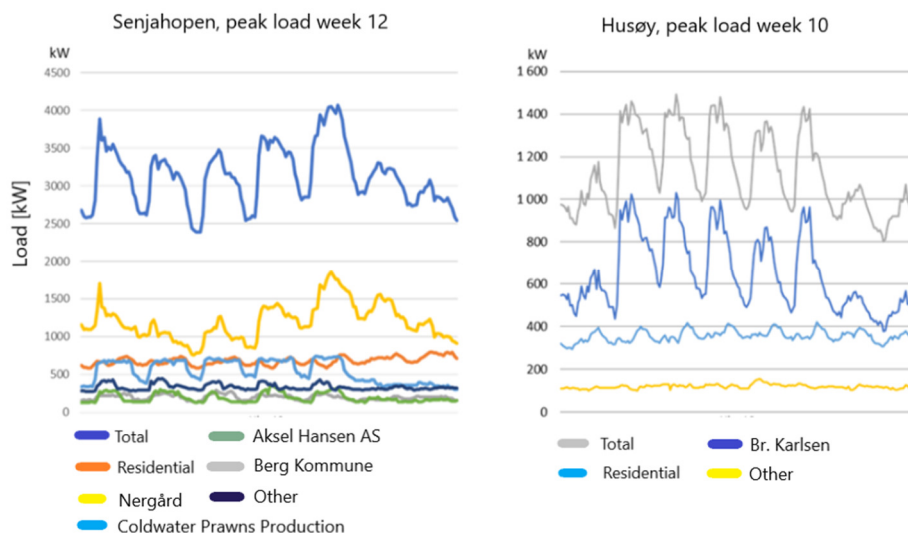
Figure 3-3 Load distribution at Senjahopen in week 12, 2018, and at Husøy in week 10, 2018 (SKS, 2019).

The 23rd of June 2020, NVE gave licence and an expropriation permission to TKN to replace the existing 66kV network line from Finnfjordbotn by a 132kV line, to increase the feeder capacity from the mainland. Also, a permission is given to install two transformers at Silsand substation (NVE, 2020). TKN has also pre-registered the construction of a new substation and a new supply line from the regional network at northern Senja, connected to the southern part of Kvaløya (SKS, 2019), circled in brown in figure 3-1.

Construction of a new regional network to Northern Senja and an upgrade of the distribution network is estimated to cost in the order of 45M€ (TKN, 2020b). This will obviously be realized in several steps, such as the two measures just mentioned, and it is desirable to postpone each step if possible. In the meantime, alternative, local solutions are being sought (SKS, 2019).

3.1.2 Surface Conditions

The surface conditions affect the reflected radiation, which has an impact on PV power production. Therefore, it should be thoroughly examined. Because of the mountainous geography at Senja, the surface conditions are diverse, as can be seen in figure 3-4. In general, the highest elevations are dominated by bare rock and heath land, while lower elevations of mixed and leaved forests, and for the eastern side also peat bogs.
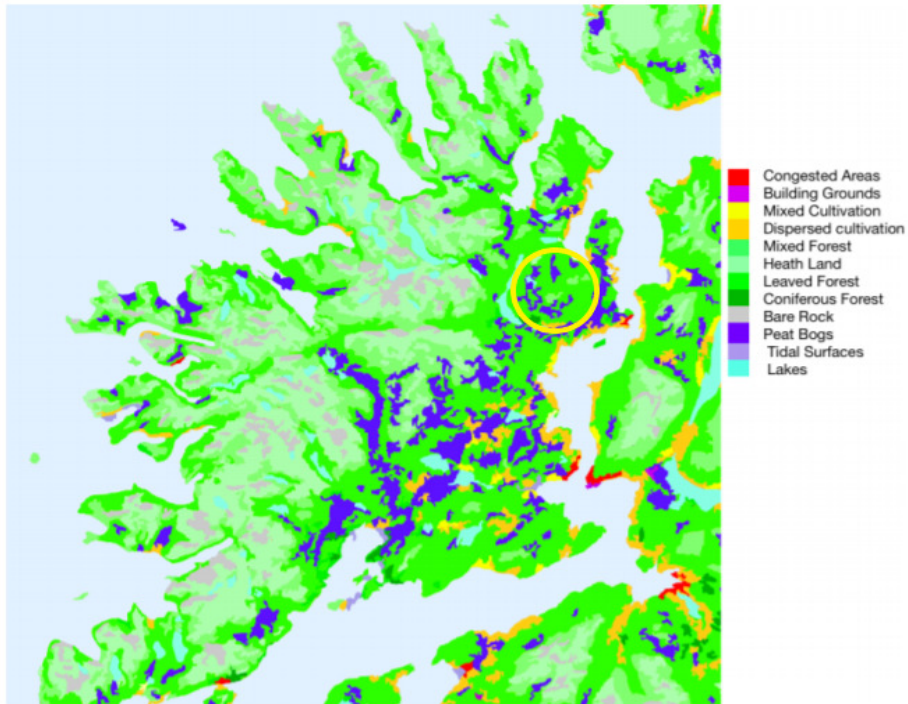
Figure 3-4 Surface conditions at Senja (Norgeskart, 2019). The area considered for PV in chapter 3-3 circled in yellow.

Due to the far north location of Senja, average temperatures are low, and winter temperatures are often below freezing point. This results in snow cover for significant parts of the year, as illustrated in figure 3-5. Figure 3-6 gives the average number of days with dry snow. The maps of snow cover are collected from seNorge, a public mapping service that is a cooperation between NVE, the Norwegian Meteorological Institute (MET) and The Norwegian Mapping Authority (Kartverket). Averages are for a reference period from 1971 to 2000 (seNorge, 2020).
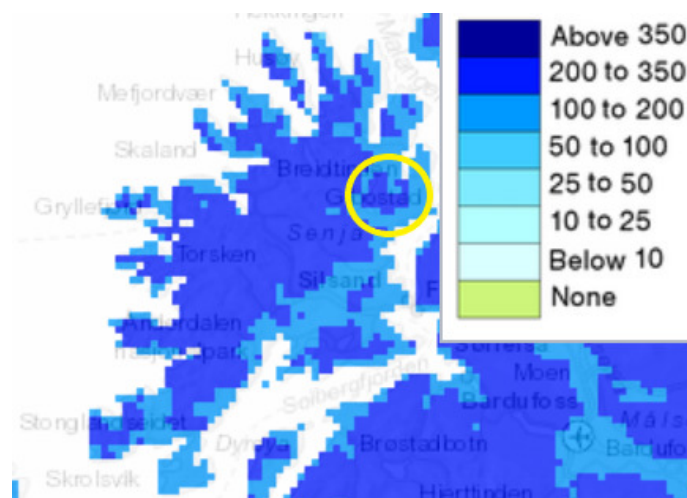
Figure 3-5 Average number of days annually with snow cover exceeding 5cm (seNorge, 2020). The area considered for PV in chapter 3-3 is circled in yellow
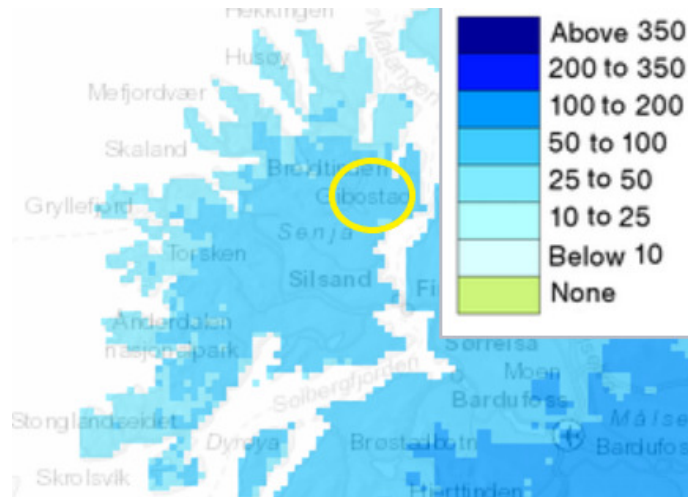
Figure 3-6 Average number of days annually with dry snow cover (seNorge, 2020). The area considered for PV in chapter 3-3 is circled in yellow

3.2 Existing Hydropower Plants at Senja

There are three already existing hydro power plants, all small sized, meaning < 10 MW installed effect, located at Senja; Lysbotn, Bergsbotn and Osteren power plant. They are all owned by a local power producer, Troms Kraft Produksjon (TKP), which is a sister company of TKN. Their locations are shown in figure 3-1.

Osteren power plant is the southernmost, and because it consists of only one magazine, with outlet to the ocean, it is unsuitable as a pumped power plant. Due to environmental restrictions, introduction of salt water in freshwater lakes is prohibited, hence Osteren power plant is not evaluated further. For the other two plants, it is beneficial for the power network and the communities at the far end of the network to have power production along the line, because this will counteract voltage drops. Nevertheless, production from these plants is regulated by optimal economical dispatch, so production does not necessarily happen when demand for power is high (SKS, 2019).

Figure 3-7 shows Bergsbotn and Lysbotn power plant, and the arrangement of their magazines are explained in the following sub chapters. Figure 3-7 also shows the power plant's precipitation fields, that boarders one another. The brown lines represent the local fields which are the most interesting, because precipitation that comes within those fields is drained down

to the lakes within the same field. The amount of drainage to each magazine depends on the area's geology. Bare mountains mostly will keep water on the surface until it reaches a lake, while marshlands might drain the water to the groundwater (NVE, 2010).
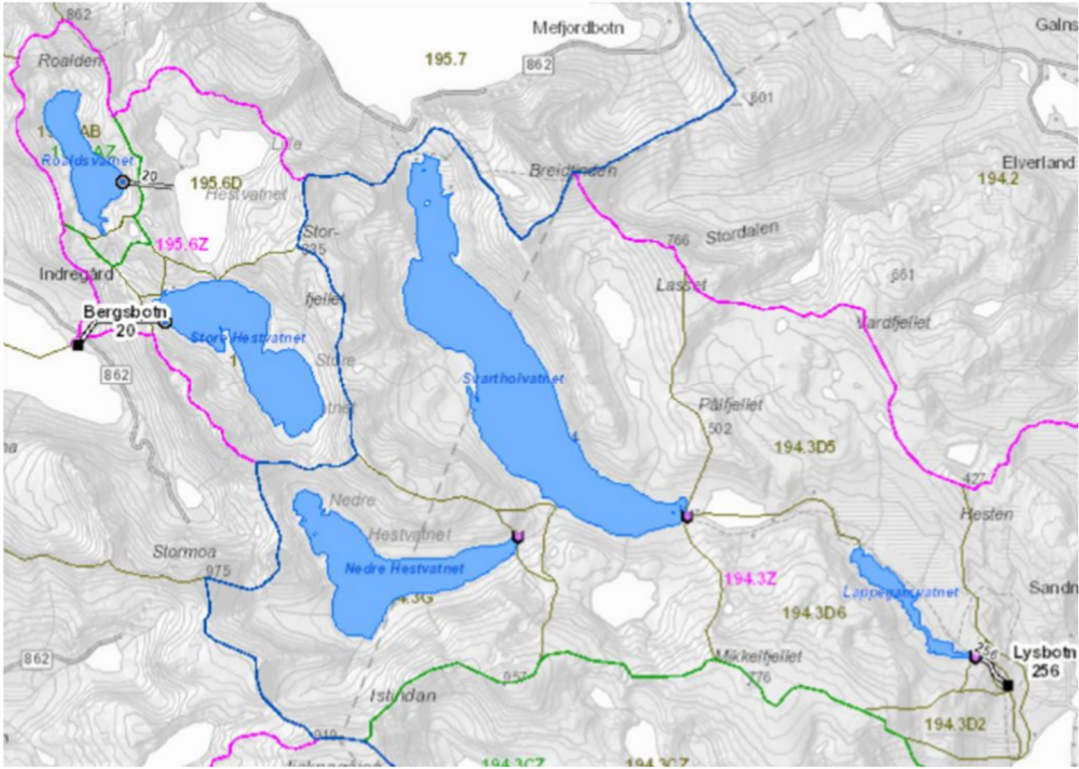
Figure 3-7 Magazines and precipitation fields of Bergsbotn power plant (left) and Lysbotn power plant (right), where the blue line shows the border between the plant's precipitation fields (NVE Atlas, 2020).

3.2.1 Bergsbotn Power Plant

Bergsbotn power plant was built in 1986, it has a head of 353m and a magazine capacity of 21.58 GWh. It has a production of 26 GWh, installed power of 7.9 MW, and an energy equivalent of 0.843 kWh/m^3 (TKP, 2020). It consists of three lakes, two of which are regulated magazines, and their characteristics are shown in table 3-1.

Table 3-1 Characteristics of Bergsbotn magazines (TKP, 2020).

Lake name:	Magazine volume [Mm^3]:	HRW [masl]	LRW [masl]
Roaldsvatn:	3.69	435.5	427.5
Store Hestvatn:	20.02	360.5	349.5

The highest magazine is Roaldsvatn, which has a manually regulated sluice gate. From there water flows to an unregulated lake, Lille Hestvatn, before it enters the lowest magazine, Store Hestvatn. Water from Store Hestvatn flows through a Francis turbine before it ends up in the ocean.

Bergsbotn is located at the north of Senja, along the distribution network which supplies Senjahopen, and it is an important player to maintain an adequate voltage level at the end of the network.

3.2.2 Lysbotn Power Plant

Lysbotn power plant was first built in 1936 but was replaced by a new plant in 1991. It has a head of 112m and a magazine capacity of 21.59 GWh. The installed power is 5.4 MW, the energy equivalent is 0.215 kWh/m^3 (TKP, 2020) and the production is 28 GWh. The plant is located at the northern part of Senja and is connected to the power distribution network which supplies Husøy. Therefore, when production occurs, Husøy and the rest of that network experience less voltage drops (SKS, 2019).

Lysbotn power plant consists of 4 lakes, 3 of them are regulated, and there is one Francis turbine from the lowest dam. The highest magazine is Nedre Hestvatn, which has a manually regulated sluice gate. The middle magazine, Svartholvatn, has a sluice gate that can be regulated from the control room at TKP (TKP, 2020b). The lowest magazine is also the smallest one, named Lappegamvatn. Between Svartholvatn and Lappegamvatn is another lake, named Mellomvatn, that is not regulated. The water that flows from Lappegamvatn through the turbine ends up in another freshwater lake, Lysvatn. Table 3-2 presents the characteristics of Lysbotn magazines.

Table 3-2 Characteristics of Lysbotn magazines (TKP, 2020b).

Lake name:	Magazine volume [Mm^3]:	HRW [masl]	LRW [masl]
Svartholvatn:	26.88	203.2	197.55
Lappegamvatn:	0.72	152.25	150.25
Nedre Hestvatn:	11.5	312.25	306.25

3.2.3 Alternative Power Regulations Exploiting the Hydropower Plants

As mentioned earlier there are strict regulations in the power marked to avoid network distributors to exploit their monopoly, and because TKN and TKP are sister companies they are subject to several regulations. There is a possibility though, for the companies to enter into a private law agreement about power support. Both Lysbotn and Bergsbotn have significantly installed power, and their locations are very suitable for voltage regulations for the distribution networks supplying Husøy and Senjahopen. A typical agreement includes the amount and effect that the producers at any time must be able to deliver, to be able to help in times of potential capacity challenges. This method is evaluated to be very effective according to the smart infrastructure concept study for Senja (SKS, 2019).

It is also possible to assure available capacity from the flexibility marked by entering an agreement between TKN and Ishavskraft, its sister company which is a local power distributor company. Such agreement would be based upon Ishavskraft committing to a minimum available flexibility in the marked, and the agreement can have a duration from weeks up to a year, depending on expediency (SKS, 2019).

3.3 Solar Power Plant Location

In Troms Kraft's project "Smart Senja", solar power has been discussed. Several different solutions have been proposed, such as PV installations at Husøy and Senjahopen. Local power production as this could help to avoid voltage drops, but there are some challenges considering installation area. What is considered the most optimal placement for small scale installations in the final report for the Smart Senja concept study, is roof top areas (SKS, 2019). Concerning the scope of this thesis, the size of such areas will not be sufficient for solar power production to drive a hybrid system of the scale evaluated.

For a large-scale solar power plant, the land area should be somewhat smooth, without too much vegetation that could cause shadings. It should be easily accessible for maintenance and situated close to the power network for which it will be connected to. When located at high latitudes at

the northern hemisphere, the most optimal position of the PV panels to assure maximum annually power output, is south facing with a relatively steep inclination angle. In case of a sloped surface, it should therefore be decreasing southwards, to avoid shadings from the PV panels in front.

3.3.1 Snauheia

After a careful evaluation of the topography and surface conditions of northern Senja, the location chosen for PV evaluation in this study is Snauheia, marked with a yellow, filled circle in figure 3-1.

Snauheia is uninhabited, and as can be seen from the map, it is situated close to the hydro power plants considered for PHES in chapter 5.1, and the power network is surrounding the area. The terrain is relatively flat, and as can be seen in chapter 3.1.2 it mostly consists of mixed or leaved forest and some peat bogs. Snauheia is situated around 300masl, with the highest point at 344masl, and there are several forest roads leading up the hill. In addition to the previously mentioned benefits of this location, it is also partly hidden from the public eye and the elevation probably causes more wind that can work as a cooling mechanism for the PV modules. Also, as can be seen in chapter 3.1.2, the snow cover lasts for a long period, with high amount of dry snow, which is beneficial for the albedo effect.

3.3.2 Solar Irradiance Potential

UiT has installed two pyranometers at Senja in late 2018, one located at Husøya and one at Silsand. The latter is situated closest to the location of interest, so only measurements from this is utilized in this thesis. It was installed at the end of 2018 in conjunction with the Smart Senja project, and it is mounted on top of a roof, free from shadings, and measures global horizontal irradiation, GHI. The coordinates of the pyranometer are 69.26° N, 17.93° E, and it is marked in the map in figure 3-1. The pyranometer is a thermophile pyranometer, which is known for

great accuracy, and the one installed at Silsand is an Apogee-SP510s, with measurement insecurity reported to be ± 5% (Apogee, 2018).

Since GHI has not been measured at Senja before 2018, a study was performed by T.T. Jacobsen in 2019 (Jacobsen, 2019) to evaluate solar irradiation potential at Silsand at Senja. Silsand is situated only about 14 km south of Snauheia, so it is expected to have somewhat similar potential. In the study, measurement data was collected from Holt in Tromsø, the closest GHI measurement station that has performed measurements over a period of several years. Holt is situated about 50km northeast of Snauheia, and the climate at Snauheia and Holt is relatively similar (MET, 2020). Even though, since Silsand and Snauheia are located further inland than Holt, it is expected that the solar irradiance might be a bit higher due to less clouds than at Holt.

In Jacobsen's study, measured data from Holt for the year 2017 was compared to simulated data from a reanalysis dataset developed by the European Centre for MediumRange Weather Forecasts (ECMWF). The ECMWF reanalysis 5, ERA5, was used, which has a 31 km spatial resolution. By statistical analysation by the Pearson correlation and bias, it was found that the ERA5 reanalysis dataset had a very high yearly correlation to the measurement data for most part of the year. The bias also showed little deviation, and the simulated data only overestimated the measured data by 3,7%. An evaluation of the year 2017 was also performed by comparing it to the other years where measurements have been done. This evaluation was a bit weak since there were only seven years of measurements. Even though, for this period 2017 showed a 5.9% higher GHI than the average.

Based on the findings in Jacobsen's study, it was chosen to scale the ERA5 modelled data for Silsand by 95%, and the final yearly GHI then amounted to about 747.5 kWh/m^2 (Jacobsen, 2019). A similar GHI value is therefore expected for Snauheia.

3.4 Wind Power at Senja

Wind power has been considered at several occasions for Senja, and also mentioned in the final report for the Smart Senja concept study (SKS, 2019). The coastal area of Northern Norway has good potential for wind power. Due to the complementation to solar resources, it

is considered a promising element in a renewable hybrid system containing a PV plant at Senja. Nevertheless, wind power has not been the focus of this thesis, so as an equivalent for wind resource potential, data from Fakken wind park at Vannøya is utilized in this study.

Fakken wind park is located about 120 km North-East of the two hydro power plants at Senja considered for PHES in chapter 5.1, as shown in the map in figure 3-8. Fakken wind park was built in 2012, consists of 18 Vestas V90 wind turbines of 3 MW each, which makes up an installed capacity of 54 MW. Each tower has a height of 80 metres, and the radius of the blades is 45 metres. The power plant's production is 130 GWh, and the owner is TKP (TKP, 2020).
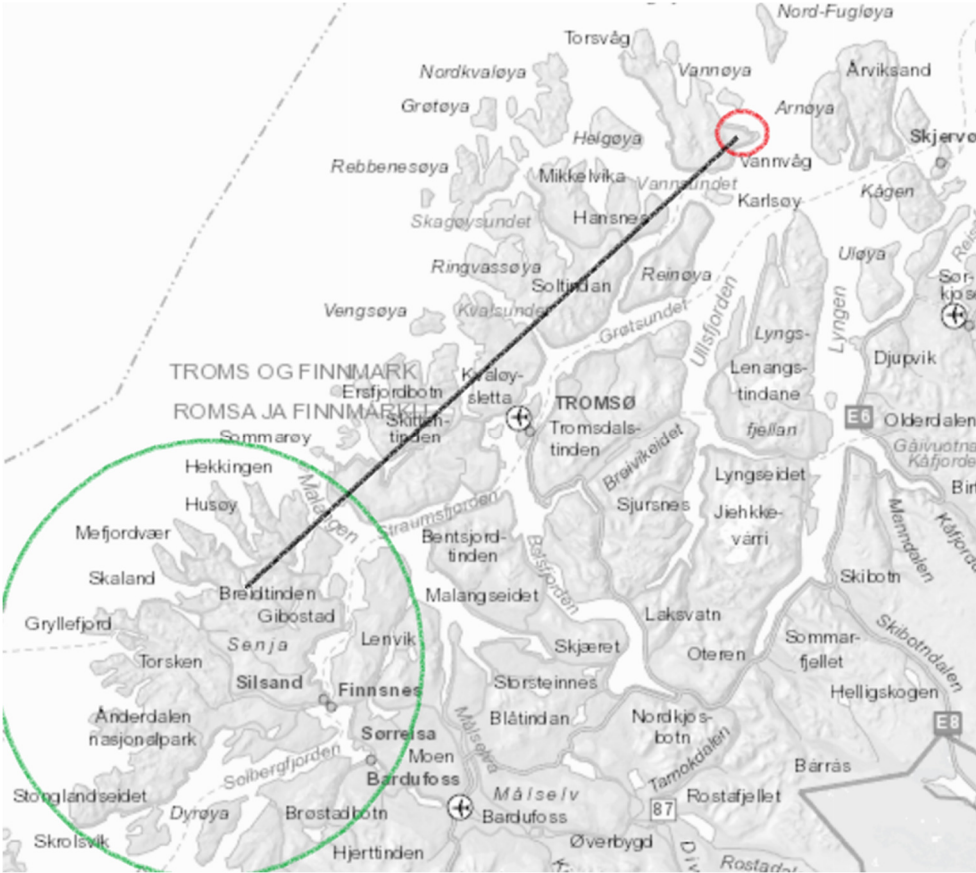
Figure 3-8 The location of Fakken wind park, circled in red, relative to Senja, circled in green. The black line connecting Fakken wind park and Bergsbotn/Lysbotn power plant measures about 120km (NVE Atlas, 2020).

4 Data and Method

Different methods have been used to evaluate PHES potential, solar power potential, wind power potential, and hybrid system solutions. The following chapter describes all methods utilized, as well as which data is used in the study and evaluations of the different components in a renewable hybrid system, and from whom the data is provided.

4.1 HOMER Pro

The main tool in this analysis is the Hybrid Optimization Model for Multiple Energy Resources, HOMER Pro, developed by the National Renewable Energy Laboratory, NREL (HOMER, 2020). This is one of the most widely utilizes software's regarding analyzation of complex renewable energy systems. It provides opportunity to implement several power technologies and analyse their behaviour. HOMER Pro holds a library of numerous system components and gives access to several weather resource data and modelling possibilities. It also provides opportunity for importation of measured data, as well as data from PVSyst, the software used to evaluate PV systems, explained in chapter 4.5. HOMER Pro also has an optimization tool, which can calculate, based on preference, best price, most optimal number of components, best cycle charging for storage etc. The disadvantage of the software is that it provides restricted access to the coding, so the user has little ability to interact or debug if preferred.

4.2 Provided Data Regarding PHES

TKP has provided data, given as Excel files, from locations and time periods requested to evaluate PHES potential at Senja. These data include production from the three power plants during 2018, and water levels for all magazines during the same year. To evaluate whether 2018 was a normal year regarding precipitation and water inflow, data was provided by TKP and

MET. TKP provided annual production data, given in GWh, for all the hydro power plants for the last 7 years, shown in table 4-1.

Table 4-1 Annual production in GWh for the hydro power plants at Senja for the last 7 years (TKP, 2020b).

År:	2013	2014	2015	2016	2017	2018	2019
Bergsbotn:	22.9	25.8	31.2	23.0	27.1	28.3	28.7
Lysbotn:	27.7	29.9	28.2	25.0	30.1	25.7	30.4
Osteren:	12.4	13.2	16.2	14.1	15.5	13.1	15.1
Sum:	**63.0**	**69.0**	**75.5**	**62.0**	**72.7**	**67.1**	**74.3**

From MET, precipitation data was received for two measurement stations, listed in table 4-2. Figure 4-1 illustrates precipitation deviation from the mean given in ml for the two stations that have measurements for 2018. The mean values are calculated from a reference period between 1961 and 1990, and for stations installed during, of after, this reference period, the mean is estimated by interpolation and usage of nearby situated stations. This is the situation for both stations considered, and their location is shown as blue crosses in the map in figure 3-1.

Table 4-2 Precipitation measurement stations information (MET, 2020)

Station number:	Station name:	Measurement	Masl:
88200	Senja – Laukhella	Aug 1997 – c.d.	9
88460	Grunnfarnes	Sep 1986 – c.d.	3
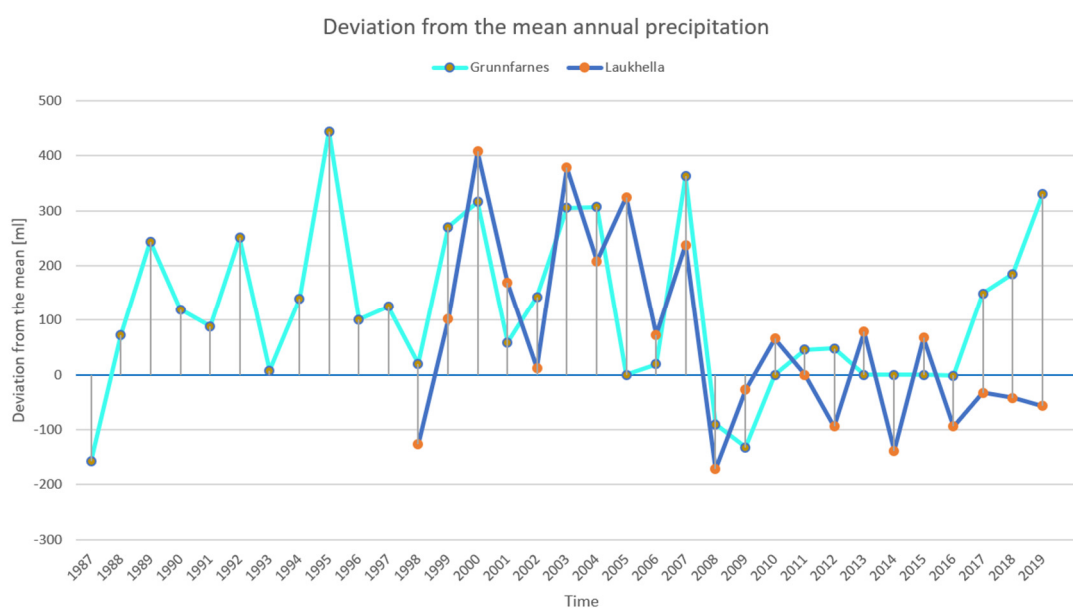
Figure 4-1 Precipitation deviation from the mean for Grunnfarnes and Lauhelle measurement stations (MET, 2020)

54

4.3 Method for Evaluating PHES Potential

TKP has provided all information needed regarding the hydro power plants of interest. Measurement data for registered water levels over the year 2018 was provided as Excel files, and there were some errors in the data sets that were corrected for as follows:

Magazine volume was missing for one lake, Lappegamvatn at Lysbotn, so an estimation is done by calculating the volume based on magazine height and lake area at HRW provided by NVE Atlas. This will obviously be an overestimation, since lake area at LRW will be smaller, so this must be kept in mind if Lappegamvatn should be considered further.

Since there are no available information regarding lake area at LRW for any of the magazines, a simplification is done regarding magazine volume for all lakes. Equal volume is assumed at each level of magazine height between LRW and HRW. This will cause some error since volumes in fact will be greater at higher levels. Values are missing for water level data at Roaldsvatn, Bergsbotn, 9/9-23/9 and Nedre Hestvatn, Lysbotn, 7/9-23/9. A mean is taken from the last day before and the first day after the gap in the measurement data and filled into the data gap. Some data points were obviously wrong, creating huge spikes. Such errors where erased using the quartile method (Dawson, 2017) and replaced by taking the mean between the hour before and the hour after the error.

Dates for adjusted data includes;

- For Nedre Hestvatn, Lysbotn: 15/1, 14/3, 18/4, 28/6, 26/10, 27/10, 28/10, 7/11, 22/12, 23/12, 25/12, 31/12. For the first 11 days of January there seems to be an error resulting in low water height, but since there is no data before this period it is left unadjusted.
- There are also periods with rapid water level change for Svartholvatn, Lysbotn, specifically for the 18/4, 22/4 ad 23/4. However, there are no obvious hourly errors, so no adjustments are done for those periods.
- For Lappegamvatn, Lysbotn, no adjustments are made.
- For Roaldsvatn, Bergsbotn: Several rapid water level changes occur, but no obvious errors, so no corrections are made, except for the previously mentioned missing data.
- For Store Hestvatn, Bergsbotn: 1/1, 2/1, 3/1, 15/1, 5/8 and 28/8.

Using the cleaned data, an analysis of available storage capacity is done in Excel. The amount of residual volume in the magazines and possible energy output from this storage capacity is calculated. For all designs where a new turbine would have to be installed, the plant efficiency is set to 0.90, and pumping efficiency to 0.85. These values are based upon good state-of-the-art values introduced in chapter 2.2 and 2.3 and are further used to calculate the energy equivalent for specific construction. The results are presented in graphs constructed in Python.

4.4 Provided Data for The Solar Power Plant Evaluation

UiT provided access to an online data base for measurements from the pyranometers at Senja. Data from the pyranometer at Silsand was downloaded as an Excel file for the last 12 months, with hourly resolution. The data is presented as a graph in figure 4-2. However, it was reported by Boström and Hardersen at UiT that there had been some issues concerning measurements, so the data has gaps and is incomplete (UiT, 2020).
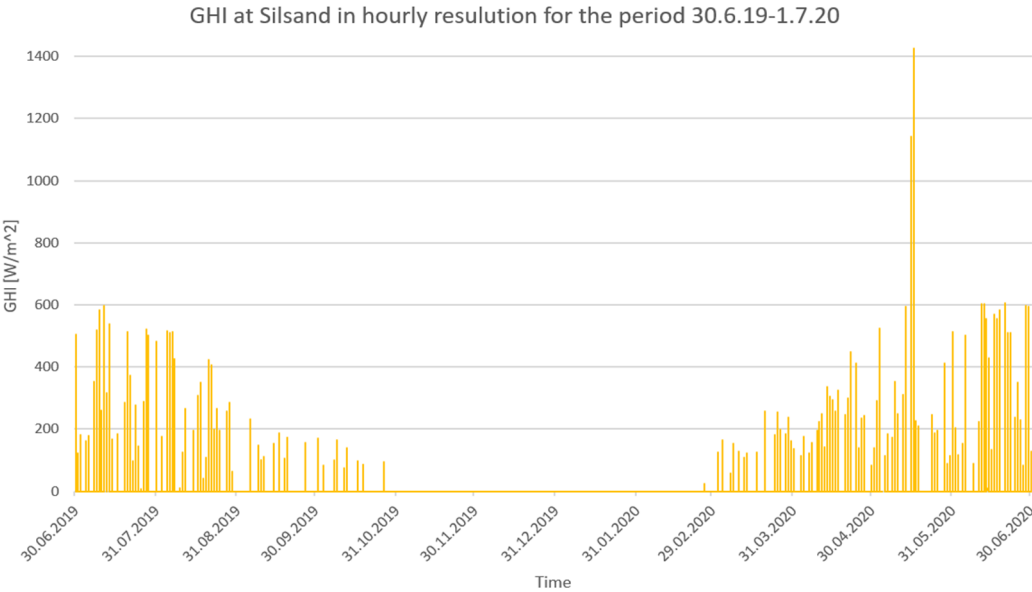
Figure 4-2 GHI from the pyranometer at Silsand for the period 30.6.19-1.7.20.

MET provided meteorological data for an evaluation of temperature and cooling effect from wind at the location considered. It was given access to modelled data of Senja from the software

NORA3. NORA3 is produced by downscaling <u>ERA5</u>, using the non-hydrostatic numerical weather forecasting model HARMONIE-AROME (Cy 40h1.2) (MET, 2020b). Also, a Matlab code was provided for easier evaluation of the data.

4.5 Method for Evaluating Solar Power Potential

Solar irradiation data from <u>UiT</u> was evaluated using Excel. It was found that out of 8760 cells, 69 where empty, corresponding to 0,79%. Those where filled in using the average value of the cell before and after. Also, a few unreasonably high values were calculated using the quartile method (Dawson, 2017) , and four outliers were found for two data points at the 15th and two for the 16th of May 2020. Those where corrected for by replacing them with the average value of the cell before and after. The period between the 15th and 21st of May contained several cells showing 0 GHI during daytime, which is highly unlikely. Such cells where replaced by measurements for the same hour of the day before or after. The errors from corrected data must be kept in mind when evaluating the results. However, even after cleaning the data set, the errors where still so severe that it was chosen to utilize modelled <u>GHI</u> instead.

<u>HOMER</u> Pro also has a PV evaluation tool, but it is restricted regarding system design, input values, output parameters etc. Therefore, the software PVSyst is used instead for a more thoroughly PV evaluation. This is a software designed to be used by architects, engineers, and researchers (PVSyst, 2020). The output can easily be imported to <u>HOMER</u> Pro to combine with other energy sources and further evaluation.

PVSyst access importation of meteorological data from software's such as Meteonorm, NASA-SSE, PVGIS TMY and NREL/NSRDB. PVSyst states that there are big discrepancies between these databases since methods and models differs between the software's. An annual available irradiation comparison between 7 different meteorological software's is performed by PVSyst for different locations. For Europe this shows that all software's compared agree within 10% of the average. Of the ones most often close to the average is Meteonorm 7, not systematically over- or underestimating (PVSyst, 2020b). Meteonorm 7.2 is therefore chosen for the evaluation in this thesis.

The coordinates chosen for input in PVSyst is 69.3744°N 17.9146°E, which is a bit south of the top of Snauheia. This to ensure being on the side of the hill descending in the southward's direction, and the altitude here is 335masl.

To ensure correct sizing of the system, default temperature values are corrected for after an evaluation of provided temperature data from <u>MET</u> (MET, 2020b). Using the Matlab code provided, the lowest and highest estimated temperature from NORA3 is -22.9°C and 30.43°C, respectively. Values are rounded to -23°C and 31°C. Usual operating temperature for winter and summer time is set to average temperatures for those months; -4°C and 3°C, respectively.

The last parameter edited from default is the constant loss factor, which is originally set to a roof mounted system value of $20W/m^2K$. The value should be higher for "free" mounted systems where the air circulation is good, as is the case for the location evaluated here. Evaluating wind speed and temperature from NORA3 (MET, 2020b), the cooling effect is ought to be good. The constant loss factor is therefore set to a $29W/m^2K$, as suggested by PVSyst for ""free" mounted systems with good air circulation".

For the location, a mono facial PV power plant is simulated for 1 MW, 5 MW and 10 MW. The type of panels chosen for the evaluation is commercially established and commonly installed panels produced by JinkoSolar (NYSE: JKS). JinkoSolar was the world's largest solar panel manufacturer in 2018 (pv-tech, 2019). They distribute their products to utility, commercial and residential customers in over 80 countries around the globe (JinkoSolar, 2020). The model chosen for this system is 370Wp 34V Si-mono JKM 370M-72-V, whom have an efficiency of 21.76%/cells area and 19.17%/module area, which is a state-of-the-art value.

Inverters are also chosen from a commercially available producer, ABB, who is also well established in Norway (ABB, 2020). A sensitivity analysis is done for each PV system to decide for inverter size, model and number of inverters to be used.

By entering the PV system's desired power output, PVSyst calculates the amount and area of modules needed, as well as number of strings and ideal inverter size.

PVSyst's optimization tool is utilized to decide on orientation input. A sensitivity analysis is also performed upon this.

A set of usual albedo values are listed in PVSyst, and it gives opportunity to set the value for each month. As can be seen in chapter 3.1.2, Snauheia consists mostly of leaved and mixed forest, and some heat land. There are also areas of peat bogs, but it is unreasonable to install PV systems there. The area considered is also normally covered in snow for between 100 and 200 days each year, where about half of those the snow is dry. Based on this, the albedo values considered from PVSyst are listed in table 4-3. Some values from the software Solargis are also included (Solargis, 2020), since PVSyst lacked values for forests.

Table 4-3 Typical albedo radiation values from PVSyst and Solargis (PVSyst, 2020; Solargis, 2020)

Surface type:	Albedo value from PVSyst:	Albedo value from Solargis:
Fresh snow:	0.82	0.80-0.90
Wet snow:	0.55-0.75	-
Snow:	-	0.40-0.90
Grass:	0.15-0.25	-
Fresh grass:	0.26	-
Green grass:	-	0.20-0.25
Conifer forest (summer):	-	0.08-0.15
Deciduous trees:		0.15-0.18

Albedo settings are based on the values from table 4-3 and the overview in chapter 3.1.2. Days of snow for Snauheia is in average between 100 and 200, or between about three and seven months. About half of those are of dry/fresh snow, having an albedo value of about 0.835 when averaging the values from PVSyst and Solargis. The average value for other types of snow is 0.65 from both PVSyst and Solargis.

In this evaluation it is chosen to set albedo values to 0.85 for the winter months December through April, and 0.5 for November and May. For the other months it is chosen to use the default value of 0.2, since values for gras and forests from table 4-3 ranges from 0.08 to 0.26, and it is hard to decide on the exact vegetation for the area chosen.

A sensitivity analysis is performed for albedo inputs for the 1 MW systems. Worst case scenario is set to a default of 0.2 for the whole year, and best-case scenario is set to 0.9 for November through May and 0.2 for the rest of the year. Also, two average settings are evaluated, using the average value between fresh and other types of snow, 0.74, throughout the winter. Days with

fresh and wet snow might occur randomly for the period, and the duration of snow cover might last between 3 and 7 months. The value of 0.74 is therefore tested for 5 and 7 months. 3 months would probably overlap with the period of polar nights, so this will correspond to the worst-case scenario with a constant albedo value of 0.2.

4.6 Provided Data from Fakken Wind Park

TKP provided wind resource data from Fakken wind park, given as measured wind speed data with 10-minute resolution. The anemometer is situated 80 metres above ground at a meteorological mast. The data was given as an Excel file for the time period requested and had no empty cells or other errors.

4.7 Method for Evaluating Wind Power Potential

The main focus in this thesis is on pumped hydropower and PV, but to obtain a state of near self-sufficiency at Senja, wind power is also implemented. The evaluation is done quite briefly by utilizing wind resource data from Fakken wind park as an equivalent wind resource data for evaluated wind power production at Senja. The data from Fakken wind park is used mainly because it was easily accessible, with good resolution and it is considered so that it makes a fairly good equivalent for a North Norwegian coastal wind resource.

The measured data from Fakken wind park was imported, without any corrections, to HOMER Pro for evaluation. A wind turbine of the same size as at Fakken wind park, 3 MW and 80m hub height, was chosen for this evaluation. The model accessible in HOMER Pro of this size was Enercon E-82 E4, whom have a hub height of 84m.

4.8 Provided Data for The Renewable Hybrid System Evaluation

All previously mentioned provided data are used for the evaluation of a renewable hybrid power system at Senja. In addition, the already existing hydropower plants will be included. HOMER Pro demands monthly average water inflow, given as l/s, as input data for hydropower plants. TKP provided Excel files containing monthly averages given as GWh.

Load data is also needed to perform a simulation in HOMER Pro. Such data must be provided by TKN, but it is very time consuming to obtain such data. A PhD student at UiT had already been provided such load data for Senjahopen and Husøy for the period 1.3.2019 to 2.2.2020, with hourly resolution, and it was given permission to reuse this (UiT, 2020b).

4.9 Method for Evaluating a Renewable Hybrid System Potential

Three different renewable hybrid system designs were evaluated using HOMER Pro, one for each size of PV system. From PVSyst the results for each PV system was exported, and by using HOMER Pro's PVSyst wizard they were imported for evaluation in combination with the other components.

Measured wind and hydro resources were imported to HOMER Pro. HOMER Pro does not allow for implementation of more than one hydropower plant, so Bergsbotn and Lysbotn power plant had to be simulated as one plant, and the hydro resource hence had to be merged to one as well. With the already given energy equivalents for each power plant, the provided data given in GWh was recalculated to provide inflow given as l/s, before it was merged and imported to HOMER Pro. Only monthly average values could be simulated from this, so the production output from the hydropower plants will be flat each month, and not as fluctuating as in reality. The output production for this constructed plant was controlled against the total actual production from the power plants for this year, and a difference of only 1% was found. The hydropower plant was included in all simulations since it already exists, while the optimization tool was used for the wind turbines.

61

A firm evaluation of <u>PHES</u> potential was performed, and the option considered most suitable was added in the design. HOMER Pro has only one pumped hydro component, and since its size is of only 245 kWh, several such components had to be added until the total size was somewhat equivalent to the one desired. The chosen <u>PHES</u> system was included in all simulations, since this is one of the main components evaluated.

HOMER Pro requires load data for one year, so an estimate was produced from the provided data for Senjahopen and Husøy for the missing 26 days. A mean was calculated using the last 26 days of January 2020 and the first 26 days of March 2019. The data series also had to be manipulated to fit the period for all the other input data. The period from 1.1.20 to 2.2.20 was moved to the beginning of the series, to represent 1.1.19 to 2.2.19. Also, this data was only for Senjahopen and Husøy, whom is highly influenced by the seafood industry, so a simple scaling was performed by the following procedure: From Statistics Norway (<u>SSB</u>), information was collected regarding population and consume. The latest number for power consumption per household was 16 000 kWh in 2016 (SSB, 2018b). It was found that the total number of residents at Senjahopen and Husøy together was 605 in January 2019 (SSB, 2020). Regarding average number of persons per household, the number was 2,05 for Northern Norway, and 2.29 for sparsely populated areas (SSB, 2020). A mean was taken from these numbers, giving an estimated number of households at Senjahopen and Husøy to be 280, and 2128 for the ret of Northern Senja. Consumption for these households then amounted to an average value of 511 kW each hour, and this was subtracted from the total, yielding an average consumption for industry alone. The value for households will obviously be higher at wintertime and lower at summertime but considering that household consumption only makes up a small fraction of the total consumption, the deviation in household consumption during a year is not calculated. For the remaining consumption, mainly from the seafood players as shown in figure <u>3-3</u>, the consumption is normalized based on the seven players included and scaled up based on other industries at Northern Senja. These includes Skaland Graphite AS, Nord-Senja Fisk in Botnhamn, Akvafarm AS in Bergsbotn, Salmar Nord at Lysnes, Senja Fiskeri in Fjordgard, 2 kindergartens and 3 schools with associated pools. The scaling factor is hence set to 1.42. The total estimated consumption is then the sum of consumption for households at Senjahopen and Husøy, households for the rest of Northern Senja, industry at Senjahopen and Husøy, and industry at Senjahopen and Husøy multiplied by 1.42.

5 Results and Discussion

In this chapter, evaluations and results are discussed regarding pumped hydroelectricity storage, solar and wind potential for a combination in a renewable hybrid power plant system at Senja. The PHES option that is considered the most optimal is used further in the renewable HPP system evaluation, along with all three PV systems evaluated.

5.1 Possibilities for Conversion of Already Existing Hydropower Plants Into Pumped Hydroelectricity Storage

In this chapter, an evaluation of the possibility of converting already existing hydropower plants at Senja is performed. Production from all power plants are given in figure 5-1, but Osteren power plant was considered not suitable for conversion, so it is not evaluated further.
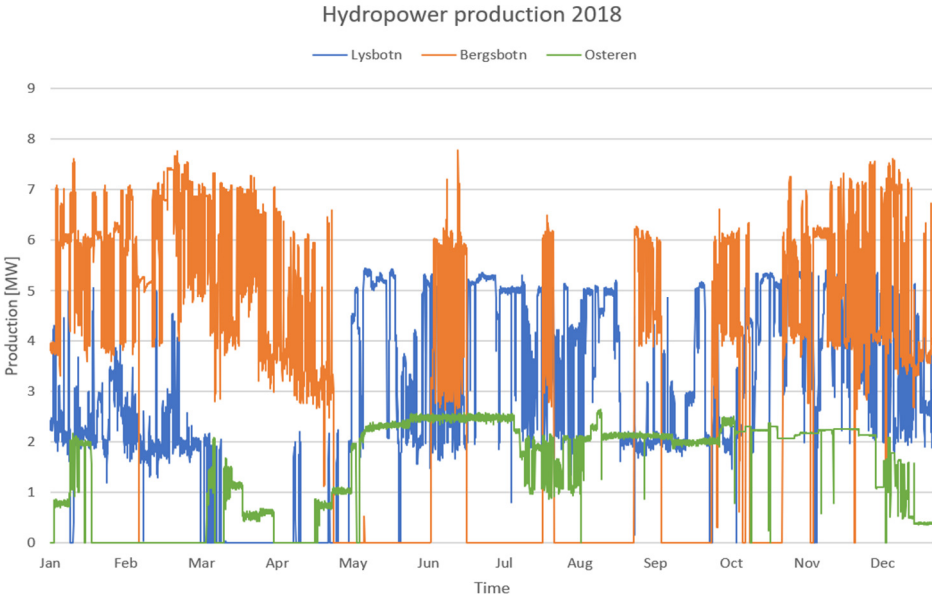
Figure 5-1 Mean hourly production from all hydro power plants at Senja in 2018

TKP provided all data requested, but there were several gaps and errors in the measurement data regarding water level, so corrections had to be made. Even after the corrections it is

suspected that there are periods regarding water levels that still holds errors, but it was concluded that these errors will not affect the results. The cleaned water level measurement data is presented as graphs in figure 5-3.
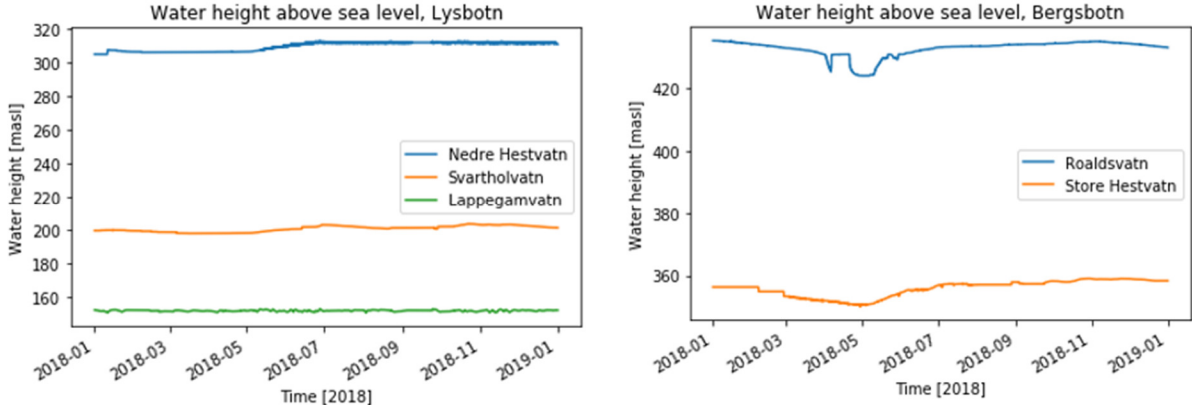
Figure 5-2 Water height above sea level for the magazines at Lysbotn and Bergsbotn power plant

When this evaluation was performed, the latest data regarding water levels was for the year 2018. Below, an analysis is performed to evaluate whether 2018 was a normal year regarding water levels at these hydropower plants.

5.1.1 Evaluation of 2018 as a Normal Year

Since only one year, 2018, is considered, an evaluation is done using provided data from TKP and MET, presented in chapter 4.2, to consider whether this was a representable year for hydropower at Senja.

As can be seen from table 4-1 in chapter 4.2, the mean annual production for Bergsbotn over the seven years given was 26.71 GWh. In 2018 the production was 28.3 GWh, which is a higher, but not an extreme value. For Lysbotn the mean annual production was 28.14 GWh, and for 2018 it was 25.7 GWh. Here it was a bit lower, but not extremely. Seven years is a short period to be used as an estimation for a mean annual production, and these values are not necessarily representative for the precipitation, due to the storage capacity. Water has most certainly been

stored from the year before, and from 2018 to the next year. Nevertheless, production within normal ranges points towards a normal year.

Precipitation measurements from the measurement stations at Grunnfarnes and Laukhella is illustrated in figure 4-1. These show that precipitation for 2018 at Grunnfarnes, which is located at the west coast of Senja, was 184.7 ml above the average of 1160 ml, which is only 16% higher. Laukhella is situated at the east side of Senja, and here 2018 was a bit dryer than normal, with 41.6 ml less precipitation than the average of 1000 ml, so only 4% lower.

For these measurements there are also some possible errors that needs to be kept in mind. Firstly, the annual mean precipitation for the measurement stations are for the period 1961-1990 and done by interpolation. New calculations will be done by MET in 2021 for the last 30 years. When calculating the mean from the actual measurements done for Grunnfarnes and Laukhella, 2018 is closer to the mean for Grunnfarnes and further away for Laukhella. Secondly, as can be seen in the map in figure 3-1, the measurement stations are located a bit south of the power plants, so even if Bergsbotn is located at the west side and Lysbotn at the east side of a mountain ridge, the local weather can differ substantially from that of the measurement stations. Even though, it must be mentioned that both the westernmost power plant production and precipitation measurements are a bit above average, while the easternmost power plant production and precipitation measurement are both a bit lower than the mean.

From the data provided, no concrete conclusion can be drawn, except that 2018 was not an outlier concerning either hydropower production or precipitation measurements from nearby measurement stations. 2018 might therefore be considered a relatively normal year with respect to precipitation.

5.1.2 How PHES Potential is Evaluated

Using provided data from TKP regarding water level, calculations are done in Excel, and graphs are constructed in Python to present residual volume in the five power plant magazines considered. Also, graphs are constructed to illustrate the amount of energy that could have been

generated if this residual volume would be used. These calculations are based on the calculated energy equivalent for each construction. The graphs for residual volume and the possible energy generation if this volume would be used, the residual volume energy content, will obviously have the same shape. The focus is on the unit on the y-axis, showing how much energy this volume could produce.

As mentioned in chapter 4.3, there are estimations and simplifications done that must be kept in mind. The water level data had some errors, there is only one year examined, and the energy equivalent is calculated based on a fairly good plant efficiency. Also, the magazine volumes will differ substantially if the power plants are converted into PHES, since pumping and generation will occur frequently in turn. The results occurring next must therefore be considered as rough estimates, as a way to investigate the possibility to utilize already existing magazines, and cannot be used as evaluation of total power output etc.

Equations used for the calculations for PHES are equation 2-4 for the energy equivalent, equation 2-6 for power input (P_{pump}), equation 2-2 for power output (P_{gen}), and equation 2-5 for the roundtrip efficiency (RTE).

All height and distance measurements in the following subchapters are collected from the public mapping service Norgeskart (Norgeskart, 2019).

It is worth reminding the reader that the graphs showing volume, are residual volumes, not actual volume. This to better illustrate the potential for pumping.

5.1.3 Results and Evaluation of Bergsbotn Power Plant as PHES

The results from figure 5-4, illustrating residual volume at Bergsbotn, show that the magazines here is at its lowest level during the months between March and June. This is consistent with the theory from chapter 2.2.3 about typical water levels in Norwegian magazines. Note that Roaldsvatn is for some period below LRW.
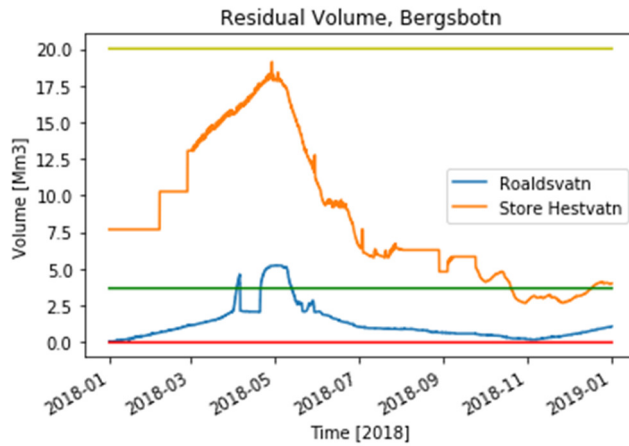
Figure 5-4 Residual volume, Bergsbotn. The red horizontal line represents volume at <u>HRW</u>, while the green and yellow horizontal line represent volumes at <u>LRW</u> for Roaldsvatn and Store Hestvatn, respectively

.

Since the lowest magazine, Store Hestvatn, has an outlet to the ocean, it is not suitable to pump water back up here because of environmental restrictions. If this power plant should be used for <u>PHES</u>, another turbine/pump or PaT must be installed at another location at the power plant. There are four suitable locations, as shown in figure 5-5, but two of these have the challenge that a permission to regulate Lille Hestvatn is required. It is worth noticing that the horizontal distance is the shortest distance measured on the map, and a longer distance might be required due to geological conditions. A summary for the different layouts is given in table 5-1.
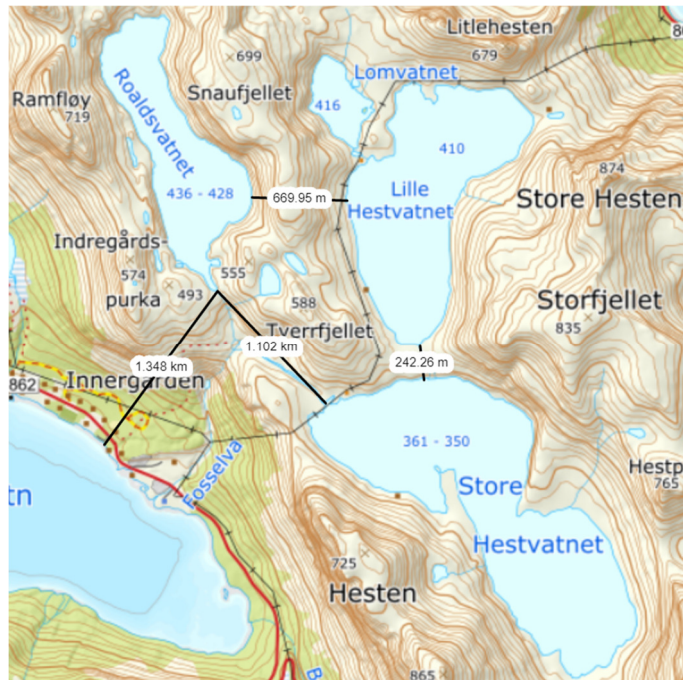
Figure 5-5 Four alternative layouts for using Bergsbotn power plant as PHES illustrated by black lines. The lines are giving the horizontal distance, and the height of the lakes are given by values in blue (Norgeskart, 2019).

Table 5-1 Summary for alternative layouts for using Bergsbotn power plant as PHES

Layout:	Horizontal distance:	Height difference	Combined volume:	Restrictive magazine:
Roaldsvatn – Store Hestvatn	~ 1102m	67m - 86m	23.71 Mm^3	3.69 Mm^3 (Roaldsvatn)
Store Hestvatn – Roaldsvatn - ocean	~ 1348m	67m - 86m /428m - 436m	23.71 Mm^3	3.69 Mm^3 (Roaldsvatn)
Roaldsvatn – Lille Hestvatn	~ 670m	17.5m - 25.5m	Above 3.69 Mm^3	Unknown
Lille Hestvatn – Store Hestvatn	~ 242m	49.5m - 60.5m	Above 20.02 Mm^3	Unknown

Since Lille Hestvatn is unregulated, it is challenging to estimate PHES potential for layouts involving this lake, since there is no knowledge about potential magazine volume, but for the solutions involving the two already regulated magazines the potential is promising. Except for the months around April and May in 2018, where both the regulated magazines are close to, and below, LRW, there is a considerable potential for PHES at Bergsbotn. Water could be regulated between the magazines without exceeding regulation limits, and for instance the period where Roaldsvatn was below LRW in 2018 could have been avoided. At the same time, this low water level may also be caused by the process of emptying magazines before spring snow melt flooding, so pumping in this period might not be feasible anyways.

One drawback for the designs involving Roaldsvatn is, however, that Roaldsvatn is a relatively small magazine, so the regulatable volume would be restricted by it. Also, the terrain between Roaldsvatn and the other two lakes are steep and challenging to access. For the layout between Roaldsvatn and Lille Hestvatn, there already exist a tunnelled water gate through the mountain, wide enough to fit a pump (TKP, 2020b). For the layout between Roaldsvatn and Store Hestvatn, a water way would have to be constructed, probably through pipes. This is a laborious process with great environmental impact that also would require permission, and the terrain is known to be avalanche-prone (TKP, 2020b). Environmental impact, economy and possible gain from this layout would therefore have to be considered thoroughly.

The other alternative for Bergsbotn power plant is to install a pump from Store Hestvatn, or Lille Hestvatn, to Roaldvatn, and a turbine at Roaldsvatn with outlet to the ocean. In this way

one could pump water higher up from an already high elevation, for instance at periods of surplus energy from PV or wind production. In that way one could gain more power from a higher energy equivalent when there is a deficit of production from other sources. The pumping height is then relatively small, between 17.5m and 25.5m from Lille Hestvatn, and between 67m and 86m from Store Hestvatn. The head between Roaldsvatn and the ocean is between 428m and 436m. Average heights are used in calculations.

Calculations are done for each PHES layout involving regulated magazines at Bergsbotn power plant, by using typical good efficiencies as explained in chapter 4.3. Plant efficiency is set to 0.90, pumping efficiency to 0.85, and a flow rate of 2.5 m^3/s. Because the same numbers are used in every calculation, the roundtrip efficiency will be approximately the same for all designs, except for when the pumping and the generating height is different.

Results for designs involving regulated magazines are given in table 5-2. Note that the RTE for the last two layouts will not be an actual round trip, and hence the value will be far above 100%.

Table 5-2 Design results for Bergsbotn PHES options

Design:	Magazine volume:	e:	Capacity:	P_{pump}	P_{gen}	RTE:
Store Hestvatn - Roaldsvatn	3.69 Mm^3 (Roaldsvatn)	0.171 kWh/m^3	0.63 GWh	2.01 MW	1.54 MW	0.76
Lille Hestvatn to Roaldsvatn to ocean	3.69 Mm^3 (Roaldsvatn)	1.056 kWh/m^3	3.90 GWh	0.62 MW	9.51 MW	15.34
Store Hestvatn to Roaldsvatn to ocean	3.69 Mm^3 (Roaldsvatn)	1.056 kWh/m^3	3.90 GWh	2.19 MW	9.51 MW	4.34

Based on the calculated energy equivalent from table 5-2, and the residual volume presented in figure 5-4, a graph illustrating "residual volume energy content" is constructed. The graph shows the energy that could have been produced if Roaldsvatn was filled, both for outlet to Store Hestvatn and outlet to the ocean and is shown in figure 5-6.
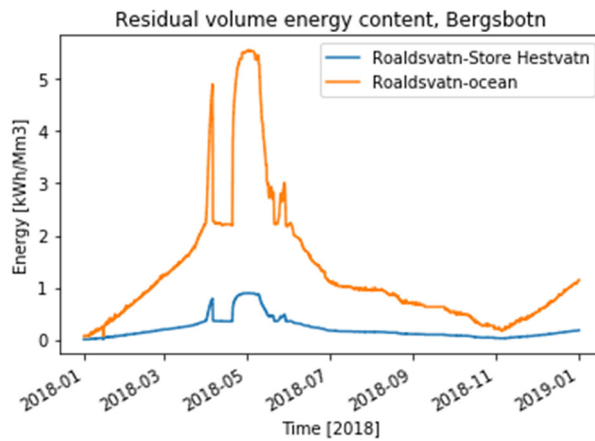
Figure 5-6 Residual volume energy content for Roaldsvatn at Bergsbotn power plant, with energy equivalents calculated in table 5-2.

The energy equivalent is 25% greater at Roaldsvatn than at Store Hestvatn, so if the pumping process is done in times of surplus energy, this could have been a feasible solution. The big drawback here is that Roaldsvatn is relatively small, and there is also no guarantee that surplus energy will occur. Additionally, there is already a turbine installed at Store Hestvatn, which relies on the water content from both Lille Hestvatn and Roaldsvatn, so it would probably not be feasible to have two parallel turbines with outlet to the ocean.

A last alternative solution for Bergsbotn power plant, is that a pump, PaT or reversible turbine could be installed between Bergsbotn and Lysbotn power plant. This could either be between Store Hestvatn and Nedre Hestvatn or Store Hestvatn and Svartholvatn. This option is discussed further in the section for results and discussion about combining Bergsbotn and Lysbotn power plant.

5.1.4 Results and Evaluation of Lysbotn Power Plant as PHES

The results for residual volume at Lysbotn power plant is presented in figure 5-7. For scaling reasons Lappegamvatn is illustrated in a separate graph as well.
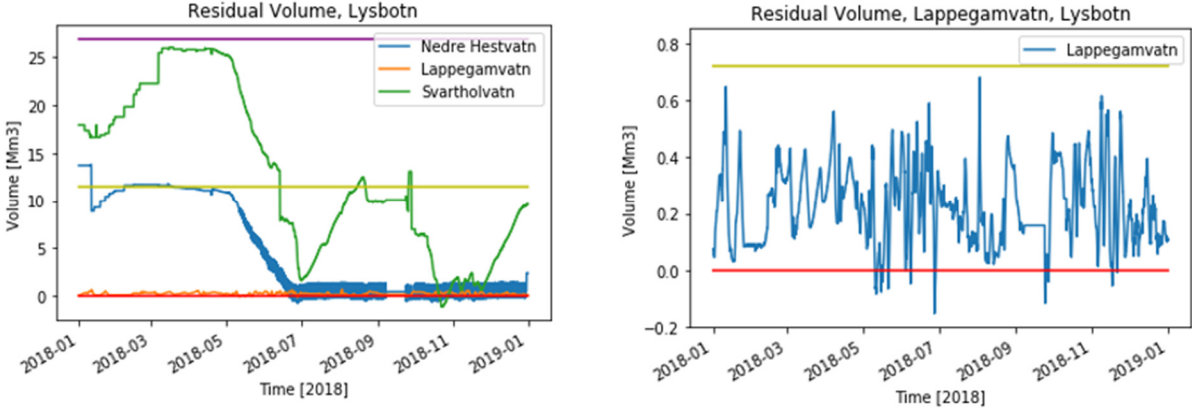
Figure 5-7 Left: Residual volume, Lysbotn. The red horizontal line represents volume at HRW, and the purple and yellow horizontal line represent volumes at LRW for Svartholvatn and Nedre Hestvatn, respectively. Right: Residual volume for Lappegamvatn alone. The red and yellow horizontal line represents HRW and LRW, respectively.

Figure 5-7 shows that the water volumes for the largest magazines are at its lowest during the first half part of the year. During the last half part of the year the highest magazine, Nedre Hestvatn, is at HRW or a bit above, so no storage capacity is available. The middle magazine, Svartholvatn, also has some periods at near HRW or above, at the start of July and between the end of October until December.

Lappegamvatn is the smallest magazine, so it is easily emptied and refilled. The upper magazines are used as supplies when needed. As can be seen from the right at figure 5-7, the volume at Lappegamvatn is rapidly fluctuating throughout the whole year.

PHES potential at Lysbotn power plant is evaluated for locations between the regulated lakes, as well as for between Lappegamvatn and Lysvatn, an unregulated lake where the power plant has its outlet. The three considered designs are shown in figure 5-8. Note that horizontal distances are the shortest distance measured from the map, except for between Svartholvatn and Lappegamvatn, where water pipes would probably been constructed around a steep mountain side. A summary is given in table 5-3.

Figure 5-8 Three alternative layouts for using Lysbotn power plant as PHES illustrated by black lines. The lines are giving the horizontal distance, and the height of the lakes are given by blue values (Norgeskart, 2019).

Table 5-3 Summary for alternative layouts for using Lysbotn power plant as PHES

Layout:	Horizontal distance:	Height difference	Combined volume:	Restrictive magazine:
Svartholvatn – Lappegamvatn	~ 2591m	45.3m - 52.95m	27.60 Mm^3	0.72 Mm^3 (Lappegamvatn)
Lappegamvatn – Lysvatn	~ 1337m	128.25m - 130.25m	Unknown	Unknown
Nedre Hestvatn – Svartholvatn	~ 700.66m	103.05m - 114.7m	38.38 Mm^3	11.5 Mm^3 (Nedre Hestvatn)

Lappegamvatn is a small magazine, so there is little opportunity to use water from this magazine to pump up to the next magazine, Svartholvatn. The regulatable volume would be restricted by the magazine volume at Lappegamvatn, which is only 0,72 Mm^3. Also, the height difference is small relative to the horizontal distance, with Mellomvatn in between, and the environmental impact by guiding water through pipes here would be great.

A more suitable option for using Lysbotn power plant as PHES would be to install a PaT, pump/turbine or reversible turbine between the two upper magazines, which are also the largest ones. From figure 5-7 there seems to be opportunity to utilize these magazines as PHES throughout most of the year 2018, except for the period around the start of November where both magazines are at HRW.

One drawback for this option though, is that the location is quite far from any infrastructure, so transportation and installation would require additional environmental impact. Permission would be required for this, as well as for extension of power network to this location. Troms Kraft are already planning to install a 22 kV power line from Lappegamvatn to Svartholvatn, to supply the water gate, that as of today is driven by a battery, diesel generator and solar panels (TKP, 2020b). This power line will be about 5 km, leaving only 2 km remaining to the evaluated PHES location between Nedre Hestvatn and Svartholvatn.

Other alternatives for Lysbotn power plant would require permission to regulate additional lakes. One of them is Lysvatn, located below Lappegamvatn. This is the only option that allows for utilization of an already installed turbine, by installing an additional pump from Lysvatn to Lappegamvatn. The magazine volume of Lappegamvatn is quite small, while the area of Lysvatn is large in comparison, 3,6 km^2. It has a mean depth of about 12m (NVE Atlas, 2020), hence the regulation will probably be quite small. Even though, Lappegamvatn is sometimes close to, or above, HRW, and for those periods there are no available storage capacity. This is probably due to water being regulated from Svartholvatn and could hence been avoided if preferred.

Nevertheless, letting water down from the upper two magazines is less costly, and it is only between March and June in 2018 that both of those are close to LRW, so a pump/turbine between Lappegamvatn and Lysvatn would probably be redundant here. It is worth mentioning though, that during these months is a part of the year where hybrid systems containing solar energy has good potential for Senja (Jacobsen, 2019). Storage of surplus energy would then be required, so this option might be of interest after all.

Results for PHES designs evaluated at Lysbotn power plant are given in table 5-4.

Table 5-4 Design results for Lysbotn PHES options

Design:	Magazine volume:	e:	Capacity:	P_{pump}	P_{gen}	RTE:
Svartholvatn - Lappegamvatn	0,72 Mm³ (Lappegamvatn)	0.120 kWh/m³	86.4 MWh	1.41 MW	1.08 MW	0.77
Lappegamvatn - Lysvatn	0,72 Mm³ (Lappegamvatn)	0.274 kWh/m³	197.3 MWh	3.22 MW	2.46 MW	0.76
Nedre Hestvatn - Svartholvatn	11.5 Mm³ (Nedre Hestvatn)	0.227 kWh/m³	2610 MWh	3.14 MW	2.40 MW	0.76

Note that the calculated values for Lappegamvatn to Lysvatn differs from the actual already existing power plant here. This is due to several factors as a different turbine efficiency or water flow than in the calculations, losses due to friction etc. This is a good reminder of that calculations like this are only rough estimates.

The roundtrip efficiencies are about the same for all three layouts, but the regulatability is substantially different. The design between Svartholvatn and Lappegamvatn have a restricted pumping ability because Lappegamvatn is so small, so there is little available water for pumping. The small volume of Lappegamvatn also restricts the pumping ability for the design between Lappegamvatn and Lysvatn, but this could probably be regulated better by decreasing the flow from Svartholvatn in periods of surplus energy from PV or wind, requiring pumping storage. In that case, Lappegamvatn could be filled near to its <u>HRW</u>.

Either way, the best option would probably be the design between the two largest magazines, since the roundtrip efficiency is about the same, but the regulatability is much greater. Figure 5-9 illustrates the residual volume energy content, showing how much energy each magazine could have produced if the residual volume was filled. For scaling reasons, Lappegamvatn is shown in a separate graph as well. For the calculations of residual volume energy content for Lappegamvatn, the actual energy equivalent of 0.215 kWh/m3 for Lysbotn power plant is used.
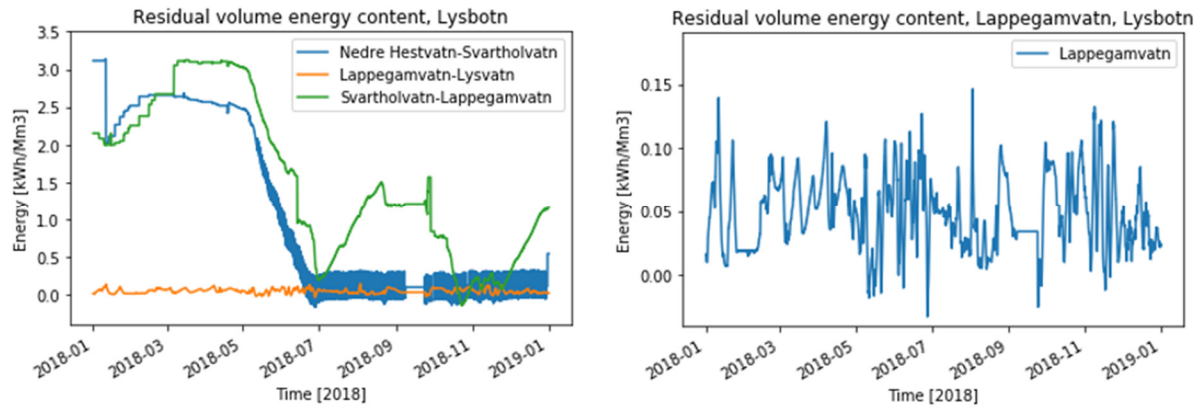
Figure 5-9 Left: Residual volume energy content at Lysbotn power plant. Right: Residual volume energy content of Lappegamvatn, Lysbotn.

Another option for using Lysbotn power plant as PHES would be to utilize lakes that have been digitally evaluated by NVE for small scale hydropower. Three of them are connected to Lysbotn power plant and are illustrated in figure 5-10. They all have a fall between 100m and 150m, but their storage capacity is small, so other alternatives would probably be more suitable for PHES.

Figure 5-10 Digitally evaluated small scale hydro power at Lysbotn power plant (NVE Atlas, 2020)

The last alternatives considered in this thesis for utilizing Lysbotn power plant as PHES is also mentioned in results for Bergsbotn, by connecting one of the two highest magazines at Lysbotn, to the lowest magazine at Bergbotn with a pump, PaT or reversible turbine. These designs are presented in the next chapter.

5.1.5 Results and Evaluation of Combining Bergsbotn and Lysbotn Power Plant

The option for combining Bergsbotn and Lysbotn power plant has several benefits. As previously mentioned, Bergsbotn power plant has a much greater energy equivalent than Lysbotn power plant. The ratio is 0,843:0,215, so almost four times higher. By pumping water from Lysbotn power plant and letting it through the turbine at Bergsbotn, one would get payed almost four times more for the power produced, minus the cost for pumping. Also, figure 5-6 illustrates that the two upper magazines at Lysbotn power plant are quite full for long periods of 2018, which might indicate that there is more water at this plant than needed. Even though, Lysbotn power plant is situated at a different distribution network than Bergsbotn power plant, whom both have voltage difficulties for parts of the year. Therefore, the most optimal solution might not be a pure pump between the power plants, but a turbine as well, or a PaT or reversible turbine. In that way, a regulation between the power plants could be obtained at the same time as PHES could be utilized. Also, an additional turbine could provide higher production for the periods where the power demand is high.

Another benefit by this solution, is that the two power plants belong to different precipitation fields. Data provided by MET shows that there are differences in precipitation on the west coast and the east side of the mountain ridge separating the power plants. In general, there are often more precipitation at the west side, probably due to the high mountains at the coast (MET, 2020). A regulation alternative between the power plants could help distribute water between them as preferred.

Two different layouts are evaluated for this combination of the two power plants, one between Store Hestvatn at Bergsbotn and Svartholvatn at Lysbotn, and the other between Store Hestvatn at Bergsbotn and Nedre Hestvatn at Lysbotn. Both alternatives give the opportunity to pump water from Lysbotn to Store Hestvatn at Bergsbotn and run the water through the turbine at Bergsbotn. The layouts are illustrated in figure 5-11, but measurements are, also here, done only based on the shortest horizontal distance. Another layout between the magazines, including longer distances, might be preferable if the topography or geological conditions require it, especially if a tunnel system is required. Figure 5-12 and 5-13 show the residual magazine volumes for the two different layouts.
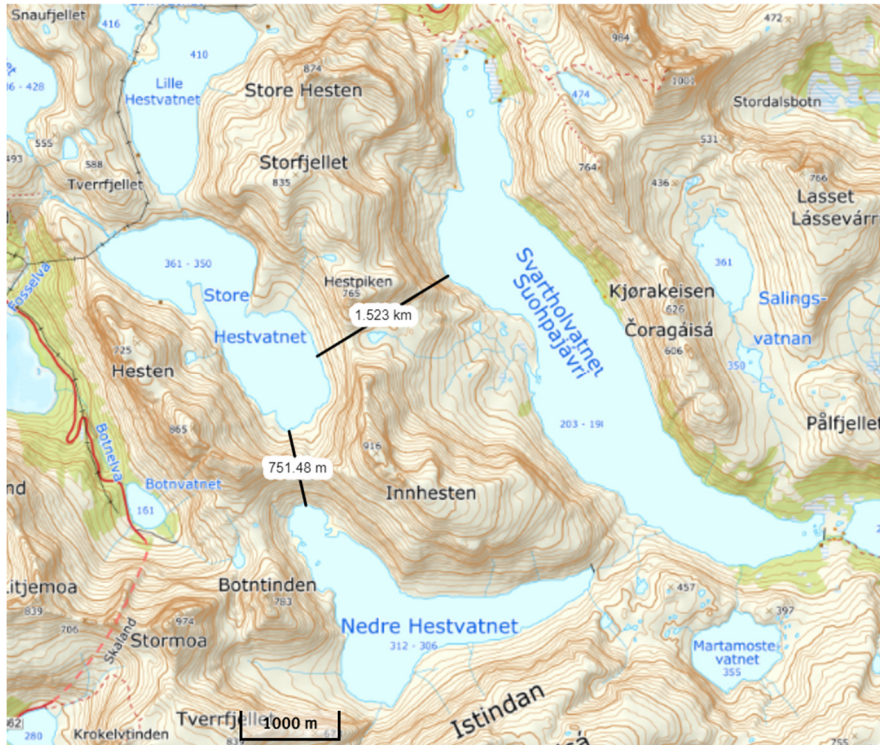
Figure 5-11 Two alternatives for combining Bergsbotn and Lysbotn power plant as PHES illustrated by black lines. The lines give horizontal distances, and the height of the lakes are given by blue values (Norgeskart, 2019).
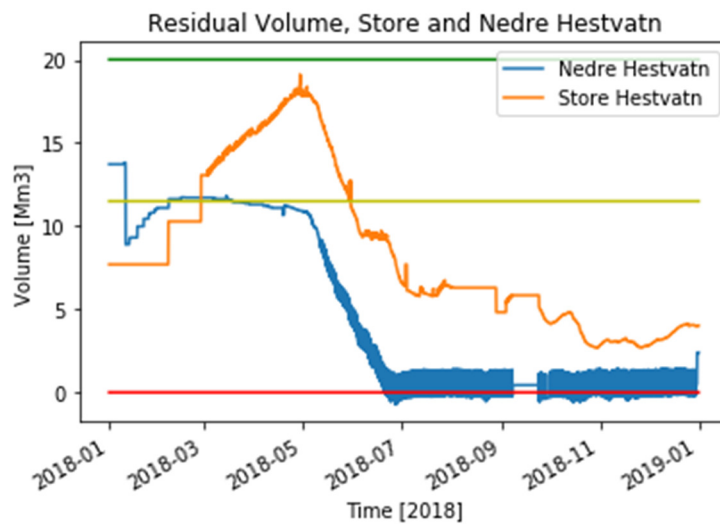
Figure 5-12 Residual volume for Store Hestvatn, Bergsbotn, and Nedre Hestvatn, Lysbotn. The red horizontal line represents volume at HRW, while the green and yellow horizontal line represent volumes at LRW for Store and Nedre Hestvatn, respectively.

.

77
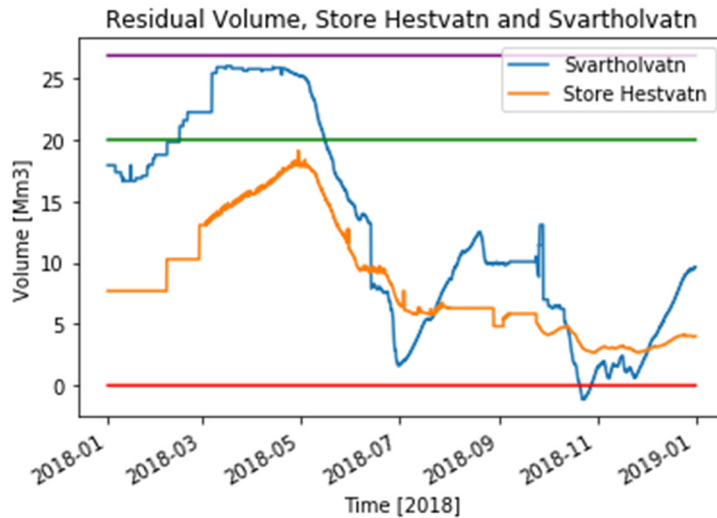
Figure 5-13 Residual volume for Store Hestvatn, Bergsbotn, and Svartholvatn, Lysbotn. The red horizontal line represents volume at HRW, while the green and purple horizontal line represent volumes at LRW for Store Hestvatn and Svartholvatn, respectively.

Figure 5-12 shows that there is little pumping capacity from Nedre Hestvatn to Store Hestvatn for the first five months of the year, when Nedre Hestvatn is at, or below, LRW. Nevertheless, if a PaT or reversible turbine would be installed here, the water levels could be regulated by letting water down from Store Hestvatn. With that solution, there would be potential for PHES throughout the entire year, and water could also be reused.

Figure 5-13 shows that Svartholvatn is close to LRW between March and May, but due to the great volume of this magazine, there is still capacity for pumping. The rest of the year also have promising prospects for PHES capacity, and the period in October where Svartholvatn is above HRW could have been avoided by pumping. A summary of the layouts is given in table 5-5.

Table 5-5 Summary for alternative layouts for combining Bergsbotn and Lysbotn power plant as PHES

Layout:	Horizontal distance:	Height difference	Combined volume:	Restrictive magazine:
Store Hestvatn - Svartholvatn	~1523m	146.3m-162.9m	46.90 Mm^3	20.02 Mm^3 (Store Hestvatn)
Store Hestvatn – Nedre Hestvatn	~751.48m	37.2m-54.2m	31.52 Mm^3	11.5 Mm^3 (Nedre Hestvatn)
Store to Nedre Hestvatn to ocean	~751.48m	37.2m-54.2m / 349.5m-360.5m	31.52 Mm^3	20.02 Mm^3 (Store Hestvatn)

78

The greatest challenges for these two designs are the accessibility to the locations and the fact that there is a relatively high mountain ridge in between. A tunnel would probably have to be constructed, which is both costly a laborious. There is one advantage though, for the design between Store Hestvatn and Nedre Hestvatn, that NATO and The Norwegian Armed Forces have already constructed a tunnel passing between the two magazines, up to a radar construction at the top of the mountain Innhesten (Forsvarsbygg, 2007). This provides an opportunity for a cooperation between NATO/The Norwegian Armed Forces and TKP. If an agreement then is made, and the tunnel is suitable, the construction process and cost could be reduced.

The design between Store Hestvatn and Svartholvatn is probably the most expensive and laborious of all the designs, with a tunnel construction of more than 1.5 km. Both these designs would require an extension of the power line from anything between 1.5 km and 2.5 km. The calculation results for the two designs of combining the power plants are shown in table 5-6.

Table 5-6 Design results for combining Bergsbotn and Lysbotn as PHES.

Design:	Magazine volume:	e:	Capacity:	P_{pump}	P_{gen}	RTE:
Store Hestvatn to Svartholvatn	20.02 Mm^3 (Store Hestvatn)	0.378 kWh/m^3	7.57 GWh	4.45 MW	3.40 MW	0.76
Store Hestvatn – Nedre Hestvatn	11.5 Mm^3 (Nedre Hestvatn)	0.111 kWh/m^3	1.28 GWh	1.31 MW	1.01 MW	0.77
Store to Nedre Hestvatn to ocean	20.02 Mm^3 (Store Hestvatn)	0.863 kWh/m^3	17.27 GWh	1.31 MW	7.77 MW	5.93

The roundtrip efficiency is, as expected, about the same for the first two designs, since the same numbers are used for flow, turbine and pump efficiency. For the last option it is much greater, since this is not a real roundtrip. The pumping height is only about 8% of the generating height. This means that by investing 1.31 MW in pumping, one could generate 7.9 MW at Bergsbotn. If the water is rather let down to Lysbotn power plant the generation would instead be 5.4 MW. The difference is 1.19 MW, so this could be a favourable option.

The greatest difference between the two first designs is the regulatable volume, about twice the size for Store Hestvatn and Svartholvatn. Also, the energy equivalent and power output is much greater for this alternative. On the other hand, so is the required power input, and not to mention

the investment cost. Nevertheless, based on the year 2018, both these designs have promising prospects regarding PHES capacity. Based on the calculated energy equivalents, residual volume energy content is illustrated in figure 5-14.
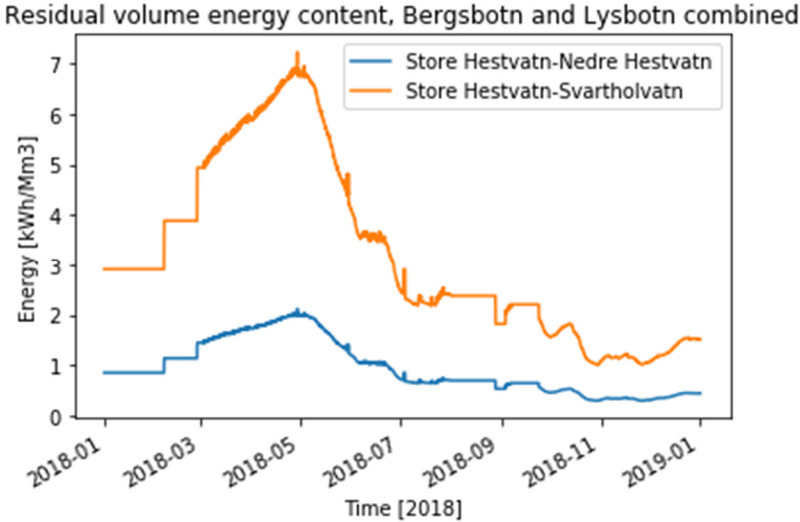
Figure 5-14 Residual volume energy content for combination of Bergsbotn and Lysbotn power plant

5.1.6 PHES Conclusion and Economics

All options considered here for converting already existing power plants at Senja into PHES are practically possible. Some of them depending on new lake regulation permit, but all of them have capacity of water regulation throughout most of the year 2018. It is still important to remember that if PHES is installed, the water levels would be much more fluctuating, and it introduces an opportunity to regulate levels as preferred.

There are little environmental impacts by converting already existing hydropower plants into PHES since the involved lakes are already regulated. Only a more rapid water level fluctuation is expected. The environmental impact is greater by introducing regulation of new lakes. Also, for some of the designs evaluated here, rivers would be affected when installing new turbines or pumps. Some designs involve tunnel construction, which will have less impact on surface conditions and the visual aspect.

The most promising designs are probably the once involving the largest magazines, Store Hestvatn at Bergsbotn power plant, and Nedre Hestvatn and Svartholvatn at Lysbotn power plant. The design between Nedre Hestvatn and Svartholvatn has good capacity without requiring tunnel construction, hence probably a lower investment cost. The water level at Nedre Hestvatn is quite full for half the year 2018, but by installation of a reversible pump, this water could be regulated between Nedre Hestvatn and Svartholvatn.

The designs combining Lysbotn and Bergsbotn power plant have some advantages, since it opens for regulation between the plants. Also, since the energy equivalent is greater at Bergsbotn power plant, one could utilize excess water from Lysbotn power plant there instead. The design between Store Hestvatn and Svartholvatn has the greatest capacity, but due to the long tunnel that would have to be constructed, it is expected that the design between Store and Nedre Hestvatn would be more favourable.

What is probably the greatest uncertainty in this evaluation is the economic aspect of each option. Nevertheless, economics must be considered against other factors. For instance, if no other solutions are found to relieve the already existing power network, a severe upgrade or new network must be installed. As mentioned previously, that is estimated to become very costly. However, a full cost analysis of the options presented in this work is so extensive that it will require another separate thesis subject of its own.

Nevertheless, a simple cost analysis is done here for the two designs combining Bergsbotn and Lysbotn power plant. Based on the average investment cost of converting already existing hydropower plants in Norway, introduced in chapter 2.3.4, estimated to be between 1680 €/kW and 2525 €/kW (Sira-Kvina, 2007), a rough analysis is given in table 5-7.

Table 5-7 Rough cost analysis of the PHES designs combining Bergsbotn and Lysbotn power plant.

Design:	Installed power:	Cost:
Store Hestvatn – Svartholvatn:	3.40 MW	5712000€ - 8585000€
Store – Nedre Hestvatn	1.01 MW	1696800€ - 2550250€

Based on the findings in this evaluation for PHES, the most promising design is estimated to be a construction of a reversible turbine between Store Hestvatn at Bergsbotn and Nedre Hestvatn at Lysbotn. This design is hence used for the HPP evaluation in chapter 5.4.

5.2 Evaluation of PV Power Installations at Senja

In this section an evaluation of three different sizes of a solar power plant design is done in PVSyst for the location at Snauheia.

First, the results from using measurement data from the pyranometer at Silsand during the period 1.7.19 to 30.6.20 is presented for a 1 MW mono facial system. However, due to the severe errors and deviation of GHI from both the Meteonorm 7.2 data and the study done by T.T. Jacobsen (Jacobsen, 2019), presented in chapter 3-3-2, the Meteonorm 7.2 model is utilized for further evaluations. Also, all other systems are evaluated from January through December for a normal year.

5.2.1 Results from Measurement Data from Silsand

When importing cleaned measurement data from the pyranometer at Silsand into PVSyst, several error messages appeared, such as for all time steps showing GHI equal zero. Also, a warning was given about time mismatch, which can cause very high errors. This was attempted to be corrected as advised by PVSyst, by the function "Time shift", but no values where entirely without errors. The best results where for a time shift of -2, yielding a time mismatch of 17 minutes. A test run was performed for this importation, and by using input values as explained in chapter 4.5, the output achieved is presented in table 5-8:

Table 5-8 Output values from a 1 MW mono facial system using measurement values from the pyranometer at Silsand

GHI [kWh/m^2]:	Generated energy [MWh]:	PR [%]:
641.0	647.8	89.80

By the study done by T.T. Jacobsen, one would expect the GHI to be about 750 kWh/m^2. This is about 16.6% higher than the result here. When performing the same run, only with modelled data from Meteonorm 7.2, the result for GHI was 759.6 kWh/m^2, which is 18.6% higher. This indicates significant errors in the imported measurements from the pyranometer at Silsand.

Hence, this will not be used in further evaluations, and the Meteonorm 7.2 model is utilized instead. The default year in PVSyst is 1990, which cannot be edited, but has no practical significance.

5.2.2 Sensitivity Analysis on PV Input Values

By inserting input values as explained in chapter 4.5, PVSyst calculates the size and performance of the system. A sensitivity analysis was performed for inclination angle with respect to yearly irradiation yield, albedo values and inverter size for the 1 MW system. The results are shown in figure 5-15, and table 5-9 and 5-10.
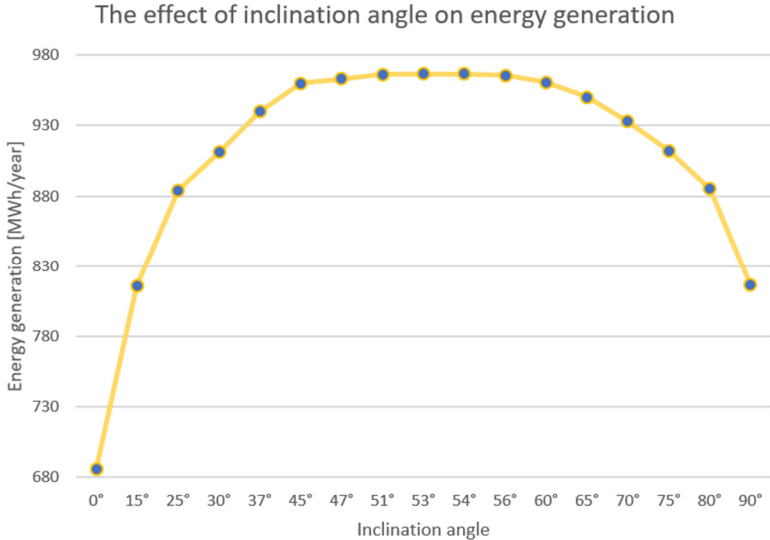
Figure 5-15 The effect of inclination angle on energy generation

PVSyst's optimization tool shows that the inclination angle resulting in 0% losses is between 51° and 54°. It is clearly shown from figure 5-14 that small changes of the inclination angle around the most optimal has a small effect on the system performance. The effect increases further away from the optimal. An inclination angle of 53° were chosen. For this angle, the azimuth angle may vary between ±3° without further losses. The azimuth angle is chosen to be 0°. In reality a lower inclination angle might be preferred because it demands less spacing between the rows of PV modules since less shading then will occur.

Table 5-9 Sensitivity analysis of albedo values. All months not mentioned are set to the default value of 0.2.

Albedo settings:	Generated energy [MWh/y]:	Yield [kWh/kWp/y]:	PR [%]:
0.74 Nov-Mar	934.8	934	91.87
0.74 Nov-May	957.3	957	91.74
0.85 Dec-Mar + 0.5 Nov + May	954.9	954	91.76
0.90 Nov-May	965.8	965	91.70
0.20 Jan-Dec	928.5	928	91.88

As can be seen from table 5-9, the energy production differs with 37.3 MWh, or about 4%, between the best and worst-case scenario. It is also shown that the two months increased duration of snow cover has a greater impact on production, than a 16% change in albedo value from 0.74 to 0.90.

Table 5-10 Sensitivity analysis of inverter size

Inverter size:	Generated energy [MWh/y]:	Yield [kWh/kWp/y]:	PR [%]:
2 x 400kW (Slightly undersized)	947.4	947	92.35
3 x 400kW (Slightly oversized)	954.6	954	93.05
2 x 500kW	960.3	960	93.61
3 x 500kW (Slightly oversized)	955.1	955	93.10
1 x 875kW	962.8	963	93.85
1 x 1000kW	**966.6**	**966**	**94.19**
1 x 1050kW (Slightly oversized)	964.4	964	94.01

From table 5-10 it can be seen that both the smallest and largest inverter systems have less energy generation than the most optimal sized systems. This is caused by losses explained in chapter 2.4.7. The inverter chosen for the 1 MW mono facial system will therefore be the 1000 kW inverter.

The same analysis for inverter size was performed for all three systems.

5.2.3 Evaluation of a PV System at Senja

After performing the sensitivity analysis, an inclination angle of 53° was chosen. The albedo values chosen, 0.85 from December through April, and 0.5 for November and May, proves to be the median of the five different settings tested. These values will hence be used for all systems evaluated. The inverter sizes must be decided for each PV system. By inserting the chosen input values, PVSyst calculates system sizes, performance ratio and energy generation, and several other output values that are not included here. Normalized energy production and performance ratio over the year is shown for the 1 MW system in figure 5-16, and the system sizes, arrangements, yield, energy generation and performance ratio are shown in table 5-11.
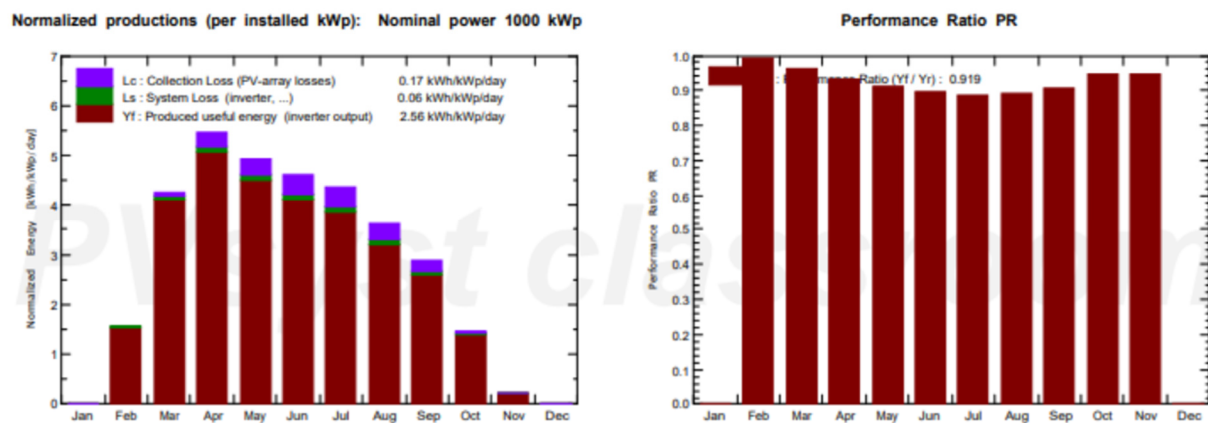
Figure 5-16 Normalized production and performance ratio for a 1 MW solar power plant

Table 5-11 Mono facial PV system sizes

System:	1 MW	5 MW	10 MW
Inverter:	1000kW 500-950V	3x1560kW 470-850V	3x1560kW 470-850V
Modules needed:	2704	13515	27030
Number of strings:	208	795	1590
Modules in series:	13	17	17
Area of modules:	5247m^2	26224m^2	52448m^2
Land area needed:	3401m^2 - 29906m^2	16714m^2 - 151534m^2	33430m^2 - 303077m^2
Yield:	966 kWh/kWp/y	965 kWh/kWp/y	965 kWh/kWp/y
Generated energy:	966.4 MWh/y	4827 MWh/y	9653 MWh/y
PR:	94.19%	94.10%	94.10%

85

The inverters that gave the best output values was the model TL 50Hz CORE-1000.0-TL for the 1 MW PV system, and the model TL 50Hz ULTRA-1500.0-TL for both the 5 MW and 10 MW systems. The performance ratio and the yield are approximately the same for all three systems.

Land area is calculated by estimating row spacing by equation 2-17, but the area is highly dependent on the arrangement of panels. It is chosen to use a solar angle above the horizon, α = 10°, meaning that no shading of rows behind will occur above this angle. The depth of a row equals 1.2m with the panel and angle chosen, and the row spacing must then be a minimum of 10.0m. Note that this is the spacing required on a horizontal surface, and for instance for a south facing slope, the required distance will be smaller. The smallest obtainable area is given if the modules are placed in only one row, and with a one metre spacing between strings. The largest required area is given if all modules are placed behind one another, but this solution is both unpractical and a highly unlikely arrangement.

Figure 5-17 illustrates estimated area at Snauheia if the number of rows equals the number of modules in series. Calculated area for the 1 MW system is then 28006m^2, 140611m^2 for the 5 MW system, and 284833m^2 for the 10 MW system. Note that no spacing is included within a row in this calculation, the slope of the hill will demand less spacing between rows than calculated, and other arrangements will result in other sizes. The simulated production from each system is presented in figure 5-18.
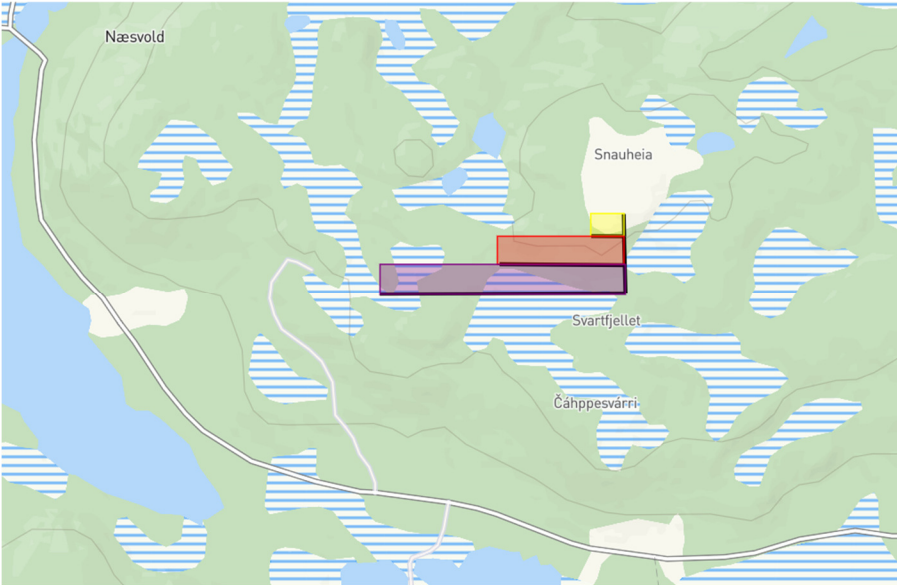
Figure 5-17 Illustration of approximately sizes for PV systems of 1 MW (yellow), 5 MW (red) and 10 MW (purple) at Snauheia
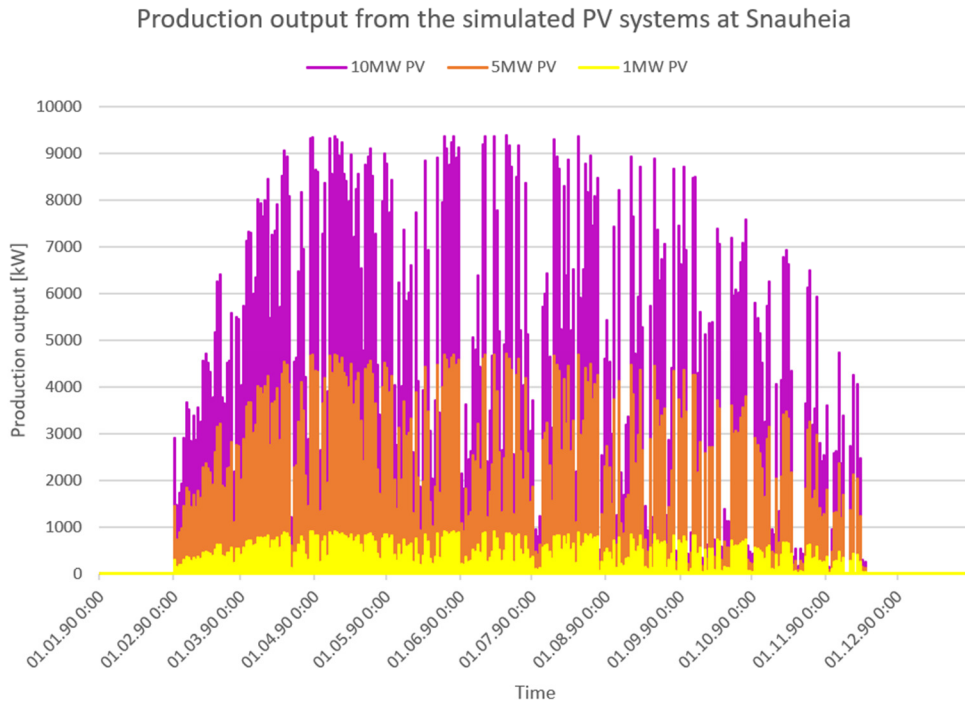
Figure 5-18 Production output from the simulated PV systems at Snauheia, with 1990 as the default evaluation year.

5.2.4 PV Conclusion and Economics

The evaluation of PV systems at Snauheia indicates that there is good potential for solar power exploitation most of the year, obviously except for the period of polar nights. It must be emphasized though, that this simulation is done based on modelled data, and hence might deviate from an actual case. Based on the study performed by T.T. Jacobsen (Jacobsen, 2019), a small downscaling of GHI would probably be appropriate, but since it is considered of less than 2%, it is not included in this evaluation.

The environmental impact of PV installation is mainly visual. There is no noise or moving mechanisms involved, and at this location at Snauheia this PV installation would probably only be visible for hikers etc.

Based on the average installation costs for PV in 2018, estimated by IRENA (IRENA, 2019a), introduced in chapter 2.4.8, the cost for each PV system at Snauheia would be approximately

as follows: 1.023 M€ for the 1 MW system, 5.12 M€ for the 5 MW system, and 10.23 M€ for the 10 MW system.

Based on the forecast for 2030, the equivalent installation cost for each system 10 years from now would be as follows: Between 0.288 M€ and 0.71 M€ for the 1 MW system, between 1.44 M€ and 3.53 M€ for the 5 MW system, and between 2.88 M€ and 7.05 M€ for the 10 MW system.

5.3 Wind Power Plant at Senja

When the size of all other power sources is set in HOMER Pro, wind power is supplemented to achieve a state of near self-sufficiency. A full self-sufficiency state is not required, since Senja is provided with power from the mainland. By selecting the wind turbine of 3 MW as explained in chapter 4.7, HOMER Pro calculates the most optimal number of wind turbines for each HPP, based on the wind resource added. Wind speed data from Fakken wind park throughout the year 2019 is shown in figure 5-19.
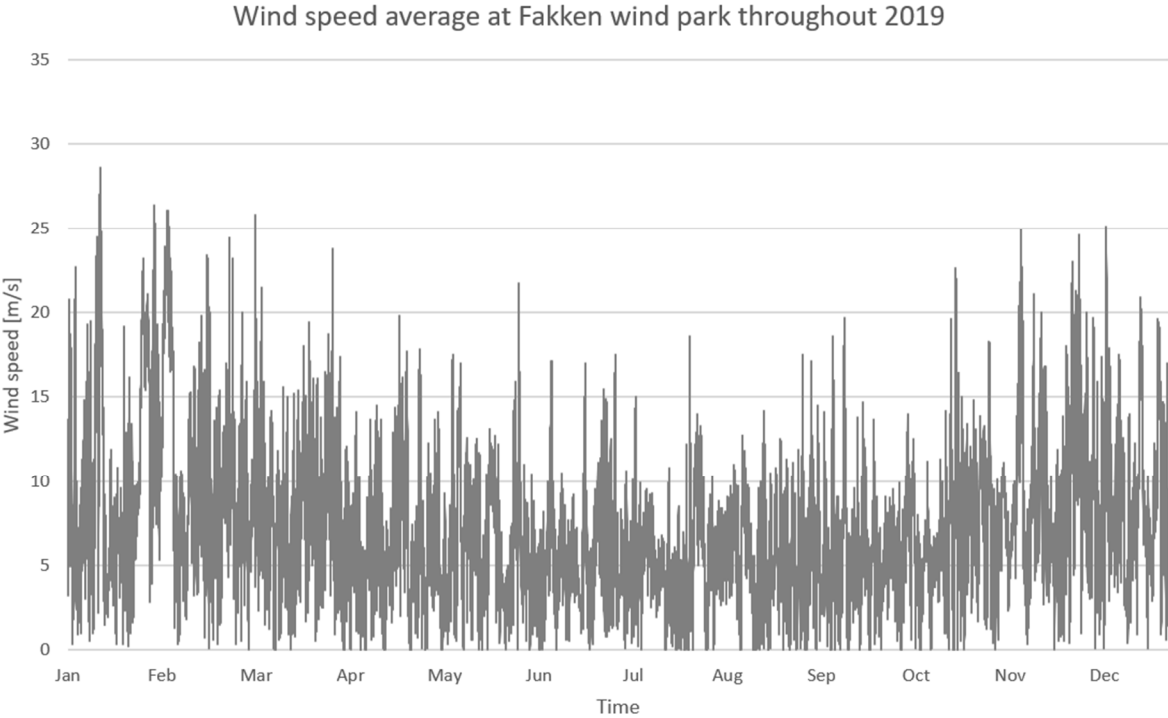

Figure 5-19 Measured wind speed from Fakken wind park during 2019, with 10-minute resolution (TKP, 2020b)

The greatest environmental impact of wind power is the land area required, the visibility from long distances and disturbances from movement and noise. Even though, for many of the simulated hybrid systems here, few wind turbines are required, which do not occupy such great land area. A rough measurement from Fakken wind park shows that the 54 MW installed wind power takes up about 3 km^2. This estimate to about 0.17 km^2 for each wind turbine. The advantage of wind power at Senja is that the wind resource is greatest simultaneously as the peak periods in consumption. Based on the average installation costs from IRENA (IRENA, 2019b), presented in chapter 2.5.5, each such wind turbine would have a cost of 3.79 M€.

5.4 Results and Evaluation of Renewable Hybrid Power Plants at Senja

Considering the evaluation of solar, wind and PHES potential, there seems to be a good potential for HPP at Senja. The coastal climate in the north of Norway results in fluctuating occurrence of precipitation, wind and sun (Dybdahl, 2016). Hence, a combination of hydropower, wind power, PV and PHES should be able to stabilize the power production. Also, the excess amount of sun during summer season, makes a good source for seasonal energy storage. Wintertime is considered a dry season for Norway, and at the same time energy peak demand is caused by both electrical heating of domestic houses and high production in the fishing industry at Senja.

For the evaluation of HPP, performed in HOMER Pro, some inputs are kept constant. The PHES design considered the most promising, between Store Hestvatn at Bergsbotn and Nedre Hestvatn at Lysbotn, yielding a capacity of 1.01 MW is included in all simulations. So is the already existing hydropower plants and the scaled load, shown in figure 5-20. Note that for Senjahopen and Husøy, the measurements for January 2019 really are the measurements for January 2020, February is constructed, and the consumption for Northern Senja is scaled as described in chapter 4.9. The only component varied is the PV system input from PVSyst. Three different designs for HPP are produced based on the different sizes of PV power plants presented in chapter 5.2.3. By using HOMER Pros optimization tool, the optimal number of wind turbines are found for each of the three systems.
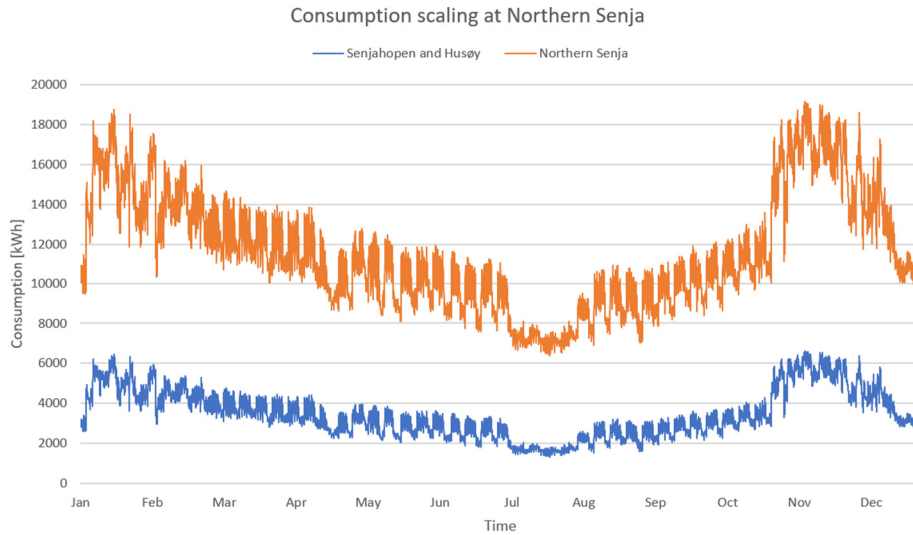
Figure 5-20 Consumption at Husøya and Senjahopen in blue, and for all of Northern Senja in orange.

5.4.1 HPP with 1 MW PV

The renewable hybrid system with 1 MW PV is first simulated without any wind turbines. Its behaviour during the year is shown in figure 5-21.
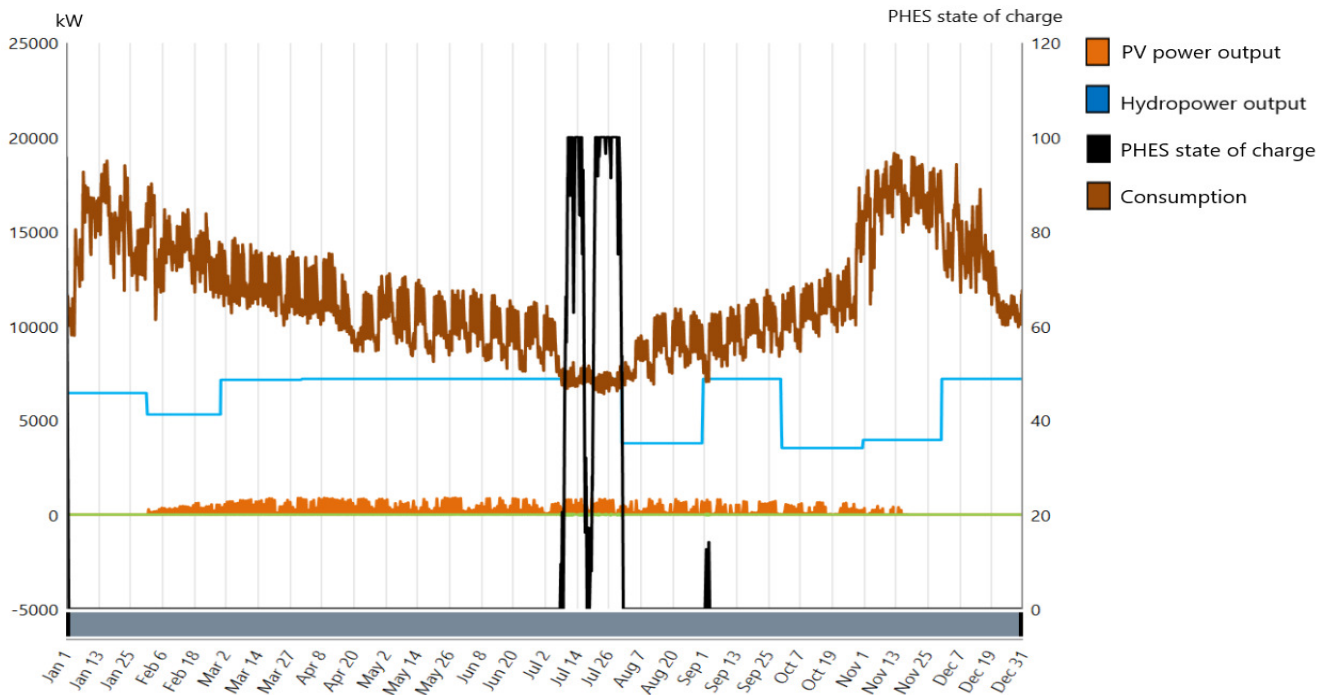
Figure 5-21 Behaviour during 2019 of the HPP with 1 MW PV and no wind power

The PHES is originally 100% charged, but due to lack of power production, its 1.01 MW is emptied so fast that it can hardly be seen on the figure. It is only refilled by surplus energy production during some periods in July, when consumption is at its lowest. Since hydropower could only be simulated with monthly values, the rapidly changing production is not shown. It was found that in the month of July there was some excess energy production, which could not be stored in the PHES that was already full. This can rather be sold and distributed elsewhere. Otherwise, the hydropower production could have been reduced during that period, and the water content in associated magazines could have been saved for later.

The number of wind turbines that was found optimal, by HOMER Pro, for this system was 6-7 turbines, and the case with 7 turbines is shown in figure 5-22.
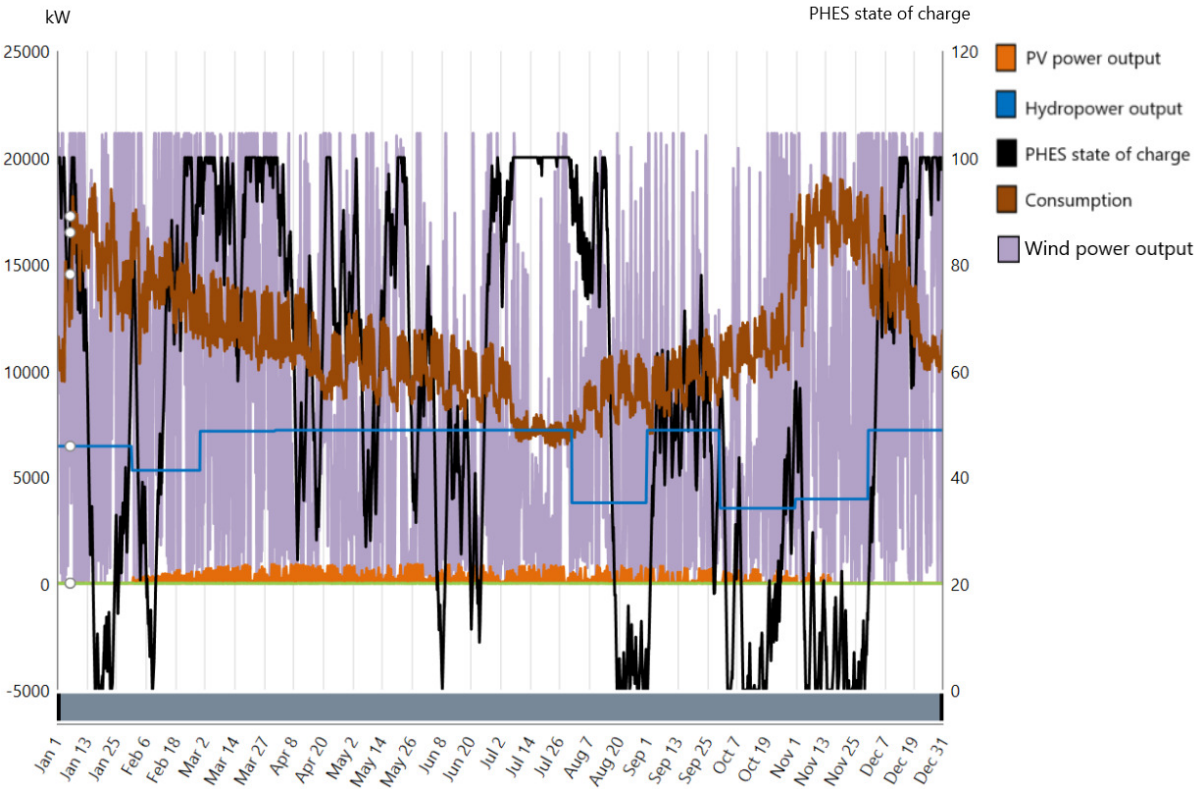
Figure 5-22 Behaviour during 2019 of the HPP with 1 MW PV and 7 wind turbines

Below 6 turbines, the state of charge of the PHES was at 0% for large parts of the year where the load is highest. Above 7 turbines the state of charge is near 100% for most of the year. For the periods where it is not, adding more wind turbines is not contributing much to the charging. This can be seen in figure 5-23, where 20 wind turbines were added for the sake of investigation.

91
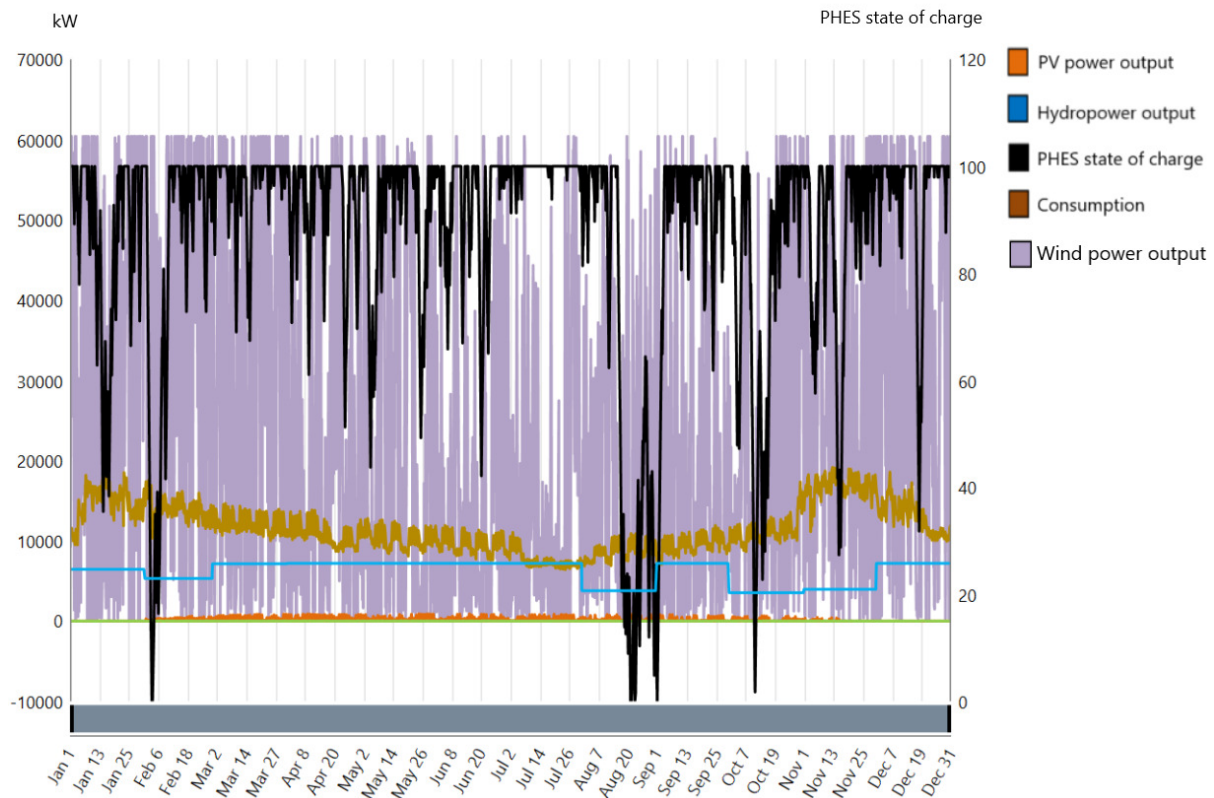
Figure 5-23 Behaviour during 2019 of the HPP with 1 MW PV and 20 wind turbines

The reason for why additional wind turbines have so little impact on the state of charge of PHES is a combination of sparse wind resources at that time, simultaneously as the hydropower production is low. Regarding the hydropower production, this could in reality been regulated.

Nevertheless, the behaviour of the PHES could probably have been better managed and distributed throughout the whole year by regulation of the hydropower production. It must be kept in mind that the hydropower plant and the PHES would in reality be part of the same system, and the actual hydropower production is much more fluctuating than in these simulations. Hence, the behaviour of both the hydropower production and the PHES will differ a lot from these simulations. If the hydropower was run tactically regarding power production, a hybrid system of 1 MW PV and less than 6 wind turbines might also have provided a state of near self-sufficiency. It is also emphasised that a complete self-sufficient state is not the goal here, since Northern Senja is supplied by power from the grid anyways. The goal is evaluate implementation of local power production and storage, to stabilize the local power network.

5.4.2 HPP with 5 MW PV

Without any wind power, the 5 MW PV renewable HPP shows the same tendency as with the 1 MW PV, where the PHES is emptied within the first days of January. Only during July is it above 5% charge, and for most of July it is full. The point of near self-sufficiency is found around 3 wind turbines, and the behaviour of the system is shown in figure 5-24.
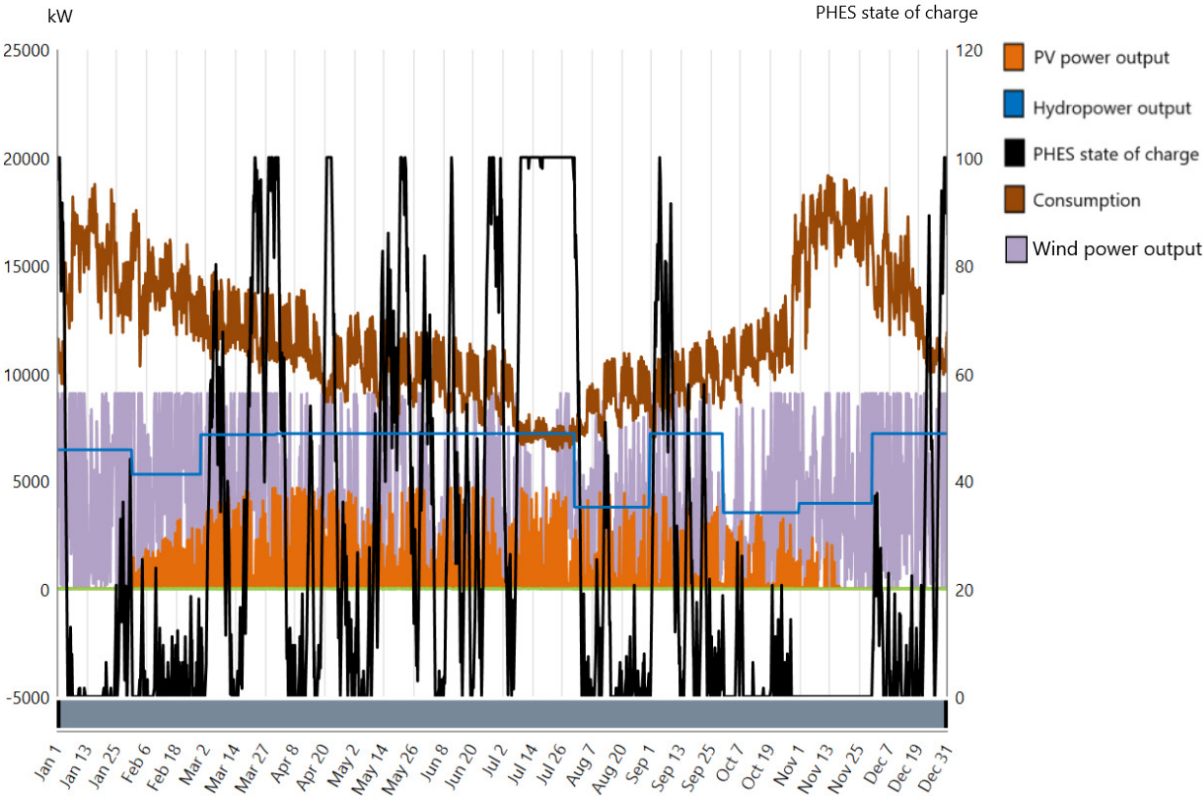
Figure 5-24 Behaviour during 2019 of the HPP with 5 MW PV and 3 wind turbines

It can be seen that there are periods where the PHES is empty, but as mentioned for the 1 MW PV system, this could be regulated by the hydropower production. With 4 wind turbines there is overproduction of energy for several periods, which could be sold or better regulated as mentioned previously. Both for the state of overproduction when the PHES is full, and underproduction when the PHES is empty, could be regulated by interaction with the grid, in addition to the previously mentioned hydropower regulation.

93

5.4.3 HPP with 10 MW PV

The behaviour throughout 2019 of the renewable hybrid power plant with 10 MW PV and no wind power is shown in figure 5-25.
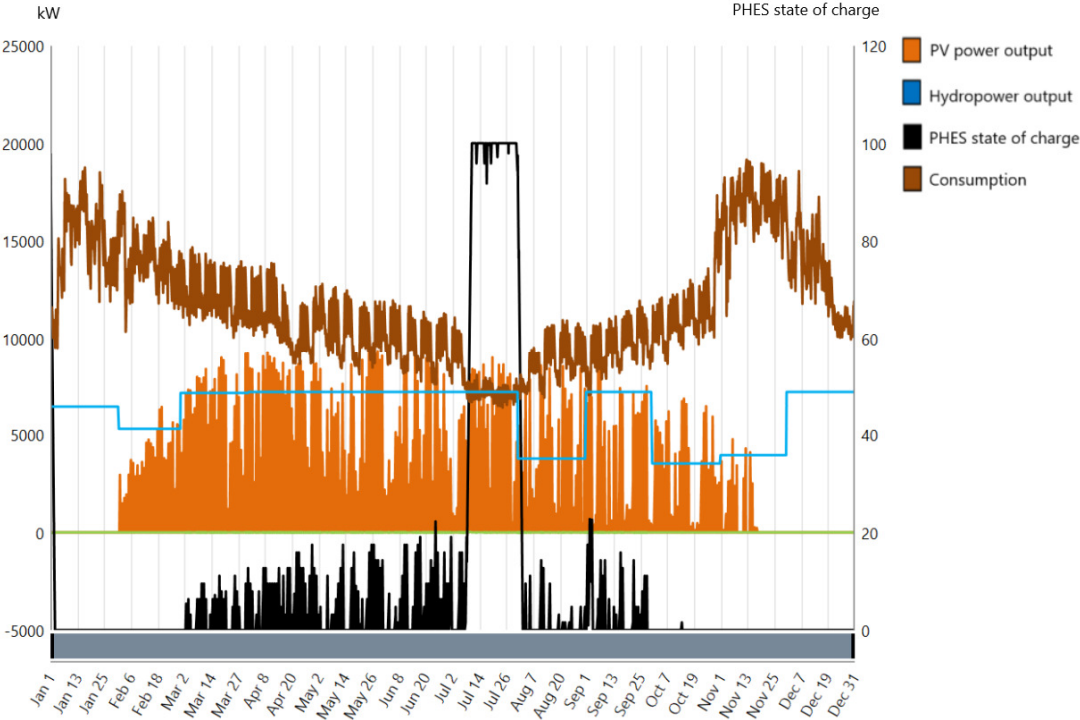
Figure 5-25 Behaviour during 2019 of the HPP with 10 MW PV and no wind power

Obviously, since this is the system with the largest PV power plant, it is also the system that is able to charge the PHES the most without any wind power. At the same time, the additional power production from PV happens, as expected, at a time of the year when consumption is at its lowest. The point of this study is to try and find a combination of PV, wind and PHES that could contribute to additional power production in times of high demand, which is wintertime for Senja. Seasonal storage of hydro is also highly desired, mainly driven by the need for additional power production at wintertime. By filling and saving hydro in the magazines of the hydropower plants one could achieve higher hydropower production in times of high demand. So even if PV power is produced at a different time than when the highest demand occurs, it could still indirectly contribute to additional power production at wintertime. This happens both by providing the opportunity to reduce hydropower production at summertime, saving water for later, as well as pumping water to a higher level if surplus production from PV occurs. By that one could gain more power from that water at a later instance.

It is easy to see from these simulations how the different components behave, but it has proven challenging to estimate, based upon these simulations, how such a system would act in real life. This is due to the fact that import of energy from outside of Northern Senja is not included in the simulations, and in reality, there would be an interaction with the grid, yielding a greater leeway. Also, since the storage of the already existing hydropower magazines is not shown, it is challenging to estimate the true storage of the HPP. For many of the simulations the PHES is discharged at fall time, but the true storage in the already existing hydropower magazines are not shown and would probably be higher than if PHES was absent. A better simulation method is proposed for further work to address this obstacle.

Nevertheless, the result for the 10 MW PV system shows some potential for storage during summertime, where there, for some parts of July, is surplus power production when the PHES is full. In addition to storage in this period, hydropower production could have been reduced, or power could be sold and distributed elsewhere. It is questionable though, if even a 10 MW PV system would contribute to satisfactory result regarding seasonal storage of hydro. By addition of only one wind turbine, the result is much more promising, as shown in figure 5-26.

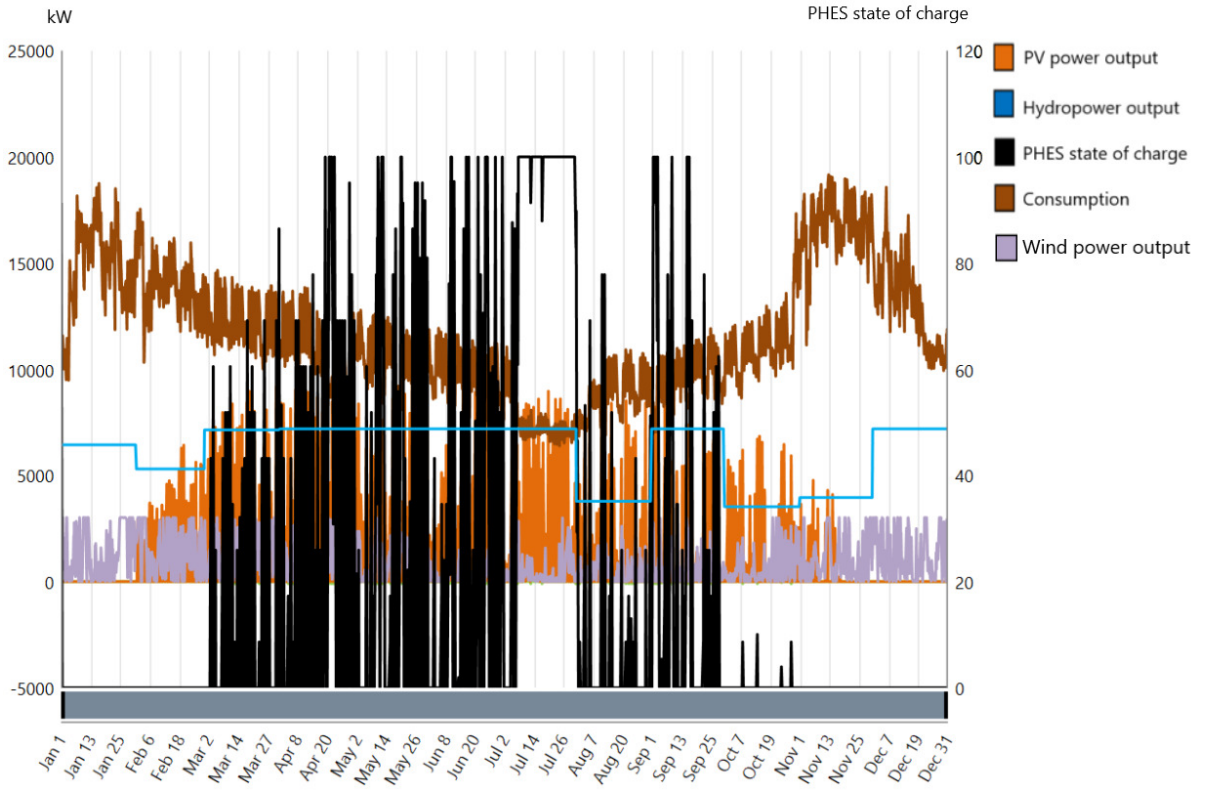*Figure 5-26 Behaviour during 2019 of the HPP with 10 MW PV and 1 wind turbine*

95

If hydropower was run more tactically, as is done in real life, it could complement the PHES better, and the graphs for PHES and hydropower would probably fluctuate more. It is also expected that the PHES state of charge would be more at a medium range during the whole year, since it in fact is the lowest magazine of Bergsbotn power plant, and the act of pumping is hence not a requirement for the PHES to be charged.

If several wind turbines are added to this 10 MW PV HPP, the state of charge for PHES is near 100% during summertime, and for wintertime it will behave as for the other systems. For evaluation of wintertime regarding wind power in the HPP, figure 5-26 shows that 1 wind turbine is not sufficient to provide the power required, in addition to the hydropower, during wintertime. It must be emphasised that all additional power production will be useful even if the system is not near self-sufficiency. 1 wind turbine would produce some local power, and hence the equivalent amount of power would not be needed from the grid outside of Northern Senja. 3 wind turbines are illustrated in figure 5-24, 7 wind turbines in figure 5-22, and 20 wind turbines in figure 5-23. The state of charge of the PHES illustrates whether there is surplus or deficit of power production, as it is charged or discharged, respectively, at that time. The more wind turbines added, the more the PHES is charged at wintertime as well. More than 7 wind turbines are estimated to exceed the state of near self-sufficiency for Northern Senja, even without any PV power production. From only wind implementation one would not get the same effect of PHES charging during summertime, since there is less wind resource then, but this is mainly based upon the number of turbines installed. The best solution though, is not necessarily the system with the highest production, as discussed in the following sub chapter.

5.4.4 HPP Conclusion and Economics

All additional local energy production will most likely be positive contributions to the power situation at Northern Senja. For the intermittent wind and PV production, it is of interest to stabilize the production by storage, and PHES seems as a promising option. At the same time as already existing hydropower plants can be upgraded to PHES, the option considered here as the most promising one, would add an extra water turbine to the system. This was the 1.01 MW design combining Bergsbotn and Lysbotn power plant with a reversible turbine, and this

contributes to the opportunity of additional power production in periods of high demand. Also, this specific PHES design provides two options. One could either retain the pumped water within the plant by letting it back down to Lysbotn power plant, or one could let the pumped water from Lysbotn through the turbine at Bergsbotn, where the energy equivalent is almost four times higher. With this design, the water could be regulated between the power plants as desired, providing better regulation.

As mentioned previously, it is challenging to estimate the exact behaviour of the HPP's, both because hydropower production could not be simulated in hourly steps, and, even if it could, its behaviour would have been completely different if a PHES was introduced. In reality the hydropower plants and the PHES would be one system, and in simulations the hydropower plants would probably been better simulated as a PHES. This is because they hold storage capacity, and preferably will produce power when there is demand, and will hold back production when it is not, just as the simulated PHES. If the regular hydropower plants would be simulated this way, one would probably see that their state of charge would be higher when included in a HPP, at least during fall, and maybe during wintertime as well.

Nevertheless, the simulations give a pointer regarding the behaviour of the system, and it proves to be promising for several options considered. Based upon the simple economic evaluations for each technology, given in chapter 5.1.6, 5.2.4 and 5.3, the installation costs for each HPP considered the most optimal is listed in table 5-12. What is considered the most optimal is based on the number of wind turbines estimated, by HOMER Pro, for each size of PV system. The sizes of hydropower are 5.4 MW and 7.9 MW, and PHES is 1.01 MW, for all designs.

Table 5-12 Roughly estimated installation costs for HPP's at Senja

HPP design:	PHES [M€]	PV [M€]	Wind [M€]	Total [M€]
1 MW PV, 21 MW wind:	1.70 - 2.55	1.02	26.54	29.26 - 30.11
5 MW PV, 9 MW wind:	1.70 - 2.55	5.12	11.38	18.20 – 19.05
10 MW PV, 3 MW wind:	1.70 - 2.55	10.23	3.79	15.72 – 16.57

The installation cost is estimated to be highest for the system with the most installed power in general, but it is important to remember that the installation cost alone will not determine which system is most profitable. For this, a firm LCOE calculation should be performed, suggested as further work.

When comparing to the estimated cost of a total upgrade of the power network at Northern Senja, estimated to be in the order of 45M€ (TKN, 2020b), all HPP's considered here are less expensive. Whether the network surrounding the HPP would require some upgrade anyways is not evaluated in this thesis and is hence proposed as further work. What is important to keep in mind regarding this cost comparison is that a power network upgrade is a mere expense, while implementation of power production is an investment and has a basis for profit.

Also, the economy is not the only factor involved when evaluating such systems. When looking at land area requirements, the 5 MW PV system is estimated to require about 0.14 km^2, while one single wind turbine of 3 MW is estimated to require about 0.17 km^2. Both wind and PV have their own advantages and disadvantages. When deciding on which technology to implement, one should also consider production method, environmental impact of installation, operation and maintenance, as well as their end-of-life management options.

In addition to the difference in price and land area required, PV and wind have the best resources at different times of the year, so a combination would perhaps be preferable. Wind power could directly add production during high demand at wintertime. PV power production could reduce the required hydropower production during summertime, perhaps contribute to pumping of PHES, and hence indirectly help off with the wintertime demand, by providing seasonal storage of hydro.

To conclude, all three HPP systems considered here shows promising results, and other combinations is most certainly also possible.

6 Conclusion and further work

6.1 Summary

In this study, possible implementation of distributed renewable energy and storage is evaluated to improve the unstable power supply experienced at Senjahopen and Husøy, and the surrounding area, at Northern Senja. By combining implementation of PV and wind power plants, with already existing hydropower and converting part of the already existing hydropower plants into pumped hydroelectricity storage, several renewable hybrid power plants are proposed.

An evaluation of already existing hydropower plants at Senja have been considered for conversion into pumped hydroelectricity storage (chapter 5.1), based on data about magazine water height in 2018. Potential for PV power plants and wind power plants was also evaluated (chapter 5.2 and 5.3), and based on this, different combinations of renewable hybrid power plants were constructed (chapter 5.4).

9 different PHES designs were evaluated in this study, and all solutions are considered practically suitable, at least for the year 2018 that was the only year considered. Some solutions seemed more promising, especially the two options combing Lysbotn and Bergsbotn power plants, where water could be retained within the plants and regulated as desired. This would also yield the possibility of pumping water up from Lysbotn power plant and running it through the turbine at Bergsbotn power plant, where the energy equivalent is almost four times higher. Two different designs were suggested for this, giving a PHES production capacity of 3.40 MW and 1.01 MW. The latter was considered the most suitable because of less construction expenses and was therefore the only solution considered in the HPP evaluation.

The potential for PV power was found to be good, with performance ratios above 94%, and three different plant sizes were evaluated. For wind power there were not performed any

analysis for Senja, but the wind resource from a relatively nearby plant, Fakken wind park, was used as an equivalent resource.

Along with the already existing hydro power plants and the PHES solution considered the most optimal, the different sizes of PV power plants were used to decide on the number of wind turbines for each renewable hybrid power plant. Three systems were simulated throughout the year 2019, and all of them showed promising results. Wind and solar resources are found to complement each other, so systems containing both gives the best results for the PHES.

Nevertheless, conclusions from the simulations in HOMER Pro are somewhat limited, since hydropower production have poor resolution with only monthly average values, and the production would have been substantially different if hourly values could have been used. Production from hydropower would also differ a lot if PHES was introduces. Another weakness of this study is that only one year, 2018, was evaluated for PHES potential, and for hydro and wind resources, only 2019 was considered. The result might have been different if other years was considered, or if an average year was calculated and utilized.

Based upon the data provided and the years considered, the results promising. Northern Senja is prone to power supply instabilities, and local power production is considered a positive contribution that could help off with this issue. The period between October through March is the most challenging, where the seafood industry, located at the far end of the power distribution network, requires high power supply.

The power feeding capacity from the mainland is limited, and the already existing hydropower plants located at Northern Senja are crucial players in maintaining an adequate voltage level. The local power company, Troms Kraft, in cooperation with UiT, is evaluating possibilities for alternative solutions to a total upgrade of the power network, estimated to cost in the order of 45M€ (TKN, 2020b). One solution could be implementation of the HPP's considered in this thesis, where the investment costs ranges from 15.72 M€ to 30.11 M€. While the power network upgrade is a mere expense, HPP implementation is an investment that has a basis for profit.

From the evaluation of the different technologies it is found that wind power resources are greatest at wintertime, simultaneously as the peak power demand period occurs, and wind power implementation could hence contribute directly to power supply. PV power production

is obviously greatest at summertime but could indirectly contribute to higher power production at wintertime by reducing the demand for hydropower production at summertime. In this way, hydro is stored for later, and by integration of a pumped hydropower plant, surplus power from PV could also be used for pumping and additional seasonal storage. Based upon this evaluation it is considered that a HPP could help relieve the power network as Northern Senja in times of high demand.

6.2 Concluding remarks

To avoid a complete upgrade of the power network at Northern Senja, distributed renewable energy seems as a promising option. In that way the production is also closer to the demand, and with the PHES options considered here, the storage could help control intermittent production, and could also be utilized as seasonal storage. Both PV power, wind power and PHES potential is considered good at Northern Senja, and in combination with the already existing hydropower plants, it could have made up a quite satisfactory renewable hybrid power plant. With local power production and seasonal storage, the power network could have been somewhat relieved, and an upgrade could possibly be postponed.

6.3 Further work

Based on the findings in this thesis, some examples for topics of further work is given, to extend and improve the study.

- **Improved measurement data**

  An evaluation should have been performed spanning several years for the wind and hydro resource. Preferably, an average year should have been calculated for the evaluation. For the hydro resource, hourly values should have been obtained, and the wind resource should have been measured at sites considered for wind power at Northern Senja. Satisfactory GHI measurements should also have been collected, preferably at locations considered for PV installations. Temperature and wind speed measurements could also help decide on the cooling effect.

- **Power network analysis**

  An uncertainty factor that has arisen during this thesis is the question of how much additional power production the power network at Northern Senja can handle. A study regarding the power network is hence suggested as further work, to, amongst other things, clarify whether a network upgrade is required even if a HPP is constructed.

- **Improved simulation of PHES in HOMER Pro**

  It was found that there is an option of simulating PHES in HOMER Pro as a battery, where the size and other inputs can be constructed to give one single unit. This would probably simulate the preferred system better than by using several of the built-in PHES systems in HOMER Pro. This is suggested done as further work, and along with it the already existing hydropower plants could have been included. This because hydropower plants with great reservoirs in reality functions as storage, and produce power when demanded, and not as simulated by HOMER Pro, where production happens simultaneously as inflow occurs.

- **Simulations of PHES in software's specialized for such**

  There exists software's specially designed to evaluate and simulate the behavior of PHES, and such simulations are suggested to perform for further evaluations of the most promising PHES options considered here.

- **Extended cost analysis**

  One of the most crucial factors regarding a considered renewable hybrid power plant at Senja is the economy. A firm cost analysis is hence suggested as further work for the three HPP systems considered in this thesis.

To conclude, a renewable hybrid power plant containing a reliable energy storage system with a large enough storage capacity seems to be a good solution to maintain power quality at a satisfactory level at Northern Senja without upgrading the network considerably. Converting already existing hydropower plants into pumped hydro energy storage seems to be a good option to meet this requirement. Wind power installations could help off with power production during peak demand periods, and PV power production could provide seasonal storage of pumped hydro

Bibliography

ABB (2020). *New.Abb.Com/no/om-oss*

Andreani, L. C., Bozzola, A., Kowalczewski, P., Liscidini, M., & Redorici, L. (2019). Silicon solar cells: Toward the efficiency limits. Advances in physics.

Andrews, J., & Jelley, N. (2007). *Energy science: Principles, technologies, and impacts*. Oxford University, New York.

Antal, B. A. (2004). *Pumped storage hydropower: A technical review*. University of Colorado, Boulder.

Apogee. (2018). Sp-510 user manual.

ARC (2020). *Arctic centre for sustainable energy; renew*

Bonsor, K. (2019). How hydropower plants work.

BOR. (2005). Reclamation, managing water in the west. U.S. Department of the interior bereau of reclamation power recourses office; hydroelectric power.

Bowden, G. J., Barker, P. R., Shestopal, V. O., & Twidell, J. V. (1983). *The weibull distribution function and wind power statistics*. University of New South Wales, Kensington, NSW 2033, Australia.

Breeze, P. (2014). *Power generation technologies (second edition)*.

Bristol, D. S. (2016). Solar heads for the hills as tower technology turns upside down.

Charmasson, J. (2016). Large scale balancing and storage from norwegian hydro hydrobalance project. *Sintef energy research, trondheim, norway*

Dawson, R. (2017). How significant is a boxplot outlier?

Diaf, S., Notton, G., Belhamel, M., Haddadi, M., & Louche, A. (2008). Design and techno-economical optimization for hybrid pv/wind system under various meteorological conditions. *AppliedEnergy,85(10):968– 987*.

Djohra, S., Mustapha, K., & Hadji, S. (2014). Technical and economic study of a stand-alone wind energy system for remote rural area electrification in algeria. *Renewable Energy and Power Quality Journal*, 638–643.

DOE. (2017). U.S. Department of energy; global energy storage database. from Department of Energy (US)

DOE. (2020). U.S. Department of energy, global energy storage database; energy storage systems program.

Dybdahl, A. (2016). *Klima, uår og kriser i norge gjennom de siste 1000 år*: Cappelen Damm akademisk.

EERA. (2016). *European energy research alliance. Eera joint program sp4 - mechanical storage; fact sheet 1 – nov 2016. Pumped hydro energy storage*.

EERE. (2020). Office of energy efficiency & renewable energy: Crystalline silicon photovoltaics research.

energysage. (2020). Smarter energy decisions; what size solar inverter do i need?

Forsvarsbygg. (2007). Nato-radar på senja i drift.

HOMER. (2020). Homer energy.

Hukseflux. (2007). *Hukseflux, thermal sensors; how to calculate pv performance ratio and performance index: According to the latest iec 61724 standard series*.

IEA. (2019). International energy agency; hydropower additions are not fully on track with the sustainable development scenario.

IRENA. (2012). International renewable energy agency; renewable energy technologies: Cost analysis series; hydropower.

IRENA. (2016). International renewable energy agency; end-of-life management, solar photovoltaic panels, june 2016.

IRENA. (2019a). International renewable energy agency; future of solar photovoltaic: Deployment, investment, technology, grid integration and socio-economic aspects (a global energy transformation: Paper), abu dhabi.

IRENA. (2019b). International renewable energy agency; future of wind: Deployment, investment, technology, grid integration and socio-economic aspects, executive summary: A global energy transformation paper, october 2019.

IRENA. (2019c). International renewable energy agency; renewable energy now accounts for a third of global power capacity, 02 april 2019.

IRENA. (2019d). International renewable energy agency; future of solar photovoltaic: Deployment, investment, technology, grid integration and socio-economic aspects.

IRENA. (2020). International renewable energy agency; renewable capacity highlights, 31 march 2020.

Jacobsen, T. T. (2019). *Distributed renewable generation and power flow control to improve power quality at northern senja, norway.* UiT - The Arctic University of Norway, Tromsø, Norway.

Jacobson, R. (2016). Where do wind turbines go to die? *Inside Energy.*

JinkoSolar. (2020). Jinkosolar.Eu/en/.

Khalid, A., Mitra, I., Warmuth, W., & Schacht, V. (2016). Performance ratio – crucial parameter for grid connected pv plants.

Kougias, I., Aggidis, G., Avellan, F., Deniz, S., Lundin, U., Moro, A., . . .Theodossiou, N. (2019). Analysis of emerging technologies in the hydropower sector. *Renewable and Sustainable Energy Reviews 113.*

LAZARD. (2019). Levelized cost of energy and levelized cost of storage 2019.

Lia, L., Vereide, K., & Kvaal, B. (2016). The new strategy for psp in norway – medium sized projects in existing power scheme.

Marabito, A., & Hendrick, P. (2019). *Pump as turbine applied to micro energy storage and smart water grids: A case study.* Université Libre de Bruxelles (ULB), Belgium.

Masters, G. M. (2013). Renewable and efficient electric power systems. John wiley & sons.

MET. (2020). Meteorologisk institutt (norwegian meteorological institute); provided observational data.

MET. (2020b). Meteorologisk institutt (norwegian meteorological institute); provided modelled data from nora3/windsurfer.

Milnes, M. (2017). Aecom design build; civil, mechanical engineering: The royal academy of engineering: The mathematics of pumping water.

Nielsen, T. K. (2015). Simulation model for francis and reversible pump turbines, department of energy and process engineering, ntnu - norwegian university of science and technology, trondheim, norway. *International Journal of Fluid Machinery and Systems, IJFMS.202015.8.3.169, 8*(3). 10.5293

Norgeskart (Cartographer). (2019). Public mapping service. Retrieved from norgeskart.no

NREL. (2013). National renewable energy laboratory; solar energy and capacity value: U.S. Department of energy, office of energy efficiency and renewable energy, operated by the alliance for sustainable energy, llc.

NVE. (2007). Norges vassdrags- og energidirektorat (the norwegian water resources and energy directorate); vassdragskonsesjon.

NVE. (2010). Norges vassdrags- og energidirektorat (the norwegian water resources and energy directorate); veileder i planlegging, bygging og drift av små kraftverk.

NVE. (2019). Norges vassdrags- og energidirektorat (the norwegian water resources and energy directorate).

NVE. (2019b). Norges vassdrags- og energidirektorat (the norwegian water resources and energy directorate: Om kraftmarkedet og det norske kraftsystemet.

NVE. (2019c). Norges vassdrags- og energidirektorat (the norwegian water resources and energy directorate); kraftproduksjon.

NVE. (2019d). Norges vassdrags- og energidirektorat (the norwegian water resources and energy directorate): Fakta; nr. 7/2019, teknologianalyser 2019; kostnader for kraftproduksjon 2018.

NVE. (2019e). Norges vassdrags- og energidirektorat (the norwegian water resources and energy directorate); fakta: Kostnader for kraftproduksjon 2018.

NVE. (2020). Anleggskonsesjon: Troms kraft nett: Ref.: 201904820-103.

NVE Atlas. (2020). Puplic mapping service.

OED. (2014). Olje- og energidepartementet (the norwegian minestry of petroleum and energy); strømforsyning og strømnettet. .

OED. (2015). Olje- og energidepartementet (the norwegian minestry of petroleum and energy); fakta 2015 energi- og vannressurser i norge.

OED. (2020). Olje- og energidepartementet (the norwegian minestry of petroleum and energy); energifakta norge: Strømnettet.

OED. (2020b). Olje- og energidepartementet (the norwegian minestry of petroleum and energy); energifakta norge: Kraftproduksjon.

Patocka, F. (2014). *Environmental impacts of pumped storage hydro power plants*. NTNU - Norwegian University of Science and Technology, Trondheim, Norway.

Perán, F., & Suárez, A. (2019). Transformation of conventional hydro into pumped-storage: A new future business line for the electricity sector.

pv-tech. (2019). Top 10 solar moduel suppliers in 2018.

PVSyst. (2020). Pvsyst.Com : Photovoltaic systems.

PVSyst. (2020b). Pvsyst: Help. From https://www.Pvsyst.Com/help/meteo_notes_data_source_comparisons.Htm.

Rosvold, K., & Hofstad, K. (2019). Store norske leksikon; midlere årsproduksjon. SNL.

Sanden, C. H. (2011). Her er det flest soltimer på jorda.

seNorge. (2020). From senorge.No.

Sira-Kvina. (2007). Sira-kvina power company; extension of tonstad hydropower plant included pumping: Application for license.

SKS. (2019). *Troms kraft nett as, ishavskraft, troms kraft produksjon as, nodes as, enfo as, eaton electric as, powel as, solbes as, uit – arctic centre for sustainable energy, sjømatindustrien; sluttrapportering på konseptutredning: Smartinfrastruktur nord senja*.

Skårerud, J. R. (2020). Vannkraftnæringen frykter norge kan miste evnen til å vedlikeholde egne vannkraftverk: Vind setter vannkraft i fare.

Solanki, C. S. (2016). *Solar photovoltaics; fundamentals, technologies and applications. Third edition*. Bombay: Department of Energy Science and Engineering, Indian Institute of Technology Bombay.

Solargis. (2020). Solargis.Com/albedo.

SSB. (2018). Statistisk sentralbyrå (statistics norway): Rapporter 2018/16: Tilgang og anvendelse av elektrisitet i perioden 1993-2017.

SSB. (2018b). Statistisk sentralbyrå (statistics norway): Vi bruker mindre strøm hjemme.

SSB. (2020). Statistisk sentralbyrå (statistics norway): Innbyggere per område 2019.

Statkraft. (2019). Energy sources; hydropower.

Statkraft. (2020). Vindkraft; en energikilde i vekst.

Statnett. (2018). Statnett (system operator of the norwegian power system); slik fungerer kraftsystemet.

Storli, P.-T. S. (2020). Hydrocen; pumpeturbin i eksisterende kraftverk.

Stortinget. (2020). *Innstilling fra finanskomiteen om revidert nasjonalbudsjett 2020, om tilleggsbevilgninger og omprioriteringer i statsbudsjettet for 2020, om endringer i skatter og avgifter i statsbudsjettet for 2020, om økonomiske tiltak i møte med virusutbruddet og om redegjørelse av finansministeren om revidert nasjonalbudsjett.*

Sönnichsen, N. (2019). Global solar thermal energy capacity additions by country 2006-2018.

Tande, J. O. G. (2006). Sintef; impact of integrating wind power in the norwegian power system. *ResearchGate*.

TKN (2020b). [Personal email conversation].

TKP. (2020). Troms kraft produksjon; våre kraftverk.

TKP (2020b). [Personal email conversation].

UiT (2020). [Personal communication with professor t. Boström and r. Hardersen].

UiT (2020b). [Personal email conversation with phd odin eikeland].

Vartiainen, E., Masson, G., & Breyer, C. (2017). European pv technology and innovation platform steering committee. Pv; lcoe and competitiveness working group.

Wizelius, T. (2010). *Vindkraft i teori och praktik* (2nd ed.).

WWEA. (2020). World wind energy association; world wind capacity at 650,8 gw, corona crisis will slow down markets in 2020, renewables to be core of economic stimulus programmes.

Yang, C.-J. (2016). Pumped hydroelectric storage: Center on global change, durham, nc, united states, p.25.